



Kent Academic Repository

Pampush, James D., Morse, Paul E., Fuselier, Edward J., Skinner, Matthew M. and Kay, Richard F. (2022) *Sign-oriented Dirichlet Normal Energy: alinging dental topography and dental function in the R-package molaR*. *Journal of Mammalian Evolution* . ISSN 1064-7554.

Downloaded from

<https://kar.kent.ac.uk/96710/> The University of Kent's Academic Repository KAR

The version of record is available from

<https://doi.org/10.1007/s10914-022-09616-6>

This document version

Author's Accepted Manuscript

DOI for this version

Licence for this version

UNSPECIFIED

Additional information

Versions of research works

Versions of Record

If this version is the version of record, it is the same as the published version available on the publisher's web site. Cite as the published version.

Author Accepted Manuscripts

If this document is identified as the Author Accepted Manuscript it is the version after peer review but before type setting, copy editing or publisher branding. Cite as Surname, Initial. (Year) 'Title of article'. To be published in **Title of Journal** , Volume and issue numbers [peer-reviewed accepted version]. Available at: DOI or URL (Accessed: date).

Enquiries

If you have questions about this document contact ResearchSupport@kent.ac.uk. Please include the URL of the record in KAR. If you believe that your, or a third party's rights have been compromised through this document please see our [Take Down policy](https://www.kent.ac.uk/guides/kar-the-kent-academic-repository#policies) (available from <https://www.kent.ac.uk/guides/kar-the-kent-academic-repository#policies>).

Journal of Mammalian Evolution

Sign-Oriented Dirichlet Normal Energy: Aligning Dental Topography and Dental Function in the R-package molaR. --Manuscript Draft--

Manuscript Number:	JOMM-D-21-00070R2	
Full Title:	Sign-Oriented Dirichlet Normal Energy: Aligning Dental Topography and Dental Function in the R-package molaR.	
Article Type:	Original Article	
Keywords:	DNE; molar; mammalian dentition; occlusal sulci; enamel furrows; dental sharpness; curvature sign orientation	
Corresponding Author:	James D. Pampush, Ph.D. High Point University High Point, NC UNITED STATES	
Corresponding Author Secondary Information:		
Corresponding Author's Institution:	High Point University	
Corresponding Author's Secondary Institution:		
First Author:	James D. Pampush, Ph.D.	
First Author Secondary Information:		
Order of Authors:	James D. Pampush, Ph.D.	
	Paul E. Morse	
	Edward J. Fuselier	
	Matthew M. Skinner	
	Richard F. Kay	
Order of Authors Secondary Information:		
Funding Information:	Directorate for Social, Behavioral and Economic Sciences (2018769)	Dr. James D. Pampush
	Directorate for Social, Behavioral and Economic Sciences (2018779)	Dr. Richard F. Kay
	European Research Council (819960)	Dr. Matthew M. Skinner
Abstract:	<p>Dirichlet normal energy (DNE) is a dental topography measurement aimed at capturing occlusal sharpness and has shown promise for its ability to sort primate molars according to perceived shearing ability. As initially implemented, this measurement does not differentiate concave versus convex contributions to surface sharpness. This is problematic because the DNE-signal derived from concave aspects of an occlusal surface measures a sharp 'edge' oriented inward towards the enamel dentine junction rather than outward towards food contact. The inclusion of concave DNE in dietary analyses of molars possessing deep occlusal sulci—such as those found among hominoids—inflates the perceived functional sharpness of these teeth. Concave-inflated DNE values can be misleading, being interpreted as indicating that a particular taxon is more adapted for processing fibrous food than is warranted. The modification of the DNE measurement introduced here 'Sign-oriented DNE' alleviates this problem by elimination of concave sharpness from analyses, allowing investigations to focus on features of occlusal surfaces plausibly linked to shearing, cutting, or shredding of food materials during Phases I and II of the masticatory power stroke. Convex DNE is just as effective at sorting non-hominoid primate molars into traditional dietary categories as the initial applications of the orientation-blind version of the measurement, and</p>	

produces more theoretically coherent results from hominoid molars. Focusing on- and improving the connection between measurement and occlusal function will enhance the ability of dental topography to make meaningful contributions to our collective understanding of species' dietary ecologies.

Dear Dr. Croft,

Thank you for reconsidering our manuscript, “Sign-Oriented Dirichlet Normal Energy: Aligning Dental Topography and Dental Function in the R package molaR” (JOMM-D-21-00070R2), for publication. We feel that our first revision addressed all of the major suggestions/critiques of the two reviewers, and the paper was made much stronger for it. In this second round of revisions, we have further adjusted our language to accommodate some of the new criticisms from Reviewer 2 (R2), but take issue with apparent differences in opinion between us and this reviewer, with capitulation to their perspective fundamentally undermining our central critique of the field of dental topography—something that we consider essential to the manuscript’s aims. R2 states:

This paper appears to have two main objectives: improve the DNE method, and defend the functional interpretation of DNE. The first one is very easy, and I am completely convinced that it is valuable. The second objective appears to generate many tangents in the paper that are not particularly necessary and are generally overly long. I think the manuscript is currently poorly set out, including extensive and sometimes repeated discussions on topics that are really only tangentially related. It appears that the majority of the text added to the Introduction is not particularly informative for the main focus of this manuscript, and can safely be shortened or removed. A lot of the material added in the Methods is also a literature-based review of DNE and would be more relevant in the Introduction or Discussion, and can be significantly shortened, retaining only the modification of the calculation of DNE.

R2 correctly diagnoses the two main thrusts of this paper: [1] to critically assess and improve the DNE measurement in light of tooth functionality, and [2] to make clear that given its detachment from homology, DNE’s (and dental topography measurements in general) utility is as an estimate of the tooth’s functional abilities. It is surprising to see the reviewer ready to accept the clear benefits of the first goal, but to miss the obvious connection with the second. Indeed, these two goals are deeply intertwined, since the rationale for the DNE improvement is based on the measurement being useful in a functional context. R2 seems to find our critique of prior implementations of DNE and dental topography generally as “tangential” despite their foundational importance for our study in the first place. This appears to be in direct opposition to the assessment of Reviewer 1 (R1), who previously requested that these aspects of the manuscript be expanded. Given what appears to amount to a disagreement in opinion about the utility of dental topography as an approach (as R2 states, “The Results and Discussion section are good” and offers no comments or edits in this portion of the manuscript), we think R2 should be encouraged to publish a critique of this paper rather than blocking us from clearly and fully laying out our argument and position. As we have already addressed a large number of edits from both reviewers in our first round of revisions and R1 is pleased with our current revision, we advocate that the pages of the literature—not confidential peer-reviewed comments—is where the debate between R2’s interpretation of dental topography and our own should take place.

Because we need to make several points at length to defend the construction of our manuscript, some of R2’s comments are addressed here before the regular table of comments.

Best regards,
James D. Pampush

Reviewer 2:

A lot of the material added in the Methods is also a literature-based review of DNE and would be more relevant in the Introduction or Discussion, and can be significantly shortened, retaining only the modification of the calculation of DNE.

R2 dismisses our deductive analysis of DNE as ‘a literature review,’ a stance we take issue with and to which we must respond.

The original paper defining DNE for use in dental topography (Bunn et al. 2011) contains only a very technical and somewhat opaque description of the DNE measurement. After describing their surface preparation, they write (pg. 250-251):

The Dirichlet energy is defined to be the extent to which the normal map expands in orthogonal directions: if u and v denote orthonormal direction on the surface, and $n(p)$ denotes the normal at point p on the surface, then locally the normal map expands as $e(p) = \|n_u\|^2 + \|n_v\|^2$, where n_u and n_v denote the derivatives of the normal n in the directions u and v , and $\|\cdot\|$ denotes the Euclidean norm (length) of a vector. The function over the tooth surface $e(p)$ is called energy density. The global measure of curviness is then defined by summing up these local energies over the tooth surface: $E = \int_M e(p) dvol(p)$, where we integrate with respect to the surface area $dvol(p)$.

In case the directions u and v are not orthonormal, the energy density is calculated by $e(p) = tr(G^{-1}H)$, where $G = \begin{pmatrix} \langle u, u \rangle & \langle u, v \rangle \\ \langle u, v \rangle & \langle v, v \rangle \end{pmatrix}$, and $H = \begin{pmatrix} \langle n_u, n_u \rangle & \langle n_u, n_v \rangle \\ \langle n_u, n_v \rangle & \langle n_v, n_v \rangle \end{pmatrix}$

and $\langle \cdot, \cdot \rangle$ denotes the Euclidean inner-product (dot product). In the discrete surface case, we first approximate the normal of the surface at the each vertex as the normalized average of the normals of its adjacent triangular faces. We then use the previous equation for calculating the energy density in each triangle (assuming that the map n is piecewise linear the energy density is constant in each triangle), see Figure 2. Then, we sum the densities multiplied by the area of the faces to get the approximated total energy: $E = \sum_{\Delta \in Faces} e(\Delta) \cdot area(\Delta)$ where Δ is traversing over all the triangles in the tooth surface.

Most readers and users of DNE do not find this description particularly helpful. The next major publication to employ DNE (Winchester et al. 2014) did not expand on this description, and outside of the members of our authorship, no other users of DNE have published further details of how the measurement works. In a 2016 paper (Pampush et al. 2016, American Journal of Physical Anthropology) we are the first describe the energy-density calculation as being based on osculating circles and in the supplemental materials provide more effective visual aids than those provided in either Bunn et al. 2011 or Winchester et al. 2014. By using the osculating circle approach and moving away from the matrix algebra description (like above), we are able to show exactly how the measurement works using a simple hemisphere giving readers and users of DNE access to the internal construction of the measure in ways not previously offered (see Spradley et al. 2017 American Journal of Physical Anthropology, and Pampush et al. 2019 American Journal of Physical Anthropology). In this manuscript, we expand on our more thorough description of the DNE calculation, and directly connect the osculating circle measurement approach with successful correlation of knife stabbing depth (i.e., a performance metric, see Hainsworth et al. 2006 cited in text). This is *not* a review of the literature—it is a coherent, approachable deduction of how

the measurement works including a previously undescribed link with function that together advocate for why our proposed alteration is necessary. We have opted to place this in the methods, since Bunn et al. 2011 describe the ‘mathematical background’ for DNE in their methods. This deduction is not only one of the explicit goals of our paper, it is a useful contribution for the larger dental topography research community to better understand be fully informed as to how the DNE measurement operates.

R2 makes an about face from their prior critique with the following comment:

L144-153: the corollary of this section is that DNE is merely an 'abstraction of the morphology' as no studies have 'correlated [DNE] with performance outcomes' during mastication. Later in the manuscript the authors expound on the theoretical basis of DNE likely measuring some aspects of sharpness that will affect force to fracture food, but this has not been directly demonstrated for DNE.

The section of text (L144-153) the reviewer is referring to states:

In contrast to standard dental measures, the landmark-free approach which advantages the dental topography measurements also has the effect of disassociating them from models of tooth function and performance. Topography measurements are abstract expressions of surface-wide dental morphology that do not necessarily follow a clear functional rationale. To be functionally insightful, measurements used to assess dental morphology must be correlated with performance outcomes—which is best assessed by chewed-food particle size and/or chew strokes or chewing time—but can also be inferred through other means. Otherwise, these measurements are just abstractions of the morphology, and while they may still be useful for tracking broad changes or trends in tooth form, they cannot inform adaptive hypotheses or dietary reconstructions without clearer links to the known modes of masticatory function.

This section of our text follows the specific description of mastication which links homologous landmarks (i.e., tooth cusps) with leading models of tooth function, providing us the rationale for these assertions. Following this text, we deductively analyze DNE and do in fact explicitly link the method of the measurement with performance outcomes (the section R2 described as “unnecessary literature review,” as noted above).

To better clarify our position, we have rewritten this section to read:

In contrast to standard dental measures, the landmark-free approach which advantages the DT measurements also has the effect of disassociating them from models of tooth function and performance. Topography measurements are abstract expressions of surface-wide dental form that may segregate different morphologies, but do not necessarily follow a clear functional rationale. To be functionally insightful, measurements used to assess dental morphology must be correlated with performance outcomes—which is best assessed by chewed-food particle size and/or chew strokes or chewing time—but can also be inferred through other means. Otherwise, when detached from homology these measurements are unmoored abstractions of the morphology, wherein two dramatically different dental Bauplanē with little-to-no clear resemblance might generate identical DT values. Outside of testing explicitly functional hypotheses, it is unclear what value DT measurements would hold in a phylogenetic context since the measures can disguise homoplasy as homology.

R2 later writes:

L188: do the authors seriously think that dental topographic measurements have been developed without any consideration of their likely functional consequences? The authors need to cite specific studies here to show which metrics they are referring to - which dental topographic measurements are a 'black box operation'? Which have been postulated

and then implemented without some degree of 'first principles' (the 'third method') being put forward? This is not to say that all of these methods are equally insightful about dental function and correlation with diet, but these are all strong words to be said in a manuscript that cannot push these issues forward beyond a minor improvement in one metric.

We think a clear link with function is at the core of the value of dental topography measurements, and that some of these approaches have been developed without any particular regard to the function of the teeth. Rather it seems, some of these measurements were developed because computing abilities have made them possible, and they have been justified post-hoc via re-sorting dental morphologies among known functional categories. There are several examples of this. In the paper we note that OPC does not appear to have a strong functional link for bunodont teeth, but at least the original authors have tried to articulate one using their original, more diverse dental sample. Other dental topography measurements such as Relief Index, Slope, Angularity, and Portion de Ciel Visible do not have clear functional rationales, or only very weak ones. We can offer specific deductive critiques of what we perceive to be 'black box operations' among the listed DT measurements if the editors require it.

We are trying to take a positive stance with our current paper and wish to only vaguely reference what we view as mis-steps by other researchers. There is too much to unpack regarding the production, justification, and use of many dental topography metrics (a criticism of each metric potentially representing a paper unto itself), and we would rather keep the focus on how to properly use this updated version of DNE, and to suggest the appearance of 'red flags' in other measurements. Dental topography as a subdiscipline is—in our opinion—in a very precarious moment of legitimacy. We want to use this paper to help push the use of these metrics in a certain direction and would prefer to leave discussion of the failures of other metrics or their applications to other publications after positioning Convex DNE appropriately. As noted above, R2 appears to differ in their opinion and/or interpretation of the field and its handling of methods. If this is so, then their perspective should be published in response to our manuscript so that a public dialog can emerge with the aim of strengthening and validating the field.

R2 takes issue with our description of OPC, but appears mistaken in their understanding of the metric:

L261: the formulation of OPC does not assume that 'the boundaries between differently-oriented patches represent cutting "tools": it is designed to correlate with the number of features on a tooth, but not that each 'patch' is a tool in itself. When the number of hemispherical cusps on a tooth increases from one (OPC~8) to two (OPC~16), we expect that the number of potential interactions between teeth and food doubles; it is not intended that the number of tools is 8 in the first, and 16 in the second tooth. Food can be fractured by both cusp and bladed tooth components - a tooth does not have to have blades to fracture food (see fundamental studies on dental function, as set out by Lucas 2004).

Evans et al. 2007 (Nature) created and defined OPC. In describing their new method, they write (pg.78, emphasis added):

“...An effective way of increasing processing capability is to add features onto the teeth that allow more food to be divided in each occlusal stroke. If we view teeth as ‘tools’ for breaking down food,¹¹ this is like adding extra tools to the tooth that function in food breakdown. **This is similar in meaning to ‘breakage sites’.**¹⁰ ‘Dental complexity’ is then any measure of the number of features, tools or breakage sites on a tooth.”

Clearly the authors are using the term ‘breakage sites’ as the feature OPC is expected to correlate with. They cite Lucas 2006 “Dental Functional Morphology” for this definition of breakage sites, but Lucas does not offer a direct definition in his book. He refers again to ‘breakage sites’ in the book, but then cites earlier works including Lucas et al. 1985 and Lucas et al. 1986, neither of which offer a clear definition. However, Lucas (2006) does cite van der Glas et al. 1992 (Journal of Theoretical Biology) in reference to breakage sites, and these authors define breakage sites as follows pg. 105:

“A breakage site is defined as part of the occlusal surface of the post-canine teeth which is suitable for breaking particles of a particular size.”

Again, this is a pretty vague definition, but it seems to be a generalization of the features of a tooth used in breaking down food and most would read this as: breakage sites = cusps and crests. We see several problems with this definition but these also extend to the OPC measurement. First, cusps and crests are most effective at breaking down different types of materials (as extensively outlined in Lucas 2006 and elsewhere). Crests are useful for shredding work-limited (tough) materials, while cusps are better for mashing soft fruits and crushing hard-objects. Conflating these two types of features within a measurement will lead to confounding ecological signals within the data unless the study design accounts for these differences in some other way. Evans et al. 2007 seemed to have accounted for this in their study design by incorporating species ranging from very simple, sectorial teeth with a few cusps and crests to those with highly complex, lophodont dentitions. Thus, the trends in their data are driven by the relative number/length of shearing crests, which the authors seem aware of when interpreting their findings (emphasis added):

Pg. 79 “For carnivorans, OPC shows a relatively clear gradation in dental complexity from low values in hypercarnivores, intermediate in the omnivores, and highest in the herbivores (Fig. 2; $P < 0.001$ for all tests) in both the upper and lower tooth rows... The rodents illustrate a similar trend of dental complexity with diet (Fig. 2)... We note that the better resolving power of OPC [other measures were not significant with dietary correlations] may be due to **its identifying distinct functional surfaces (such as wear facets), fitting with the concept of tooth crown consisting of individual ‘tools’ for breaking down food.**”

Given that the number of cusps is not drastically different between hypercarnivores and herbivores, OPC is increasing with the number of cutting crests on the postcanine teeth, while the number of cusps is being swamped out by the crest count. This is confirmed in noting that this measure works well with lophodont dentitions as other authors have shown but not with more generalized dentitions involving the typical tribosphenic cusps (Pineda-Munoz et al. 2017). Indeed Evans uses this interpretation in a follow up paper on the evolution of horse molars to argue that they show an increasing shearing efficiency throughout their North American lineage because an increase in OPC counts through time is linked to the evolution of more complex and lophed molars (Evans and Janis 2014, Ann. Zool. Fennici). For clades with conservative occlusal features (such as primates), OPC reveals no clear trends among taxa even when contrasting frugivores and folivores, showing a weak correlation between the measurement and the functional demands of teeth (Winchester et al., 2014)

As evidenced above, framing this argument requires a lot of space and we were trying to keep it short in the actual manuscript since this is not a paper about OPC. We have significantly modified our discussion of OPC to reflect this more nuanced perspective but thought the editors could benefit from this discussion in evaluating our manuscript against R2's comments.

R2 has an additional compound comment regarding DNE, its utility, and the deductive analysis:

L199: given how much space the authors give to the first two 'methods', the third method is rather superficially treated, particularly as it relates to the interpretation of DNE. How do we expect DNE to correlate with diets? If DNE measures sharpness, and sharpness affects 'the ability of the interdigitating tooth surfaces to reduce the particle size of chewed food' then why would sharpness not be maximised for all diets? Why would it differ among diets?

We have superficially treated the third method here because we plan on using it to explicate what the DNE measurement is capturing when deployed. We feel this terse introduction to deductive logic prepares readers for the longer discussion of the DNE measurement this reviewer previously referred to as a 'literature review.'

In the deductive analysis of DNE we have 2 main goals: First to show that DNE is a surface-wide extension of the osculating circle approach to measuring sharpness. Second, to show that this measure seems to be effective when applied to knives, that is, when used in a functional context.

This third method is not dependent on diet or dental morphology as the other two are. It is purely an analysis of whether or not DNE is measuring a *useful* property of a surface irrespective of the type of surface or the role of that surface. It seems a safe extension that if DNE is indeed measuring surface sharpness as we attempt to show, that this is a useful property to measure on a surface expected to be used in breaking down other objects/materials.

The reviewer then asks a set of hyperbolic questions regarding the application of DNE in a dietary ecology framework. First, we (and all other authors employing DNE in a dietary framework, to our knowledge) expect the measure to correlate with the need to cut foods and therefore the amount of tough, work-limited, dietary fiber materials in a given diet. Thus primates (and other mammals) consuming larger quantities of tough foods are expected to have higher DNE values on their teeth compared to related taxa consuming less tough food items. DNE is not always maximized because not all dietary materials are best broken down with shearing actions. Some materials are considered stress-limited; these types of materials tend to catastrophically fail when enough stress is imparted into them, as exemplified with the breaking of hard candy. Mammals possessing diets full of stress-limited foods tend to have rounded bulbous cusps and teeth capable of imparting larger force-loads into dietary objects while also dissipating these loads within their own teeth by evenly distributing the strain throughout the enamel cap avoiding the production of failure points. The 'architecture' of sharpness encourages the buildup and concentration of stress, making high DNE teeth unsuitable for hard-object crushing. Other food

materials are better ‘mashed’ rather than cut, like most ripe fruits, and the morphology best suited for this breakdown also involves rounded bulbous cusps. Thus animals with hard-objects (nuts, seeds, bark, etc.) or lots of fruit in their diets are predicted to have lower DNE values (and this has so far proven to be the case), since cutting is not as important during their masticatory events. All of this has been argued extensively in other papers, including: Winchester et al. 2014, Pampush et al. 2016 & 2018 all cited in this paper. It is strange that R2 is apparently either unfamiliar with this literature given its central importance to their critique and our manuscript, or is opting to purposefully ignore it when fielding comments we must reply to.

Reviewer 2:

L213: given the strongly worded statements about how morphologists and ecologist should be 'skeptical of the biological relevance of any surprising or incongruous dental topography findings', why is this skepticism not applied to the typical interpretation of DNE in this manuscript?

Pardon our grumpiness, but to fully explain our position, please consider this theoretical example. Suppose the dietary ecology of a group of organisms is quite well known and established. Now imagine that a new type of measurement is invented. This measurement seems to present an objectivity and attention to detail that was previously unattainable. But the measurement is quite complex to the point that even mathematically and statistically savvy people need to do a fair amount of work to understand its calculation. When applied to the known group of organisms, this new measurement seems to indicate something very surprising and maybe even a reversal in thinking regarding the dietary ecology of our organism.

Are you ready to rewrite the ecology of the organism? Or would you prefer to better understand and investigate the measurement?

It is our very skepticism about DNE, and our deductive work over the last few years in studying it and related measurements which have lead us to write this paper. Given that the motivation for this paper is skepticism of the typical interpretation of DNE, leading us to propose a modification, we find R2’s question baseless. Such a question can only logically arise from either an extraordinarily cursory or incomplete reading of the manuscript, or a deliberate attempt to generate additional comments that imply an inconsistency not present in our work.

Reviewer	Reviewer Comment	Current Location in Manuscript (if applicable)	Adjustment/Response
----------	------------------	--	----------------------------

R1.2	The authors have expanded the introduction, explained goals in more detail, and combined some figures. Most of my concerns have been considered or reasons have been given if not. To me the authors answers make sense. I'm looking forward to see the article published.		Thank you, we certainly put a lot of hard work into this paper.
R1.2	I have only one minor suggestion for improving the figures: the authors tried to combine figures, but more needs to be done: figure 2 and 4 can be combined, and figure 5 and 6 as well. In addition table 1 has a lot of empty space: I recommend to move it to the supplement and combine it with SOM Table S1.2.		We made all these changes. Moved table 1 to supplemental, combined figures 2 and 4, as well as 5 and 6.
R2.2	With the focus on defending the functional interpretation of DNE, additional effort should be put into critical evaluation of DNE - it has not been empirically tested, it is a metric of sharpness that cannot be immediately translated to a true size (e.g. radius of curvature in millimeters) that will have different consequences in the mouth of a real-sized animal. Showing both the strengths and weaknesses of all methods is essential for progress in methodological development.		<p>In this paper, we have presented the most thorough analysis of the DNE calculation yet to appear in the literature as mentioned in the comment immediately above from the earlier review.</p> <p>We deductively analyzed the measure, and then discussed the implications for the way it is calculated. We specifically addressed the size issue, and would like to remind the reviewer that the measurement is unitless, and independent of size (facts repeated in every study utilizing DNE). We and many others have noted the advantages and pitfalls of this feature of the measure. I do not think there is anything else to address regarding this comment.</p> <p>The reviewer is correct to say that the measurement has not been 'empirically tested.' We would argue that the closest example of this type of testing has occurred in a paper published by our research group (Spradley et al. 2017, American Journal of Physical Anthropology) wherein we predict based on the underlying math what the DNE of a hemisphere should be. We then scanned a rubber ball, processed it, and measured its DNE, and found it to indeed be very close to the mathematical prediction.</p>
R2.2	L58: shearing, cutting and shredding of food can also occur during Phase II and puncture-crushing.		<p>We agree. We have altered this sentence to read "during Phases I and II..."</p> <p>We opted to leave out the comment that shearing is also going on during Puncture-Crushing, since most dental morphologists would agree that the shape of molars is likely most attuned to the functional needs</p>

			during interdigitating occlusion, as noted later in the manuscript.
R2.2	L83-124: I do not think this level of detail on chewing is relevant to this study.		We disagree. In our view, most dental topography studies have focused far too little attention on how teeth actually work, as evidenced by the inclusion of Concave DNE signal in final DNE values in past studies. R1 both requested and appreciated this addition, and we think it is an important reminder. We also want our readership specifically thinking about this kind of stuff prior to reading our deductive analysis.
R2.2	L165: 'FPS, as a surrogate for swallowed food size' - do the authors mean surrogate for performance?		<p>We mean both. But we are not sure that measuring chewed food particle size will result in clear answers since a simple solution is to take additional chew strokes if the teeth are dull.</p> <p>DNE on teeth of folivores may track chew-strokes. That would probably be the best way of confirming the performance aspect of this measurement in a biological setting.</p> <p>Regardless, the reviewer's comment is about our reporting of another paper. In this section of the text, we are describing what other researchers have done to try to 'ground-truth' dental topography to performance. We are accurately describing another research group's work without directly putting words in their mouth and are uncertain anything can be done to address this particular complaint.</p>
R2.2	L177: 'where topography measurements are inferred to be functionally relevant if they successfully differentiate dental morphologies' - are these 'dental morphologies' being a priori distinguished by a human observer? Do you mean the topographic measurements are inferred to be relevant if they differentiate dentitions from animals with different diets or similar? This is what is more clearly stated in the next sentence.		<p>The full quote from our paper reads: "A second approach employs the comparative method, where topography measurements are inferred to be functionally relevant if they successfully differentiate dental morphologies. Currently this second technique is how most dental topography measurements derive their presumed efficacy—via demonstrations of their successful sorting of mammalian teeth into traditional heuristic dietary categories (e.g., insectivore, folivore, frugivore, etc., see: Evans et al. 2007; Winchester et</p>

		<p>al. 2014). With the specimens' dietary categories assigned a priori, these kinds of studies often show that these measurements are likely capturing functionally relevant properties of dental surfaces; possibly even quantifying the same features researchers have previously used to qualitatively sort teeth into dietary groups.”</p> <p>We feel like this section is clear. Perhaps we do not entirely understand the complaint of the reviewer here, but we start with a topic sentence and then build from there and don't see a clear way of improving the language here.</p>
R2.2	<p>L191: I would argue that 'classic and simpler measurements like SQ' often have fundamental misunderstandings about their functional relevance: is it the length of the crest, its angle or its sharpness that is primarily being selected for? The foundational studies argue largely for an increase in length, but that is not the only aspect of shape that differs with SQ.</p>	<p>The way SQ works is predicated entirely on measuring the relative length of shearing crests. To measure SQ, a scholar would hand-measure the lengths of shearing crests, plot them against tooth length, and take the residual of that regression. It is blind to crest sharpness or orientation. In this way, when a correlation is found between SQ and an ecological variable(s), there is no confusion as to how to make a proper interpretation, since it is a measure of crest length. This clearly refutes this reviewer's speculation that the interpretation of SQ can be ambiguous.</p> <p>If we take the reviewers comments to mean that SQ is not always <i>effective</i> in testing ecological hypotheses, then they may have a point. Perhaps SQ is not useful in certain circumstances when the <i>sharpness</i> of crests, and not their relative lengths is the target of selection. This is a very good reason to turn to the DNE metric, which accounts for both the length of the convex sharp edge, and the sharpness of the edge. However, only Convex DNE would be similar (and therefore hold the same functional value) as SQ since only the outward facing sharp ridges are of any value.</p>

R2.2	L194: this criticism of lack of quantitative correlation with feeding performance is directly relevant to DNE, and I am slightly mystified as to why the authors are so adamant to make this point several times in a manuscript that cannot answer the criticisms of the method they are employing. It is also largely a discussion point rather than being necessary for an Introduction to the topic.		<p>As we point out in several places in the manuscript, the ‘gold standard’ for confirming the value of these dental topography metrics is a correlation between chewing efficiency and the measures. We agree with the reviewer that, like the other topography measurements, DNE has not been directly investigated for its relationship to performance <i>per se</i>.</p> <p>Acknowledging this about DNE and indeed all topography measurements is important because we may still learn important things about their value when this sort of work is completed. And, of course, this is a major short-coming in their current formulations and implementation by researchers. We must acknowledge this to better inform readers, and we think this belongs in the introduction.</p> <p>However, despite this lack of direct testing, there are several reasons to think that DNE is a better topography measure than most and we have tried hard to make that case here with lots of examples and thorough deductive analysis.</p>
R2.2	L216: it seems the point trying to be made here is a specific criticism of a previous study that found that DNE did not strongly correlate with diet in great apes. It would be preferable that such criticism is more clearly stated rather than being obliquely referred to, so the reader is clear what point is being made. This is clearly a main motivation for the study but is hidden amongst many other superfluous points.		There has been some work published on great ape and hominin dental topography which we would prefer not to discuss in this paper. We want the focus of this work to be on the refinement and future application of DNE, and to discuss dental topography as a maturing discipline. Some mistakes have certainly been made, but this paper does not need to be about that.
R2.2	L224: no demonstrative link currently exists between DNE and 'chewing efficiency' - such tests have not been carried out, as was extensively discussed in the Introduction of this manuscript.		<p>We agree and this was a sloppily written sentence on our part and certainly not our intention. We have rewritten the sentence to read: “...and is expected to produce a more coherent link between the DNE measurement and functional sharpness of occlusal surfaces.”</p>



[Click here to view linked References](#)

1
2
3
4
5
6
7
8
9
10
11
12
13
14
15
16
17
18
19
20
21
22
23
24
25
26
27
28
29
30
31
32
33
34
35
36
37
38
39
40
41
42
43
44
45
46
47
48
49
50
51
52
53
54
55
56
57
58
59
60
61
62
63
64
65

**1 Sign-Oriented Dirichlet Normal Energy: Aligning Dental Topography and Dental Function in
2 the R package mo1aR.**

3
4 James D. Pampush^{1,2}, Paul E. Morse^{3,4}, Edward J. Fuselier⁵, Matthew M. Skinner^{6,7}, and Richard
5 F. Kay^{3,8}

6
7 ¹Department of Exercise Science, High Point University, High Point, NC 27260

8 ²Department of Physician Assistant Studies, High Point University, High Point, NC 27260

9 ³Department of Evolutionary Anthropology, Duke University, Durham, NC 27708

10 ⁴Florida Museum of Natural History, University of Florida, Gainesville, FL 32611

11 ⁵Department of Mathematical Sciences, High Point University, High Point, NC 27260

12 ⁶School of Anthropology and Conservation, University of Kent, Canterbury, UK CT2 7NR

13 ⁷Department of Human Evolution, Max Planck Institute for Evolutionary Anthropology, Leipzig,
14 Germany 04103

15 ⁸Division of Earth and Climate Sciences, Nicholas School, Duke University, Durham NC 27708

16
17
18 Key Words:

19 DNE; crenulated enamel; occlusal sulci; enamel furrows; dental sharpness; curvature sign
20 orientation

1
2
3
4
5
6
7
8
9
10
11
12
13
14
15
16
17
18
19
20
21
22
23
24
25
26
27
28
29
30
31
32
33
34
35
36
37
38
39
40
41
42
43
44
45
46
47
48
49
50
51
52
53
54
55
56
57
58
59
60
61
62
63
64
65

Abstract

Dirichlet normal energy (DNE) is a dental topography measurement aimed at capturing occlusal sharpness and has shown promise for its ability to sort primate molars according to perceived shearing ability. As initially implemented, this measurement does not differentiate concave versus convex contributions to surface sharpness. This is problematic because the DNE-signal derived from concave aspects of an occlusal surface measures a sharp ‘edge’ oriented inward towards the enamel dentine junction rather than outward towards food contact. The inclusion of concave DNE in dietary analyses of molars possessing deep occlusal sulci—such as those found among hominoids—inflates the perceived functional sharpness of these teeth. Concave-inflated DNE values can be misleading, being interpreted as indicating that a particular taxon is more adapted for processing fibrous food than is warranted. The modification of the DNE measurement introduced here ‘Sign-oriented DNE’ alleviates this problem by elimination of concave sharpness from analyses, allowing investigations to focus on features of occlusal surfaces plausibly linked to shearing, cutting, or shredding of food materials during Phases I and II of the masticatory power stroke. Convex DNE is just as effective at sorting non-hominoid primate molars into traditional dietary categories as the initial applications of the orientation-blind version of the measurement, and produces more theoretically coherent results from hominoid molars. Focusing on- and improving the connection between measurement and occlusal function will enhance the ability of dental topography to make meaningful contributions to our collective understanding of species’ dietary ecologies.

1
2
3
4 **65 Introduction:**

5
6
7 **66** Originally introduced by Ungar and colleagues (e.g., Zuccotti et al. 1998; Ungar and
8
9 **67** Williamson 2000; Ungar and M'Kirera 2003), dental topographic (DT) analysis is a rapidly
10
11 **68** growing and diversifying approach aimed at studying the morphological, functional, and
12
13 **69** adaptive properties of mammalian teeth. Using scanned and digitized dental surfaces, DT
14
15 **70** measurements quantitatively characterize the surface topography of tooth crowns. Some
16
17 **71** prominent DT measurements include orientation patch count (Evans et al. 2007), relief index
18
19 **72** (Boyer 2008), average surface slope (Dennis et al. 2004), and the focus of this work: an estimate
20
21 **73** of surface sharpness known as Dirichlet normal energy (DNE, Bunn et al. 2011). DNE and other
22
23 **74** DT measurements offer many advantages over homology-based dental measures, such as
24
25 **75** shearing quotient (SQ; see: Kay and Simons 1980; Kay 1984; Anthony and Kay 1993; Strait 1993;
26
27 **76** Ungar and Kay 1995; Kirk and Simons 2000), or crown height (Williams and Kay 2001; Damuth
28
29 **77** and Janis 2011). Paramount among the topography measurements' advantages is that they can
30
31 **78** be applied to teeth without requiring dental landmarks, as they are quantitative
32
33 **79** characterizations of whole or partial tooth surfaces. By side-stepping homology, these
34
35 **80** measurements can be applied to worn teeth (e.g., Ungar and Williamson 2000; Ungar and
36
37 **81** M'Kirera 2003; Pampush et al. 2018)—whose identifiable landmarks (discrete cusp tips and
38
39 **82** crests) are often obscured by wear—and they permit comparisons among clades that may not
40
41 **83** share homologous features (e.g., Evans et al. 2007; Harper et al. 2019; Selig et al. 2021).
42
43 **84** Generally speaking, DT measurements overwhelmingly derived their perceived usefulness from
44
45 **85** their ability to assign objective and distinct values to teeth supposedly possessing differing
46
47 **86** dietary adaptations (see below). The underlying assumption here is that within the context of
48
49
50
51
52
53
54
55
56
57
58
59
60
61
62
63
64
65

1
2
3
4
5
6
7
8
9
10
11
12
13
14
15
16
17
18
19
20
21
22
23
24
25
26
27
28
29
30
31
32
33
34
35
36
37
38
39
40
41
42
43
44
45
46
47
48
49
50
51
52
53
54
55
56
57
58
59
60
61
62
63
64
65

87 mammalian mastication, DT measurements are reflective of the functional abilities of occlusal
88 surfaces. However, uncritical acceptance of this assumption paves the way for misapplication or
89 misinterpretation of DT measurements, particularly when applying them to teeth which are
90 structurally distinct from reference samples. Before more thoroughly evaluating DNE, it is best
91 to review what is understood about dental function and what might be learned about dental
92 morphology from the use of DT measurements.

93 *Associating dental topography and dental function*

94 To date, there has been inconsistent and incomplete efforts made to connect dental
95 topography measurement with models or assessments of tooth function. Stepping away from
96 dental landmarks has hindered the interpretive footing of some DT measurements since
97 modeling of how teeth move and interact during mastication has traditionally been framed
98 around the interaction of various named features presumed to have functional relevance (e.g.,
99 cusp apices). Put differently, dental landmarks provide the essential vocabulary in
100 characterizing exactly which and how parts of teeth are brought together to reduce food. Initial
101 studies of mammalian masticatory movements were based on manipulation of dried skulls and
102 jaws where researchers focused on how the cusps of upper and lower teeth might complement
103 one another (Butler 1952; Mills 1955; 1963; 1967; Butler 1973; Mills 1973). Models of
104 mastication experienced a leap forward with the advent of cinefluorography and its application
105 to mammals and primates exhibiting 'primitive' dental morphologies (Crompton and Hiiemae
106 1967; Crompton and Hiiemae 1969; Kay and Hiiemae 1974c; Kay and Hiiemae 1974b; Hiiemae
107 1978). Cinefluorographic recordings showed that mastication follows a rhythmic pattern
108 arranged in two basic modes. Cycles in both modes consist of a closing movement in which the

1
2
3
4 109 lower jaws are approximated, giving way to a power stroke when forces are applied between
5
6
7 110 teeth and food. The two modes of mastication are distinguishable by the degree of occlusion in
8
9
10 111 their power strokes. In the initial mode, once a bite of food is separated and brought into the
11
12 112 mouth, the upper and lower cheek teeth are closed around it, coarsely reducing the food, and
13
14 113 mixing it with saliva in preparation for finer trituration. This so-called ‘puncture-crushing’ mode
15
16
17 114 does not involve the direct occlusion of molars during its power stroke, and is not tightly
18
19
20 115 constrained by- nor particularly informative of- the form-function relationship of molar
21
22 116 structure. In a second subsequent ‘chewing’ mode of the power stroke, smaller food boluses
23
24
25 117 are tightly pressed between teeth during the power stroke. During this second mode of
26
27
28 118 mastication, precise contacts between the teeth guide and constrain masticatory movements.
29
30 119 It is during this second operation of the power stroke—or intercuspal phase (Ross and Iriarte-
31
32
33 120 Diaz 2014)—where molar form becomes relevant to masticatory function. It has been
34
35 121 convincingly established that the complementary features of occluding molars work to reduce
36
37
38 122 food while the mandibular molars are brought upward and medially, processing food between
39
40
41 123 the interdigitating cusps (Crompton and Hiiemae 1970; Hiiemae and Kay 1972; Kay and Hiiemae
42
43 124 1974a; Hiiemae 1978; 1984). In primates and other mammals with conservative dental
44
45
46 125 morphology, most or all of the features we identify as ‘shearing’ crests come into occlusion
47
48 126 during the initial upward and mediolingually-directed Phase I of the chewing power stroke
49
50
51 127 (Crompton 1971; Kay 1975; 1977). When the teeth are fully interdigitated (in centric occlusion),
52
53 128 the upper molar protocones (and hypocones, if present) are seated in the talonid and trigonid
54
55
56 129 basins of the lower molars, respectively. Movement into this position is followed by a Phase II
57
58
59 130 movement out of centric occlusion when the surfaces of the talonid and trigonid are dragged
60
61
62
63
64
65

1
2
3
4
5
6
7
8
9
10
11
12
13
14
15
16
17
18
19
20
21
22
23
24
25
26
27
28
29
30
31
32
33
34
35
36
37
38
39
40
41
42
43
44
45
46
47
48
49
50
51
52
53
54
55
56
57
58
59
60
61
62
63
64
65

131 across the protocone and hypocone. The degree of force applied between the teeth during the
132 two phases has been debated (Wall et al. 2006; Ross and Iriarte-Diaz 2014), but certainly forces
133 sufficient to produce a distinctive pattern of scratches on planar attrition wear surfaces are
134 achieved during Phase II.

135 The adaptive significance of mammalian cheek-tooth morphology and mastication is
136 realized with the observation that—not only are the varied forms seemingly optimized to
137 efficiently triturate particular types of food materials—but that the morphological differences
138 fit within the functional expectations for how chewing works (Butler 1939; Kay 1975; Lucas
139 2006). Early studies of primate molars established that species that feed on different
140 proportions of fruit, leaves, and insects have different molar structure and that common
141 adaptive patterns were acquired convergently in many clades. Primate frugivores have small
142 teeth for their adult body size with relatively short molar crest lengths and crushing-grinding
143 basins (Kay 1975). In contrast, leaf-eating species tend to have larger teeth for their adult body
144 size with longer, sharper molar crests and larger crushing-grinding basins. These observations
145 made with standard dental measurements such as SQ have proven insightful, partly because
146 these measures were intentionally designed to capture functionally relevant information based
147 on models of how teeth interact during mastication, but also because they were explicitly
148 linked to a performance metric: chewed food particle size (Sheine and Kay 1977; Kay and
149 Sheine 1979; Sheine and Kay 1982). Since it is well established that the digestibility (extractable
150 energy), especially of high-fiber plant materials is significantly improved when they are more
151 finely triturated (McLeod and Minson 1969; Sheine and Kay 1977; Kay and Covert 1984), the
152 connection between dental measures and performance allowed researchers to convincingly link

1
2
3
4
5
6
7
8
9
10
11
12
13
14
15
16
17
18
19
20
21
22
23
24
25
26
27
28
29
30
31
32
33
34
35
36
37
38
39
40
41
42
43
44
45
46
47
48
49
50
51
52
53
54
55
56
57
58
59
60
61
62
63
64
65

153 their observations to adaptive scenarios (e.g., Kay 1984; Kay and Covert 1984; Anthony and Kay
154 1993; Kirk and Simons 2000; Allen et al. 2015).

155 In contrast to standard dental measures, the landmark-free approach which advantages
156 the DT measurements also has the effect of disassociating them from models of tooth function
157 and performance. Topography measurements are abstract expressions of surface-wide dental
158 form that may segregate different morphologies, but do not necessarily follow a clear
159 functional rationale. To be functionally insightful, measurements used to assess dental
160 morphology must be correlated with performance outcomes—which is best assessed by
161 chewed-food particle size and/or chew strokes or chewing time—but can also be inferred
162 through other means. Otherwise, when detached from homology these measurements are
163 unmoored abstractions of the morphology, wherein two dramatically different dental *Bauplan*
164 with little-to-no clear resemblance might generate identical DT values. Outside of testing
165 explicitly functional hypotheses, it is unclear what value DT measurements would hold in a
166 phylogenetic context since the measures can disguise homoplasy as homology.

167 In practice, there may be three ways of showing or inferring that a DT measurement is
168 capturing functionally relevant information about dental morphology to prove useful in testing
169 adaptive hypotheses. First, a measurement could be experimentally grounded to a functional
170 effect if it is shown to be correlated with chewed-food particle sizes or chewing time/chew-
171 stroke count. This must be done using a set of dental morphologies whose disparity of forms at
172 least encompasses the precision of the measurement, while also controlling for as many
173 aspects of food material properties and chewing mechanics as possible. As mentioned above,
174 we believe this to be the ideal approach for ecologically ground-truthing these measurements,

1
2
3
4 175 and might be best achieved with a thoughtfully designed experiment on captive or
5
6
7 176 opportunistically collected dead animals (e.g., Lanyon and Sanson 1986; Renaud and Ledevin
8
9
10 177 2017). Some progress has been made toward making these correlations. In gelada baboons
11
12 178 (*Theropithecus*), Venkataraman et al. (2014) studied food toughness and fecal particle size (FPS,
13
14 179 as a surrogate for swallowed particle size) in the field, matched with age-graded topographic
15
16
17 180 metrics on teeth from museum collections. They found that FPS is similar between prime and
18
19
20 181 old adults in the wet season, when food fracture toughness was at a minimum, but older adults
21
22 182 were less efficient (higher FPS) than prime individuals in the dry season when food toughness
23
24
25 183 was highest. They linked these findings to DT measurements (declining relief index and
26
27
28 184 orientation patch count; DNE was not measured) in older individuals. But this study did not
29
30 185 directly compare occlusal topographies with FPS, limiting confidence in their results. A number
31
32
33 186 of other studies on primates have reported on the relationships among FPS, age, and molar
34
35 187 topography (Ungar 2004; Glowacka et al. 2016; Thiery et al. 2017) but none considers all three
36
37
38 188 together, and clear documentation of the relationship between chewed-particle size and
39
40
41 189 topography measurements has remained elusive.

42
43 190 A second approach employs the comparative method, whereby topography
44
45
46 191 measurements are inferred to be functionally relevant if they successfully differentiate dental
47
48 192 morphologies. Currently this second technique is how most dental topography measurements
49
50
51 193 derive their presumed efficacy—via demonstrations of their successful re-sorting of mammalian
52
53 194 teeth into traditional heuristic dietary categories (e.g., insectivore, folivore, frugivore, etc., see:
54
55
56 195 Evans et al. 2007; Winchester et al. 2014). With the specimens' dietary categories assigned *a*
57
58
59 196 *priori* on the basis of field observations, such studies often show that these measurements are
60
61
62
63
64
65

1
2
3
4 197 likely capturing functionally relevant properties of dental surfaces; possibly even quantifying
5
6
7 198 the same features researchers have previously used to qualitatively sort teeth into dietary
8
9
10 199 groups. However, in the case of some DT measurements, these inferences are based on the
11
12 200 interpretation of patterns arising from uncertain processes; without clarity on precisely which
13
14 201 tooth features are being measured and how these measures directly relate to masticatory
15
16
17 202 function, dental topography is relegated to a black box operation that produces results
18
19
20 203 constrained to analogy and lacking in functional insight. That is, even if the new measurement
21
22 204 seems to identify patterns in teeth, those patterns need to correlate with function to be
23
24
25 205 insightful. In contrast, classic and simpler measurements like SQ have already provided the core
26
27
28 206 ecological insights and analogical frameworks these new DT measurements aim to make more
29
30 207 'objective,' and do so with clear underlying functional rationale. Without a clear correlation
31
32
33 208 with some element of masticatory performance, the new dental topography measurements will
34
35 209 remain hamstrung in their ability to speak to the functional capabilities of unusual occlusal
36
37
38 210 morphologies (such as those encountered in wear series, or in extinct organisms for whom no
39
40 211 straightforward modern analog exists), undermining their core purpose.

42
43 212 A third method relies on appealing to first principles while associating the
44
45
46 213 measurements derived from teeth (e.g., sharpness as assessed with DNE) with the functional
47
48 214 outcomes of their interactions with food materials (i.e., the ability of interdigitating tooth
49
50
51 215 surfaces to reduce the particle size of chewed food). Through a deductive reasoning process
52
53 216 starting with examination of the dental properties supposedly being captured by the various
54
55
56 217 measurements, researchers might then conclude that the results of particular measurements
57
58
59 218 must anticipate certain masticatory outcomes. Deductive logic of this kind, though largely

1
2
3
4 219 theoretical, is still necessary for the attainment of measurement consistency, and for
5
6
7 220 articulating the relationship between the measured features and functional outcomes.
8
9
10 221 Ultimately, to be useful in a dietary ecology context, these highly abstract
11
12 222 measurements of dental morphology should be grounded to masticatory function using all
13
14 223 three of the above stated approaches. They should: [1] correlate with a performance metric, [2]
15
16
17 224 effectively capture observable patterns among study specimens, and [3] offer clear underlying
18
19
20 225 functional rationale(s). Until there is clarity and certainty regarding the value of these
21
22 226 measurements in functional terms (if at all), researchers employing DT measurements should
23
24
25 227 remain skeptical of the biological interpretations arising from any surprising or incongruous
26
27
28 228 dental topography findings. In other words, if the DT measurement values from a particular
29
30 229 taxon do not conform to *a priori* expectations (e.g., molars with apparently blunt cusps yielding
31
32
33 230 surprisingly high values of sharpness), researchers would be better served to question the
34
35 231 measurements themselves (or the protocol for producing them), rather than attempting to
36
37
38 232 rewrite the known feeding ecology of the taxon under consideration.

39
40 233 In this paper, we introduce an important modification to how the dental topography
41
42
43 234 measurement DNE is expressed, by labeling and sorting the surface according to the orientation
44
45
46 235 (concave vs convex) of its curvature. This is operationalized in a revision to the R package
47
48 236 `moLaR` (Pampush et al. 2016b), and is expected to produce a more coherent link between the
49
50
51 237 DNE measurement and functional sharpness of occlusal surfaces. In presenting sign-oriented
52
53
54 238 DNE, we explore four interrelated goals. [1] First, decompose the calculation of DNE and assess
55
56 239 the components' associations with dental performance. As will be shown below, while there is
57
58
59 240 solid rationale to consider DNE the best estimate of *functional* occlusal sharpness among the

1
2
3
4 241 current suite of DT measurements, not all aspects of its final summation can be deductively
5
6
7 242 linked to masticatory performance. In particular, the concave-oriented component of total
8
9
10 243 surface sharpness is likely confounding the link between DNE measurement values and realized
11
12 244 dental performance and should be eliminated from the measurement in future applications. [2]
13
14
15 245 Second, reanalysis of previously published primate dental surfaces will show that the isolated
16
17 246 convex DNE component retains its correlations with diets high in fiber/exoskeleton
18
19
20 247 consumption. The proposed modification to DNE not only better aligns the measure with
21
22 248 current models of chewing mechanics but should also improve its precision since concave, non-
23
24
25 249 masticatory edges are eliminated from the final summation of specimen DNE values. [3] We
26
27
28 250 demonstrate below that this proposed modification to the DNE measurement is non-trivial by
29
30 251 examining great ape (Hominoidea) molars in comparison to other primate teeth. It will be
31
32
33 252 observed that not all primates (let alone mammals generally) possess similar ratios of convex to
34
35 253 concave dental surface curvature, such that the concave surface contribution to the final DNE
36
37
38 254 surface values cannot be dismissed as commonly held 'noise' when making adaptive
39
40
41 255 comparisons or interpretations. Furthermore, we will argue that without convincingly
42
43 256 connecting concave DNE to the same measurement objectives as convex DNE, the comingling
44
45
46 257 of these two components into one value produces functional and interpretive incoherence. [4]
47
48
49 258 Fourth, and finally, we examine the effects and interaction that scaling, scanning, and
50
51 259 processing of teeth into digital surfaces has on the ratio between concave and convex
52
53
54 260 components of DNE values. We will examine whether the differences among the digital
55
56 261 surfaces analyzed here are non-allometric products of the underlying morphology or artifacts of
57
58
59 262 the digitization process for completing the measurements. It is our expectation that these

1
2
3
4
5
6
7
8
9
10
11
12
13
14
15
16
17
18
19
20
21
22
23
24
25
26
27
28
29
30
31
32
33
34
35
36
37
38
39
40
41
42
43
44
45
46
47
48
49
50
51
52
53
54
55
56
57
58
59
60
61
62
63
64
65

263 analyses and alterations to the DNE calculation will make it more consistent and reliable across
264 the varied dental morphologies of mammalian taxa, and guide researchers in applying DNE for
265 meaningful ecological and evolutionary insights.

Methods:

Measurement background and decomposition of Dirichlet normal energy (goal 1)

268 When viewed from first principles (*à la* deductively), not all purported measurements of
269 topographic surface sharpness—a valuable property of teeth to measure given its expected link
270 with the ability to slice through tough or crack-arresting materials (Lucas 2006)—are similarly
271 effective and/or consistent in a dietary ecology framework. Orientation patch count (OPC), for
272 instance, is designed to count the number of ‘breakage sites’¹ on a molar and is coarsely
273 correlated with the proportion of fiber in a species’ diet across broad mammalian groups (Evans
274 et al. 2007). Ecologists have taken this to mean that the count of breakage sites tracks the
275 cutting ability of teeth (e.g., Evans and Janis 2014), since dietary fibers are generally work-
276 limited for break down (Strait 1997; Lucas 2006). That is, fibrous materials need to be cut with
277 continuous application of force, whereas stress-limited materials which will catastrophically fail
278 when enough force is applied. While the comparative analyses seem to demonstrate the
279 efficacy of OPC, considering the calculation of the measurement—which begins by sorting
280 contiguous aspects of the tooth surface according to whichever direction the feature faces
281 within an eight compass directions framework (see Evans et al. 2007; Evans and Janis 2014)—
282 suggests that it is set up to analyze lophodont teeth. In fact, OPC has proven most effective

¹ ‘Breakage sites’ are defined by van der Glas et al. (1992; pg. 105) as “part of the occlusal surface of the post-canine teeth which is suitable for the breaking of particles of a particular size.” Most dental morphologists take this to mean the outward facing crests and cusps of molars.

1
2
3
4
5
6
7
8
9
10
11
12
13
14
15
16
17
18
19
20
21
22
23
24
25
26
27
28
29
30
31
32
33
34
35
36
37
38
39
40
41
42
43
44
45
46
47
48
49
50
51
52
53
54
55
56
57
58
59
60
61
62
63
64
65

283 when deployed in clades possessing lophodont taxa, and it does not seem to correlate with
284 dietary fiber content among clades possessing more basal tribosphenic designs (Pineda-Munoz
285 et al. 2017). One might interpret this to mean that the measurement seems to work when the
286 boundaries between patches are sharp edges associated with crests, but begins to come apart
287 when teeth lack crests, for instance, even a simple hemisphere has an OPC value of eight
288 (because some part of the hemisphere will face each of the 8-compass directions) but at best
289 has only one ‘breakage site’ at the apex of the hemisphere. This limited functional
290 correspondence likely explains the success of the measurement in certain applications (e.g.,
291 Evans et al. 2007; Evans and Janis 2014) while OPC’s use among bunodont dentitions has
292 yielded fewer insights (e.g., Winchester et al. 2014).

293 On the other hand, Dirichlet normal energy (DNE)—even as conventionally
294 implemented—is one of the more promising measurements because of the way it characterizes
295 dental surfaces. DNE is a unitless and directionless, assessment of surface sharpness. It follows
296 that if DNE is indeed measuring sharpness in a functionally meaningful way, then we would
297 expect animals routinely consuming tough foods like fibrous leaves and other plant parts (or
298 insect exoskeletons) to have overall sharper occlusal surfaces—and correspondingly higher DNE
299 values—as has been previously demonstrated with some comparative studies (e.g., Winchester
300 et al. 2014). Furthermore, when DNE is mapped onto a model tooth surface, the areas
301 exhibiting the greatest Dirichlet energy density tend to correspond to the portions of the tooth
302 making functional contact during Phase I occlusion (see chewing mechanics above). Together,
303 these observations suggest that DNE is capturing functionally relevant properties of a dental
304 surface.

1
2
3
4
5
6
7
8
9
10
11
12
13
14
15
16
17
18
19
20
21
22
23
24
25
26
27
28
29
30
31
32
33
34
35
36
37
38
39
40
41
42
43
44
45
46
47
48
49
50
51
52
53
54
55
56
57
58
59
60
61
62
63
64
65

305 The DNE of a surface is estimated with the formula:

$$DNE = \sum e(p) \times area(p) \tag{Eqn (1)}$$

306 where $e(p)$ is the Dirichlet energy density about point p given by the formula:

$$e(p) = \left(\frac{1}{r_a}\right)^2 + \left(\frac{1}{r_b}\right)^2 \tag{Eqn (2)}$$

307 As can be seen from the underlying Dirichlet energy density calculation, sharpness is estimated
308 for each point on the analyzed surface by summing the two squared reciprocal radii of
309 osculating circles (r_a and r_b) found in the planes of principle curvature about each point. Point-
310 based sharpness values are summed over the entire surface to give a ‘total surface’ DNE
311 measure (for visuals and worked example, see SOM of Pampush et al. 2016a).

312 Particularly relevant to the underlying calculations in the DNE measurement is the use
313 of osculating circle radii to assess sharpness. The use of osculating circles appears to be one of
314 the more successful approaches researchers have found to quantify sharpness (e.g., Popowicz
315 and Fortelius 1997; Evans et al. 2005; Hainsworth et al. 2008), a property which has otherwise
316 proven surprisingly difficult to measure (for review see Reilly et al. 2004). In one standout study
317 of knife blades, Hainsworth and colleagues (2008) demonstrated a relationship between
318 osculating circle radii and performance (see also: McCarthy et al. 2010). While controlling for
319 the force involved and the material being stabbed, Hainsworth et al. (2008) measured the
320 osculating circle radii of blade edges before using the knives in a series of stabbing experiments.
321 From their results Hainsworth et al. (2008) note two key findings: First, they show that
322 osculating circle radii (i.e., morphology measurement) are correlated with knife penetration
323 (i.e., performance measurement), meaning that the measurement can be used to predict
324 functionality. The second point their data makes is the *way* the two measurements are

1
2
3
4
5
6
7
8
9
10
11
12
13
14
15
16
17
18
19
20
21
22
23
24
25
26
27
28
29
30
31
32
33
34
35
36
37
38
39
40
41
42
43
44
45
46
47
48
49
50
51
52
53
54
55
56
57
58
59
60
61
62
63
64
65

325 correlated. They show that the smaller the osculating circle radius (i.e., the finer the knife edge)
326 the deeper the stabbing depth—interestingly—in a negative correlation which resembles the
327 formula $y = -\sqrt{x}$ (see Fig. 10 Hainsworth et al. 2008). These results can be algebraically
328 manipulated to present a positive linear correlation between osculating circle radii and stabbing
329 penetration by taking the reciprocal of the radii and squaring them. This mirrors the
330 manipulation occurring within the Dirichlet energy density measurement (Eqn 2) with the minor
331 difference that Dirichlet energy density is measuring sharpness in two dimensions (two
332 orthogonal radii) instead of one. If sharpness is quantified in this manner and summed across
333 all points on the surface, it produces Equation 1 from above. Therefore, one can interpret DNE
334 as a natural surface-wide extension of the osculating circle approach to measuring sharpness.

Examining the underlying DNE calculation provides some insights into the expected
performance of the measurement, with two items particularly worth noting. [1] The
measurement does not account for the orientation of the sharp edge, since an osculating circle
can be placed above or below the surface and simply has to trace the curve of the point. As the
reciprocal radii are always squared to produce the Dirichlet energy density measure, the
positive or negative signs of the radial values are eliminated (Dirichlet energy density is always
expressed as an absolute value). [2] While squaring of the reciprocal radii linearize their
relationship to performance, it also has the mathematical effect of relegating most of the
surface to irrelevance in the final summation. Put differently, in a surface composed of irregular
curvatures (like a tooth with sharp cusps and crests, but relatively gently-curving walls and
basins) a small amount of the surface area accounts for the vast majority of the total DNE value.
In concert, the orientation blindness and the emphasis on relatively small portions of the

1
2
3
4
5
6
7
8
9
10
11
12
13
14
15
16
17
18
19
20
21
22
23
24
25
26
27
28
29
30
31
32
33
34
35
36
37
38
39
40
41
42
43
44
45
46
47
48
49
50
51
52
53
54
55
56
57
58
59
60
61
62
63
64
65

347 surface to define the total DNE value require researchers to be particularly cognizant of what
348 exactly it is they are measuring, especially if they plan to use those results to draw ecological or
349 adaptive inferences.

350 From the perspective of tooth shearing ability, a major flaw in the conventional
351 application of DNE as a measure of surface sharpness is its inability to distinguish concave from
352 convex components of sharpness. If DNE's utility as a dietary signal is derived from its capturing
353 of occlusal sharpness in a *functional* context (as opposed to a strictly morphological
354 assessment), then occlusal sulci, the often deep and sharp grooves on tooth surfaces, may be
355 creating an interpretive problem. As currently implemented, in-folded creases such as occlusal
356 sulci are summed as sharp elements just as are ridges and crests even though the 'sharp'
357 component of these grooves is oriented towards the inner dentine of the tooth. With the
358 current understanding of mastication, it is hard to imagine how deep and sharp sulci could
359 assist in slicing up food. Due to this lack of accounting for sharpness orientation, conventional
360 DNE measurements of tooth surfaces that combine sharp crests with crenulations and/or deep
361 sulci may misinforming functional/adaptive interpretations. During normal mastication, dietary
362 materials are unlikely to make contact with- or be deformed by- the nadirs of the deep occlusal
363 sulci, and in the event that they do, during these interactions they are being 'cupped' not 'split'
364 as they are at cusp tips or along crests and shearing ridges. Thus, when sharp, deep sulci are
365 present to a high degree, scholars may interpret high values of DNE as pointing to elevated cusp
366 and ridge sharpness, when instead the occlusal 'sharpness' measured by DNE is
367 disproportionately derived from inwardly-directed, sharply concave occlusal sulci. This may lead
368 to the understandable misinterpretation that a species is adapted to masticate higher levels of

1
2
3
4
5
6
7
8
9
10
11
12
13
14
15
16
17
18
19
20
21
22
23
24
25
26
27
28
29
30
31
32
33
34
35
36
37
38
39
40
41
42
43
44
45
46
47
48
49
50
51
52
53
54
55
56
57
58
59
60
61
62
63
64
65

369 dietary fiber than its teeth are actually equipped to efficiently process—provided DNE is being
370 used as a proxy for functional masticatory surface sharpness.

371 A simple solution is at hand to better align DNE as a functionally relevant measurement
372 of masticatory morphology: Investigated surfaces can be partitioned into concave and convex
373 components (described below), allowing researchers to disregard the concave aspect of DNE
374 and focus their functional interpretations on the outwardly sharp convex DNE value. The
375 convex component of the DNE summation represents the aspect of the tooth expected to make
376 direct contact with food materials, and therefore actually be used in food breakdown.

377 *Software and data collection*

378 The R package `molAR` is a suite of tools for performing dental topographic analyses
379 (Pampush et al. 2016b). The package allows researchers to measure the following from PLY-
380 format files (McHenry and Bajcsy 2008) that represent dental surfaces: Dirichlet normal energy
381 (DNE), orientation patch count (OPC), orientation patch count rotated (OPCR), surface slope
382 (m), and relief index (RFI). The package also contains tools for performing analyses of
383 measurement accuracy and quality, as well as visualization of these measures on digital surface
384 models. The updated version `molAR` 5.0 contains a modification to the `DNE()` function
385 incorporating a new user-adjustable argument *kappa*, which enables users to set the inflection
386 point for defining the concave versus convex portions of the occlusal surface (for specific details
387 of the calculation, and for an extreme example of sign-oriented DNE applied to a convex-
388 dominated tooth, see Online Resources 1 and 2). The default value of *kappa* is set at 0, meaning
389 that the function will partition the surface into concave and convex portions according to a
390 neutral or zero measurement of curvature. Users can adjust *kappa* anywhere between -2 to 2,

1
2
3
4 391 with negative values biasing the boundary towards concave curvature values, meaning that
5
6
7 392 $\kappa=-1$ will result in a reduced area being defined as concave, while $\kappa=1$ will have an
8
9
10 393 enlarged area of the surface designated as concave. The new DNE() function separately
11
12 394 aggregates the concave and convex contributions to the total DNE value, as well as the surface
13
14
15 395 area measurements, for the analyzed surface. As is standard when applying DNE to dental
16
17 396 surfaces (e.g., Bunn et al. 2011; Winchester et al. 2014; Pampush et al. 2016b), PLY faces with a
18
19
20 397 vertex on the boundary, and those faces with Dirichlet energy densities above the 99.9th-
21
22 398 percentile are excluded from the final DNE summation (though users can adjust these
23
24
25 399 parameters in the `molAR DNE()` function). Therefore, the function otherwise makes no changes
26
27
28 400 to the way DNE is calculated—the total DNE of a surface is constant regardless of the value of
29
30 401 κ —but this novel parameter permits deeper insight into the relative contributions
31
32
33 402 (concave or convex) to total DNE. Additionally, users can adjust κ to isolate the most
34
35 403 concave or convex portions of a surface for more detailed analysis.

38 404 Surfaces derived from dental scans of 234 minimally worn lower second molars (M_2)
39
40
41 405 were analyzed for this study. The sample includes 100 strepsirrhine specimens, 8 tarsiers
42
43 406 specimens (i.e., ‘prosimians;’ 26 total species) and 107 platyrrhine specimens (21 species) from
44
45
46 407 the data set of Winchester et al. (2014), downloaded from *MorphoSource.org* (Figure 1, Online
47
48 408 Resource Table S1; Boyer et al. 2016). These surfaces were combined with unworn lower
49
50
51 409 second molar surfaces of the hominoids *Gorilla gorilla* (N=6), *Pongo pygmaeus* (N=6), and *Pan*
52
53 410 *trogodytes* (N=7) either downloaded from *MorphoSource.org* or from *human-fossil-record.org*
54
55
56 411 (Online Resource Table S1). In preparation for measuring DNE, all the surfaces were processed
57
58
59 412 uniformly following protocols detailed elsewhere (e.g., Pampush et al. 2016a; Spradley et al.

1
2
3
4 413 2017), whereby the M₂ tooth crown was digitally segmented away from adjacent teeth as well
5
6
7 414 as its roots using *Avizo 9.5* (FEI Houston, Hillsboro, OR). Occlusal surface damage was digitally
8
9
10 415 repaired during segmentation. If the damage was so extensive as to obscure the original surface
11
12 416 contours the specimen was discarded. Digital surfaces were generated without smoothing from
13
14
15 417 the segmentation results. After cropping to the enamel cervix, surfaces were simplified and
16
17 418 remeshed to ~10,000 faces, smoothed 20 iterations in *Avizo*, and exported as PLY files for
18
19
20 419 analysis in R following previously published recommendations (Spradley et al. 2017).

22 420 Several different types of data were collected from each of the digitized dental surfaces
23
24
25 421 and specimens. Sign oriented DNE was measured on each dental surface in *molAR 5.0* with the
26
27
28 422 contributions from the concave and convex areas of the tooth partitioned using the default
29
30 423 *kappa* value of 0 (see Online Resource 1 for technical details of curve orientation assignment).
31
32
33 424 The partitioned tooth surface area was also measured. DNE ratio (DNE-R) and surface area ratio
34
35 425 (SA-R) were both calculated as concave portion divided by convex portion. Additional DNE
36
37
38 426 parameters for outlier and boundary exclusion were left at their default values (Pampush et al.
39
40
41 427 2016b). Each of the non-hominoid taxa was assigned into a traditional heuristic dietary category
42
43 428 (i.e., insectivore, folivore, frugivore, etc.) following the same designations used by Winchester
44
45
46 429 et al. (2014) when they originally published these surfaces. Additionally, three different scaling
47
48 430 measures were collected; species mean body mass for all available taxa was recovered from the
49
50
51 431 literature, tooth length was taken directly from the surfaces themselves, and scanning
52
53 432 resolution (in millimeters) was recorded for each specimen.

56 433 To investigate the dietary signal from the isolated convex component of DNE, the
57
58
59 434 Winchester et al. (2014) data set was reanalyzed comparing convex DNE with traditional dietary

1
2
3
4 435 categories using a phylogenetically controlled Markov-chain Monte Carlo sampled generalized
5
6
7 436 linear model (MCMCglmm) through the R package `MCMCglmm` (Hadfield 2010). The advantage
8
9
10 437 of using the `MCMCglmm` rather than a simple phylogenetically controlled least-squares
11
12 438 regression (i.e., PGLS, see Grafen 1989), is that in the former, data entries do not need to be
13
14
15 439 reduced to species averages and instead individual specimen measures can be used as we have
16
17 440 done here.

18
19
20 441 A series of additional `MCMCglmm`s were performed to investigate scaling allometry of
21
22 442 concave DNE and the DNE-R. Logit-transformed DNE-R was compared with log-transformed
23
24
25 443 tooth length, log-transformed body mass, and scanning resolution in models incorporating all
26
27
28 444 taxa, and within each of the taxonomic groupings. In keeping with prior dental topography
29
30 445 studies that have grouped strepsirrhines and tarsiers from this data set together into the
31
32
33 446 ecomorphological (and now systematically defunct) category ‘prosimians’ (Boyer 2008; Bunn et
34
35 447 al. 2011; Winchester et al. 2014), we employ this nomen and compare these taxa with
36
37
38 448 platyrrhines and hominoids. The phylogenetic tree used for these analyses was downloaded
39
40
41 449 from 10k trees (Arnold et al. 2010) and reflects the modern cladistic systematic consensus that
42
43 450 there are two basal clades of primates, Strepsirrhini and Haplorhini, the latter consisting of
44
45
46 451 anthropoids and tarsiers. All `MCMCglmm` analyses employed a sampling rate of 50, a burn-in of
47
48 452 3,000, and were iterated 250,000 times. All `MCMCglmm` posterior distributions were tested for
49
50
51 453 convergence using the R package `coda` (Plummer et al. 2006).

52
53 454 In addition to the `MCMCglmm`s, non-phylogenetically controlled ANOVAs were
54
55
56 455 performed examining logit-transformed DNE-R and SA-R sorted by taxonomic groupings to gain
57
58
59 456 insights into potential grade effects using base R functions (R Core Team 2017). Finally, logit-

1
2
3
4
5
6
7
8
9
10
11
12
13
14
15
16
17
18
19
20
21
22
23
24
25
26
27
28
29
30
31
32
33
34
35
36
37
38
39
40
41
42
43
44
45
46
47
48
49
50
51
52
53
54
55
56
57
58
59
60
61
62
63
64
65

457 transformed DNE-R and SA-R were compared with diet in phylogenetically controlled ANOVAs
458 within prosimians and platyrrhines using the R package `phytools` (Revell 2012).

459 **Results**

460 Summary statistics describing the mean values of DNE, convex DNE, concave DNE,
461 convex surface area, and concave surface area (with $\kappa=0$) are organized by taxonomic
462 group and diet in Table 1. The DNE ratio (DNE-R) and surface area ratio (SA-R)—both defined as
463 concave/convex—are presented in heat-map style in Table 2, illustrating that while the
464 hominoids have much higher DNE-R values, they possess relatively low SA-R values. Pie charts
465 organized by taxonomic group and diet visually present these ratios in Figure 2A and B. All raw
466 data, including the surface files used to perform these calculations are available in Online
467 Resource 3.

468 Examination of convex DNE’s diet-based sorting ability shows (as expected) that
469 insectivores and folivores tend to have higher convex DNE values than those of frugivores and
470 omnivores, reflecting their overall sharper cusps and crests (Table 3). These trends are
471 visualized in the colored histogram in Figure 3, and the differences between conventional (i.e.
472 total) DNE and convex DNE are shown in the box plots of Figure 2C.

473 Multiple MCMCglmm results are presented in Table 4, describing the statistical
474 relationships between DNE-R and two measures of size, tooth length and average species body
475 mass. MCMCglmm models in these analyses employed the entire data set as well as specific
476 examinations of the taxonomic groupings. The overall distributions of tooth length and average
477 species body mass are visualized against logit-transformed DNE-R in Figure 4A and B. Three of
478 these models returned significant correlations: DNE-R is significantly correlated with tooth

1
2
3
4 479 length across all specimens, and DNE-R is also significantly correlated with tooth length within
5
6
7 480 great apes, but not within the other groups. Finally, DNE-R is significantly correlated with
8
9
10 481 average species body mass within great apes, but not within or across the other groups.

11
12 482 Significant correlations exist between DNE-R and scan resolution across all specimens
13
14
15 483 and within great apes, as well as between concave DNE and scan resolution across all
16
17 484 specimens and within apes. Table 5 presents the results of MCMCgIimm analyses comparing
18
19
20 485 scanning resolution with two measures: DNE-R and concave DNE. Like the other set of
21
22
23 486 MCMCgIimm analyses, these use several different specimen partitions—across all specimens,
24
25 487 and then within each of the groupings (i.e., prosimians, platyrrhines, and great apes). The
26
27
28 488 relationship between scan resolution and logit-transformed DNE-R is plotted in Figure 4C, and
29
30 489 between scan resolution and concave DNE in Figure 4D. In both cases, these significant
31
32
33 490 relationships appear to be driven by gorillas, which required much lower resolutions during
34
35 491 scanning due to their significantly larger size than even the other apes.

36
37
38 492 In a *post hoc* analysis aimed at investigating the relationship between scanning
39
40
41 493 resolution against concave DNE and DNE-R, we scanned a single maxillary molar (M^2) of *Pan*
42
43 494 *trogodytes* at three different resolutions (9, 18, and 36 μm), and then subjected the different
44
45
46 495 scans to the previously described processing regime of simplifying, remeshing, and smoothing
47
48 496 to end up with three different $\sim 10,000$ face PLY files. DNE-R (concave/convex) for these
49
50
51 497 surfaces is highest for the 9 μm resolution scan at 0.875, followed by a precipitous drop off to a
52
53
54 498 DNE-R of 0.514 at the 18 μm scale. The 36 μm scan has a DNE-R of 0.431 as the relationship
55
56 499 appears to level-off (see Online Resource 3 for plots and Online Resource Table S2 for raw
57
58
59 500 values). From this analysis it is safe to conclude that as scanning resolution decreases, the

1
2
3
4 501 amount of concave DNE contained in digitized models of teeth decreases much more quickly
5
6
7 502 than does the amount of convex DNE. Thus, if any of the specimens scanned for these analyses
8
9
10 503 would be biased with methodological inflation of concave DNE it would be the specimens
11
12 504 scanned at the finest resolution. Therefore, the inflated concave DNE values observed in these
13
14
15 505 great ape molars in our sample are unlikely to be an artifact of lower scanning resolution.

16
17 506 Conventional ANOVAs comparing logit-transformed DNE-R and surface area ratios
18
19
20 507 across the taxonomic groups indicates significant differences among these groupings (Table 6).
21
22 508 This is suggestive of a grade shift between great apes and the other taxa within this sample.
23
24
25 509 Furthermore, phylogenetically-controlled ANOVAs examining logit-transformed DNE-R and SA-R
26
27
28 510 within the prosimian and platyrrhine groupings show only one significant relationship to diet,
29
30 511 among prosimians and DNE-R. These additional ANOVAs further suggest that the increase in
31
32
33 512 DNE-R and SA-R is not a product of diet, but rather suggests historical contingency in the
34
35 513 *Baupläne* of these primate molars.

36
37
38 514 **Discussion:**

39
40 515 *Utility of convex DNE for studies of dietary ecology (goal 2)*

41
42
43 516 Conventional Dirichlet normal energy is regarded as a proxy for surface sharpness (Bunn
44
45
46 517 et al. 2011; Winchester et al. 2014; Pampush et al. 2016b), a property expected to correlate
47
48 518 with fibrous and tough diets in primates (Kay 1975; Lucas 2006). However, when decomposed
49
50
51 519 and critically assessed for their functional implications, not all components of the conventional
52
53 520 DNE measurement can be deductively associated with a *functionally* sharp occlusal surface (i.e.,
54
55
56 521 a surface consisting of blades that might be expected to interact with and cut food). Notably,
57
58
59 522 concave components of the occlusal surface can consist of very sharp and deep crevices; such

1
2
3
4 523 concave features are oriented towards the enamel dentine junction and would not be expected
5
6
7 524 to directly interact with a food bolus. Obviously, this presents an explanatory challenge to
8
9
10 525 researchers using conventional DNE to ascribe dietary characteristics from occlusal surfaces.
11
12 526 Rather than arguing that concave sulci have a functional shearing role during mastication, a
13
14
15 527 more plausible stance is to argue that concave DNE contributes ‘noise’ when the measurement
16
17 528 is used as to assess a tooth’s shearing ability. Concave ‘noise’ of this kind is likely to play a role
18
19
20 529 to some degree among nearly all mammalian molars, since complex mammalian cheek teeth
21
22 530 are almost always characterized by both crevices and crests. For the continued application of
23
24
25 531 DNE among primates, it is reassuring to note that the isolated convex component of DNE—
26
27
28 532 measured from the portion of the occlusal surface oriented toward food contact—is correlated
29
30 533 with fibrous diets needing masticatory cutting, supporting Winchester et al.’s (2014) general
31
32
33 534 conclusions (Table 3, Figures 2C and 3). The reanalyzed Winchester et al. (2014) data set of
34
35 535 prosimian and platyrrhine primates shows that insectivorous and folivorous taxa from both
36
37
38 536 groups exhibit higher convex DNE values than their more frugivorous or
39
40
41 537 omnivorous/durophagous relatives (Figures 2C and 3). Close inspection of the regions of the
42
43 538 molars that produce the highest levels of convex DNE show that they are associated with
44
45
46 539 ‘shearing crests’ used in Phase I of the chewing power stroke (Figure 5), further underscoring
47
48
49 540 that convex DNE is capturing functionally relevant information. It should be noted however,
50
51 541 that the prosimians and platyrrhines contained in the Winchester et al. (2014) data set all
52
53 542 exhibit fairly similar ratios of convex to concave DNE (DNE-R Table 2). Thus the switch to
54
55
56 543 analyzing only the convex DNE component had little to no effect on the relative arrangement of
57
58
59 544 measured specimen values—and therefore pertinent dietary inferences—of these taxa. Given
60
61
62
63
64
65

1
2
3
4 545 these results, conventional DNE analyses which have previously looked at prosimians,
5
6
7 546 platyrrhines, and other close relatives are unlikely to gain new ecological insights with this
8
9
10 547 revision to the DNE measurement, even if the measure is now more theoretically consistent
11
12 548 with current models of tooth function (e.g., Ledogar et al. 2013; Winchester et al. 2014; López-
13
14 549 Torres et al. 2018; Selig et al. 2019; Selig et al. 2021). However, this new approach does appear
15
16
17 550 to have implications for analyses of great ape molars (see below), and potentially other taxa
18
19
20 551 characterized by different ratios of concave to convex DNE.

22 552 *Taxonomic differences and the functionality of concave DNE (goal 3)*

25 553 In contrast to the measures taken from prosimians and platyrrhines, great ape molars
26
27 554 tend to exhibit large amounts of highly concentrated concave DNE (i.e., DNE arising from the
28
29
30 555 concave areas of the occlusal surface; Table 1, Figure 2A). This concave DNE contribution is
31
32
33 556 particularly striking among apes because of the relatively small amount of surface area it is
34
35 557 derived from (for examples of surfaces see Figures 2A, 2B and 5). In the case of great apes, this
36
37
38 558 concave DNE contribution is likely confounding the interpretive power of the conventional (i.e.,
39
40
41 559 total-surface) DNE measurement (Figure 6) because the sharp edges of these concave features
42
43 560 are oriented inward towards the enamel-dentine junction, and are certainly not being used to
44
45
46 561 shred, slice, or cut food. When the outsized concave contribution to total DNE is included
47
48 562 during dietary interpretation of great apes, they cluster with primate folivores (Figure 2C). Such
49
50
51 563 a finding could be interpreted as indicating that great ape occlusal surfaces are relatively sharp
52
53 564 compared with other primates, and suggestive of adaptation for shearing-based mastication of
54
55
56 565 highly fibrous or mechanically tough diets. However, this interpretation does not square with
57
58
59 566 the ecologically well-characterized great ape diets typically full of fruit, nuts, herbaceous

1
2
3
4 567 vegetation, and occasionally meat (e.g., Watts 1984; Nishihara 1995; Pruetz 2006; Taylor 2006;
5
6
7 568 Kanamori et al. 2010). Mountain gorillas, on the other hand, are known to be highly folivorous
8
9
10 569 (Schaller 1963; Fossey and Harcourt 1977; Watts 1984), but were not analyzed here; our sample
11
12 570 is composed of western lowland gorillas characterized by more frugivorous diets (Doran et al.
13
14
15 571 2002; Doran-Sheehy et al. 2009). When the ape molars are assessed for only convex DNE, their
16
17 572 measures fall out with the convex DNE measurements of the platyrrhines and prosimian species
18
19
20 573 Winchester et al. (2014) labeled as omnivores (Figure 2C). This omnivore designation reflects
21
22 574 not only the reported diversity of great ape diets, but likely the current precision of the DNE
23
24
25 575 measurement when trying to characterize dietary adaptation on generalized occlusal
26
27
28 576 morphologies.

30 577 The preponderance of sharp sulci on ape teeth begs the question as to whether there
31
32
33 578 might be some relationship with tooth function or if their presence is related to how tooth
34
35 579 enamel develops. Regarding the morphogenesis of the ape occlusal sulci (and therefore the
36
37
38 580 measured concave DNE), Butler (1956) noted that sulci normally correspond in position to
39
40
41 581 valleys in the surface of the dentine. He suggested that they may be greatly exaggerated in
42
43 582 depth owing to a localized failure of enamel formation, an epiphenomenon of the restriction of
44
45
46 583 the vascular supply to the ameloblasts lying in the depths of the sulcus. If Butler is correct, deep
47
48
49 584 sulci would be an example of fabrication noise (Seilacher 1973). In keeping with Butler's
50
51 585 (1956) model, for the comparatively thick-enameled primates like *Homo*, *Australopithecus*,
52
53
54 586 *Paranthropus* or *Pongo* (Grine and Martin 1988; Shellis et al. 1998) the deep occlusal sulci are
55
56 587 possibly the spandrellic consequence of the evolution of thicker enamel driven by the need to
57
58
59 588 overcome stresses directed normal to the occlusal plane and/or exposure to dietary abrasives
60
61
62
63
64
65

1
2
3
4 589 and wear (Kay 1981; Vogel et al. 2008; Pampush et al. 2013). In such a scenario, the enamel
5
6
7 590 thickness of the cusps is the principal target of selection and the thickening of the cuspal
8
9
10 591 enamel should prove sufficient by itself to achieve functional competence with or without the
11
12 592 accompanying sulci. However this potential process cannot explain the presence of all great ape
13
14 593 deep occlusal sulci because not all have evolved thickened molar enamel (Molnar and Gantt
15
16
17 594 1977). Indeed, many Miocene apes have thick enamel without deep occlusal sulci (Alba et al.
18
19
20 595 2010). Another complication is the degree to which dentine surface complexity is echoed in the
21
22 596 outer enamel surface, a relationship with considerable variation among primates, and
23
24
25 597 particularly so among the great apes (Skinner et al. 2010). Further research is needed to
26
27
28 598 determine the potential functional value of the highly crenulated occlusal basins often found,
29
30 599 for example, in *Pongo* and the platyrrhine *Chiropotes* (Vogel et al. 2008; Ledogar et al. 2013).
31
32
33 600 Whatever the ultimate cause, our results indicate that the concave DNE contributed from the
34
35 601 sulci and inward crenulations of hominoid molars should not be viewed as tooth sharpness, as
36
37
38 602 it relates to the ability of teeth to cut through tough foods.

39
40 603 The occlusal sulci on hominoid (including human) molars are not necessarily functionless
41
42
43 604 morphogenic byproducts, although as noted above, that remains a distinct possibility. Yet,
44
45
46 605 before applying an abstract and complex measurement like DNE in the study of occlusal sulcus
47
48 606 morphology, it is worth asking some basic questions to better frame ecological hypotheses to
49
50
51 607 consciously avoid the sharpshooter fallacy² (see Evers 2017). What function do the sulci serve

52
53
54
55
56 ² As explained by Evers (2017), the sharpshooter fallacy arises when particular outcomes are assessed without
57 proper context and perceived patterns are erroneously assumed to be linked to some underlying cause. This fallacy
58 is illustrated with a parable about a poor marksman who shoots without aiming at a barn and later paints targets
59 around the bullet holes. Researchers can fall victim to this fallacy if they indiscriminately apply complex
60 measurements like DNE to morphologies without specific expectations for what they are trying to measure.
61
62
63
64
65

1
2
3
4 608 other than to separate the tooth into discrete cusps and crests? How exactly should researchers
5
6
7 609 use a measurement like DNE to functionally assess concavely oriented sulci within their
8
9
10 610 ecological hypothesis? Perhaps the sulci serve as 'stress sinks' during crushing actions, acting in
11
12 611 concert with buttressing features like the 'protostylid' and 'trigonid crest' to protect the non-
13
14 612 renewable enamel from cracks and catastrophic failure as some have speculated (Benazzi et al.
15
16
17 613 2013). If this is the case, then before applying DNE (or any other abstract topographical
18
19
20 614 measurement) it is worth examining what kind of sulcus morphology would best accommodate
21
22 615 this role and how concave DNE might correlate with that morphology. One way to approach
23
24
25 616 this is to use the optimality criterion (Parker and Maynard Smith 1990), which argues that a
26
27
28 617 morphology is well suited to counter particular loading regimes if it evenly distributes stress
29
30 618 throughout the structure, thereby avoiding the production of failure points. It is well known
31
32
33 619 that enamel cracks form from concentrated stress (Lucas 2006; Lucas et al. 2008), and sharp
34
35 620 deep sulci engender stress concentrations during loading (Benazzi et al. 2013). Cracks, even in
36
37
38 621 deep sulci, expose the underlying dentine to bacterial colonization and the development of
39
40
41 622 dental caries. In fact, deep occlusal sulci are associated with dental caries with or without
42
43 623 cracks in the enamel (Brown 1970). All other things being equal, a better morphology for
44
45
46 624 countering masticatory crushing loads would involve parabolic shaped cusps and sulcal basins
47
48 625 which would more evenly distribute stresses (Lucas 2006; Constantino et al. 2011). As this work
49
50
51 626 has shown, sharp deep sulci correlate with high concave DNE values, and thus transitively, high
52
53 627 concave DNE should correlate with the production of large stress concentrations in sulci during
54
55
56 628 heavy masticatory loading. Given the framework of this functional hypothesis, concave DNE
57
58
59 629 should be *negatively* correlated with enabling stress dissipation during hard object feeding.

1
2
3
4 630 Furthermore, if sharp, deep occlusal sulci are stress-sinks for crushing hard foods, then these
5
6
7 631 features should be associated with other adaptations for hard-object feeding like thick enamel.
8
9
10 632 The taxon possessing the largest average concave DNE in our sample is the relatively thin-
11
12 633 enameled *Gorilla gorilla*, not the thick-enameled hard-object feeder *Pongo pygmaeus*
13
14
15 634 (Schwartz 2000), the reverse of expectations under the stress-sink hypothesis.

16
17 635 Considering the above, when applying conventional DNE to a dental surface we find
18
19
20 636 ourselves at something of an interpretive impasse. Convex DNE measures outward facing
21
22 637 sharpness, plausibly linked to cutting ability and correlated with dietary toughness and fiber
23
24
25 638 content, while concave DNE measures inward facing sharpness which is likely engendering
26
27
28 639 stress concentrations that are seemingly maladaptive for crushing loads and have no plausible
29
30 640 functionality for shearing. Given this framing, we see no value in combining these two sources
31
32
33 641 of DNE into a single measurement, since they are likely tracking very different functional (or
34
35 642 even fabricational) consequences of the dental morphology, one directed outward toward the
36
37
38 643 food bolus and the other inward to the internal structure of the tooth. Additionally, it has been
39
40
41 644 shown that concave and convex DNE are not necessarily correlated across taxa, and if
42
43 645 comingled into a single measurement, researchers cannot discern whether they are measuring
44
45
46 646 outward or inward oriented sharpness. Perhaps deep occlusal sulci have some functional role
47
48 647 only realized with sufficient dental wear, but such a hypothesis is yet to be articulated or
49
50
51 648 tested. Until there is some demonstrable functional benefit for sharp concave sulci included in
52
53 649 the functional complex associated with shearing, researchers using DNE as a sharpness proxy to
54
55
56 650 study feeding ecology and adaptation are best advised to disregard concave DNE and focus on
57
58
59 651 the convex DNE component.

1
2
3
4 652 *Effects of scaling and digitization on DNE ratios (goal 4)*

5
6
7 653 While measures of convex DNE align the great apes with other primate omnivores, a
8
9
10 654 central question remains, why do these great ape molars show such radically higher values of
11
12 655 concave DNE and therefore significantly different DNE-R than their prosimian and platyrrhine
13
14
15 656 relatives (Table 2, Figures 2 and 6)? Despite the mathematical proofs indicating that the DNE
16
17 657 measurement is unitless (see Bunn et al. 2011; Pampush et al. 2016a), the size disparity among
18
19
20 658 the taxa of this study naturally point towards two inter-related forms of allometric scaling
21
22 659 concerns: methodological and biological. Methodologically, to produce faithful digital models of
23
24
25 660 their molars, the specimens in this study were necessarily scanned at different resolutions. It is
26
27
28 661 therefore possible that the increased relative amount of concave DNE among great apes is the
29
30 662 byproduct of different scan resolutions. The non-ape teeth used in this study were scanned at a
31
32
33 663 resolution of 10 and 18 μm , but the apes were scanned at lower 23-65 μm resolutions. There
34
35 664 are detectable trends between DNE-R and concave DNE with scan resolution across the entire
36
37
38 665 sample (Table 5, Figures 4), however closer inspection of these results suggests that this
39
40
41 666 relationship is driven by the gorilla sample. Gorillas exhibit not only the largest size of any of the
42
43 667 specimens in the sample, but also exhibit the largest DNE-R values (concave to convex, Table 2).
44
45
46 668 Within only the prosimians and platyrrhines, both of which have specimens scanned at the 10
47
48
49 669 and 18 μm resolutions, there are no differences in the DNE-R or quantities of concave DNE
50
51 670 (Table 5, Figure 4). The findings within the non-ape sample in which some specimens have been
52
53
54 671 scanned at roughly half the resolution of others, suggest that the inflated concave DNE
55
56 672 measures characteristic of great apes are not the result of scanning differences. Moreover, a
57
58
59 673 lower scan resolution should cause features such as narrow crests and sulci to be represented
60
61
62
63
64
65

1
2
3
4 674 as blunter rather than sharper edges on digitized surface models—the reverse of our findings.
5
6
7 675 Indeed, in our *post-hoc* analysis of an upper molar of a chimpanzee scanned at three different
8
9
10 676 resolutions, both convex and concave DNE was observed to decrease with coarser resolutions,
11
12 677 but the concave DNE does so much more dramatically than does the convex DNE component
13
14
15 678 (Online Resource 4).

16
17 679 Having discounted a methodological origin for our observations, we conclude that there
18
19
20 680 is something biologically different about great ape molars apart from their size, which is
21
22 681 producing these concave DNE results. The other size-based analyses presented in Table 4, and
23
24
25 682 Figure 4 support this suggestion. In a pattern very similar to the resolution analyses, when
26
27
28 683 compared with tooth length, DNE-R is significantly correlated across the whole data set as well
29
30 684 as within the apes but not within any other subsets of the specimens (Table 4, Figure 4B). The
31
32
33 685 analyses of species body mass averages against DNE-R (Figure 4A) showed significant
34
35 686 correlation within apes, but not within prosimians, within platyrrhines, or across the specimens
36
37
38 687 generally. Additionally, the non-phylogenetically controlled ANOVAs comparing DNE-R and SA-R
39
40
41 688 among the three groups confirm that apes stand apart from the other primates analyzed here
42
43 689 (Table 6). In concert, these findings suggest that DNE-R results are not the product of scaling
44
45
46 690 problems associated with producing the measurement nor the result of some sort of primate-
47
48 691 wide scaling phenomenon; rather they seem to be related to the biology of great ape dental
49
50
51 692 structure alone. Researchers might speculatively associate the higher levels of concave DNE
52
53 693 found on great ape molars with processes of evolving relatively thicker enamel (Molnar and
54
55
56 694 Gantt 1977), developmental interactions with the underlying dentine surface—which is
57
58
59 695 typically more complex in apes (Skinner et al. 2010)—or to a functional stress-dissipating role
60
61
62
63
64
65

1
2
3
4 696 (Benazzi et al. 2013), but as discussed above, further research is required to explore these
5
6
7 697 hypotheses and their consequences.
8

9
10 698 **Conclusions**

11
12 699 Dirichlet normal energy (DNE) is one of several new and potentially useful dental
13
14 700 topographic measurements with relevance for understanding tooth function and inferring
15
16
17 701 dietary behavior in extinct primates. This study analyzes DNE's ability to provide functionally
18
19
20 702 relevant insights when employed in dietary ecology studies of primate (and mammalian) cheek
21
22 703 teeth. Following the deductive decomposition of the measurement into its concave and convex
23
24
25 704 components, we propose a modification to the DNE measurement whereby the concave and
26
27
28 705 convex portions of the occlusal surface are partitioned into their separate contributions to the
29
30 706 total surface-wide DNE measure. The interpretive consequences of this refinement are
31
32
33 707 explored, and several major conclusions reached: [1] DNE's value is found in its ability to
34
35 708 capture functional properties of occlusal surfaces (specifically the ability to reduce the size of
36
37
38 709 food particles by shearing and/or cutting), and should be employed in the context of *functional*
39
40 710 dietary ecology hypotheses. [2] The value of DNE as a functional signal is undermined by
41
42
43 711 considering the combined concave and convex contributions to total surface-wide DNE. These
44
45
46 712 separate components of occlusal morphology have distinct (and uncorrelated) functional
47
48 713 consequences, the former being associated with the ability of teeth to comminute food and the
49
50
51 714 latter of uncertain significance but possibly related to attenuating internal stresses or an
52
53 715 artifact of enamel growth. Therefore, combining the two produces incoherence in the
54
55
56 716 functional interpretation of DNE values. [3] In the specific case of great apes and (speculatively)
57
58
59 717 other mammals exhibiting similar occlusal features on their molars (e.g., some bears, bunodont
60
61
62
63
64
65

1
2
3
4
5
6
7
8
9
10
11
12
13
14
15
16
17
18
19
20
21
22
23
24
25
26
27
28
29
30
31
32
33
34
35
36
37
38
39
40
41
42
43
44
45
46
47
48
49
50
51
52
53
54
55
56
57
58
59
60
61
62
63
64
65

718 artiodactyls, sea otters etc.), sharply grooved and inwardly oriented sulci or furrows contribute
719 ‘sharpness’ components whose function has not been established and may not be relevant to
720 the ability of the tooth to cut tough foods, and therefore add ‘noise’ to the functional utility of
721 the total DNE signal, potentially misleading inferences about the diet of investigated taxa. [4]
722 Consideration of convex DNE in isolation retains and refines the validity of previous findings
723 regarding relationships between occlusal sharpness and consumption of dietary fiber, whether
724 that be chitinous insect exoskeletons or cellulose plant fiber, while also aligning those taxa with
725 sharply concave surfaces (i.e., great apes) with the functional expectations the measurement
726 was originally intended to reflect. [5] Methodologically, large quantities of concave DNE do not
727 appear to be artifacts of the scanning and digitization process, but rather seem to be derived
728 from something distinct about the morphogenesis of particular mammalian teeth. Given these
729 findings, this refinement to DNE should help researchers using it to bring new insights to
730 dietary-reconstruction debates involving molars with deep occlusal sulci, such as those found
731 among hominins.

732 Dental topography measures offer great promise for bringing new insights to our
733 collective understanding of the function and adaptation of molar teeth, particularly in the
734 integrated context of dental lifespans. However, researchers need to articulate their questions
735 carefully while incorporating the assumptions and capabilities of these abstract quantifications
736 of morphology in their studies, and resist being seduced by the ‘objectivity’ the derived
737 numerical values seem to present. The presented refinement and discussion of DNE here
738 should help researchers effectively and intelligently deploy this measurement, and the other

1
2
3
4 739 dental topography measurements should be similarly explored for improvements and
5
6
7 740 coherence.
8
9
10 741
11
12 742 Acknowledgements
13
14 743 This research was supported by the National Science Foundation Grant Nos. 2018769 and
15
16
17 744 2018779; a Leakey Foundation grant for the project titled “Hominin dental topography in 4D: A
18
19
20 745 novel assessment of diet;” the European research Council (ERC) under the European Union’s
21
22 746 Horizon 2020 research and innovation programme (grant agreement no. 819960), and the Max
23
24
25 747 Planck Society. For access to CT scans of extant apes, we thank the Museum für Naturkunde –
26
27
28 748 Leibniz Institute for Evolution and Biodiversity Science (Frieder Myer and Christiane Funk), the
29
30 749 Max Planck Institute for Evolutionary Anthropology (C. Boesch, J-J. Hublin), and special thanks
31
32
33 750 to Simon Chapple and Mykolas Imbrasas who were involved in directly transferring scans.
34
35 751 Finally, we also thank the editors and two anonymous reviewers whose helpful comments on
36
37
38 752 early versions of this manuscript improved this work immensely. We declare no known conflicts
39
40
41 753 of interest.

42
43 754
44 755 **Figure Captions:**
45
46 756 **Figure 1:** Radial plot of phylogenetic tree used in analyses, downloaded from 10k Trees (Arnold
47 757 et al. 2010). Colored points at end of each tip indicate species’ dietary category. Colored text of
48 758 binomina indicates grouping used for analyses.
49
50 759

51 760 **Figure 2:** A and B summary pie charts showing average convex and concave contributions to
52 761 subsets of the sample. Platyrrhines and prosimians are sorted by dietary categories following
53 762 Winchester et al. (2014). Apes (plotted with red) are grouped according to genus. A illustrate
54 763 convex and concave proportions of surface DNE. B illustrate convex and concave proportions of
55 764 M₂ surface area. Note the significantly larger percentage of concave DNE derived from ape
56 765 molars, despite smaller percentage of concave surface area as compared to the other primates
57 766 analyzed here. C Overlaid boxplots of conventional (i.e., ‘Total’) DNE that incorporates DNE
60 767 from the concave portions of the tooth crown (in faded colors) and convex DNE (in bolder

1
2
3
4
5
6
7
8
9
10
11
12
13
14
15
16
17
18
19
20
21
22
23
24
25
26
27
28
29
30
31
32
33
34
35
36
37
38
39
40
41
42
43
44
45
46
47
48
49
50
51
52
53
54
55
56
57
58
59
60
61
62
63
64
65

768 colors). Prosimians and platyrrhines are sorted by dietary categories following Winchester et al.
769 (2014), while apes are grouped by genus.

770
771
772 **Figure 3:** Histogram of entire dental sample's convex DNE distribution. Colored circles represent
773 individual specimens and their dietary category. Apes are included among omnivores.

774
775
776 **Figure 4:** Scatter plots comparing logit-transformed DNE-R (ratio of concave to convex DNE)
777 with measures of taxon size and scanning resolution. A Log-transformed average species body
778 mass, collected from the literature. B Log-transformed tooth length measured from the digital
779 surfaces. C Logit-transformed DNE ratio (concave/convex) with scanning resolution; D concave
780 DNE alone. The platyrrhines and prosimians were all scanned at either 10 or 18 μm resolutions,
781 whereas apes required lower scanning resolutions due to their larger size.

782
783
784 **Figure 5:** M_2 s models of representative M_2 specimens from each taxonomic grouping, all to the
785 same scale in occlusal and oblique perspectives. Left images in each pair illustrate sign-oriented
786 DNE (scaled consistently among all specimens) in log-scale to improve visualization of surface
787 curvature. Right images in each pair illustrate convex and concave regions of the M_2 surfaces.
788 Note that in contrast to prosimian and platyrrhine folivores and insectivores, these *Pongo* and
789 *Gorilla* M_2 s show both relatively lower, more rounded cusps, and smaller, more discretized
790 concave regions corresponding to grooves and sulci. The narrow nature of these concave
791 regions accounts for the relatively lower concave area observed in ape molars (Figure 2B), but
792 also generates high DNE values (Figure 6).

793
794
795 **Figure 6:** Bar plots showing the relative contribution to total DNE from each face on the surface
796 of the representative specimens illustrated in Figure 5. Face DNE values are ordered from most
797 concave to most convex and colored consistently with the DNE plots in Figure 5. Open circle
798 along x-axis represents the inflection point where surface orientation transitions from concave
799 to convex (i.e., neutral or 'flat' orientation). Pie charts embedded in the plots show the relative
800 contributions to DNE from the concave and convex portions of each surface. Note the relatively
801 steep slopes of the prosimian and platyrrhine concave faces, while the apes show much
802 shallower slopes, indicating the larger number of concave faces making significant contributions
803 to total DNE.

1
2
3
4 805 Alba DM, Fortuny J, Moyà-Solà S. 2010. Enamel thickness in the Middle Miocene great apes
5 806 *Anoiapithecus*, *Pierolapithecus*, and *Dryopithecus*. Proc Biol Sci 277:2237-2245.
6 807 Allen KL, Cooke SB, Gonzales LA, Kay RF. 2015. Dietary inference from upper and lower molar
7 808 morphology in platyrrhine primates. PLoS ONE 10(3):e0118732.
8 809 doi:10.1371/journal.pone.0118732.
9 810 Anthony M, Kay RF. 1993. Tooth form and diet in ateline and alouattine primates: reflections on
10 811 the comparative method. Am J Sci 293A:356-382.
11 812 Arnold C, Matthews LJ, Nunn CL. 2010. The 10kTrees Website: A new online resource for
12 813 primate phylogeny. Evol Anthropol 19:114-118.
13 814 Benazzi S, Nguyen HH, Kullmer O, Hublin JJ. 2013. Unravelling the functional biomechanics of
14 815 dental features and tooth wear. PLoS ONE doi:10.1371/journal.pone.0069990.
15 816 Boyer DM. 2008. Relief index of second mandibular molars is a correlate of diet among
16 817 prosimian primates and other euarchontan mammals. J Hum Evol 55:1118-1137.
17 818 Boyer DM, Gunnell GF, Kaufman S, McGeary T. 2016. MorphoSource - Archiving and sharing 3D
18 819 digital specimen data. Paleont Soc P 22:157-181.
19 820 Brown JP. 1970. Rat molar morphology and dental caries. Caries Res 4:49-55.
20 821 Bunn JM, Boyer DM, Lipman Y, St. Clair EM, Jernvall J, Daubechies I. 2011. Comparing Dirichlet
21 822 normal surface energy of tooth crowns, a new technique of molar shape quantification
22 823 for dietary inference, with previous methods in isolation and in combination. Am J Phys
23 824 Anthropol 145:247-261.
24 825 Butler PM. 1939. Studies of the mammalian dentition—Differentiation of the post-canine
25 826 dentition. Proc Zool Soc Lond 109(1):1-36.
26 827 Butler PM. 1952. The milk-molars of *Perissodactyla*, with remarks on molar occlusion. Proc Zool
27 828 Soc Lond 121(4):777-817.
28 829 Butler PM. 1956. The ontogeny of molar pattern. Biol Rev 31:30-70.
29 830 Butler PM. 1973. Molar wear facets of early Tertiary North American primates. In: Zingesser MR,
30 831 editor. Craniofacial Biology of Primates: Symp Fourth Int Cong Primatology Vol 3: Karger,
31 832 Basel. p 1-27.
32 833 Constantino PJ, Lee JJ-W, Morris D, Lucas PW, Hartstone-Rose A, Lee W-K, Dominy NJ,
33 834 Cunningham A, Wagner M, Lawn BR. 2011. Adaptation to hard-object feeding in sea
34 835 otters and hominins. J Hum Evol 61:89-96.
35 836 Crompton AW. 1971. The origin of the tribosphenic molar. In: Kermack DM, Kermack KA,
36 837 editors. Early Mammals. p 65-87.
37 838 Crompton AW, Hiiemae K. 1969. Functional occlusion in tribosphenic molars. Nature 222:678-
38 839 679.
39 840 Crompton AW, Hiiemae KM. 1967. Molar occlusion and mandibular movements during
40 841 occlusion in the American opossum, *Didelphis marsupialis* L. Zool J Linn Soc 49:21-47.
41 842 Crompton RH, Hiiemae KM. 1970. Molar occlusion and mandibular movements during occlusion
42 843 in the American opossum, *Didelphis marsupialis* L. Zool J Lin Soc 49(1):21-47.
43 844 Damuth J, Janis CM. 2011. On the relationship between hypsodonty and feeding ecology in
44 845 ungulate mammals, and its utility in palaeoecology. Biol Rev 86:733-758.
45 846 Dennis JC, Ungar PS, Teaford MF, Glander KE. 2004. Dental topography and molar wear in
46 847 *Alouatta palliata* from Costa Rica. Am J Phys Anthropol 125(2):152-161.
47
48
49
50
51
52
53
54
55
56
57
58
59
60
61
62
63
64
65

1
2
3
4
5
6
7
8
9
10
11
12
13
14
15
16
17
18
19
20
21
22
23
24
25
26
27
28
29
30
31
32
33
34
35
36
37
38
39
40
41
42
43
44
45
46
47
48
49
50
51
52
53
54
55
56
57
58
59
60
61
62
63
64
65

848 Doran DM, McNeilage A, Greer D, Bocian C, Mehlman P, Shah N. 2002. Western lowland gorilla
849 diet and resource availability: New evidence, cross-site comparisons, and reflections on
850 indirect sampling methods. *Am J Primatol* 58(3):91-116.

851 Doran-Sheehy DM, Mongo P, Lodwick J, Conklin-Brittain NL. 2009. Male and female western
852 gorilla diet: preferred foods, use of fallback resources, and implications for ape versus
853 old world monkey foraging strategies. *Am J Phys Anthropol* 140(4):727—738.

854 Evans AR, Hunter J, Fortelius M, Sanson GD. 2005. The scaling of tooth sharpness in mammals.
855 *Ann Zool Fenn* 42:603-613.

856 Evans AR, Janis CM. 2014. The evolution of high dental complexity in the horse lineage. *Ann*
857 *Zool Fenn* 51:73-79.

858 Evans AR, Wilson GP, Fortelius M, Jernvall J. 2007. High-level of similarity of dentitions in
859 carnivorans and rodents. *Nature* 445:78-81.

860 Evers JLH. 2017. The Texas sharpshooter fallacy. *Human Reproduction* 32(7):1363.

861 Fossey D, Harcourt AH. 1977. Feeding ecology of free-ranging mountain gorillas (*Gorilla gorilla*
862 *beringei*). In: Clutton-Brock TH, editor. *Primate Ecology*. New York: Academic Press. p
863 415-447.

864 Glowacka H, McFarlin SC, Catlett KK, Mudakikwa A, Bromage TG, Cranfield MR, Stoinski TS,
865 Schwartz GT. 2016. Age-related changes in molar topography and shearing crest length
866 in a wild population of montain gorillas from Volcanoes National Park, Rwanda. *Am J*
867 *Phys Anthropol* 160(1):3-15.

868 Grafen A. 1989. The phylogenetic regression. *Phil Trans R Soc Lond B* 326(1233):119-157.

869 Grine FE, Martin LB. 1988. Enamel thickness and development in *Australopithecus* and
870 *Paranthropus*. In: Grine FE, editor. *Evolutionary History of the "Robust"*
871 *Australopithecines*. New York: Aldine de Gruyter.

872 Hadfield JD. 2010. MCMC methods for multi-response generalized linear mixed models: The
873 MCMCglmm R package. *J Statistical Software* 33(2):1-22.

874 Hainsworth SV, Delaney RJ, Ruttly GN. 2008. How sharp is sharp? Towards quantification of the
875 sharpness and penetration ability of kitchen knives used in stabbings. *Int J Legal Med*
876 122(4):289-291.

877 Harper T, Parras A, Rougier GW. 2019. *Reigitherium* (Meridiolestida, Mesungulatoidea) an
878 enigmatic Late Cretaceous mammal from Patagonia, Argentina: morphology, affinities,
879 and dental evolution. *J Mamm Evol* 26:447-478.

880 Hiiemae KM. 1978. Mammalian mastication: a review of the activity of the jaw muscles and
881 movements they produce in chewing. In: Butler PM, Joysey KA, editors. *Development,*
882 *Function and Evolution of Teeth*. London: Academic Press. p 359-398.

883 Hiiemae KM. 1984. Functional aspects of primate jaw morphology. In: Chivers DJ, Hladik CH,
884 editors. *Food Acquisition and Processing in Nonhuman Primates*. London: Acadmeic
885 Press. p 257-281.

886 Hiiemae KM, Kay RF. 1972. Tends in the evolution of primate mastication. *Nature* 240:486-487.

887 Kanamori T, Kuze N, Bernard H, Malim TP, Kohshima S. 2010. Feeding ecology of Bornean
888 orangutans (*Pongo pygmaeus morio*) in Danum Valley, Sabah, Malasia: A 3-year record
889 including two mast fruitings. *Am J Primatol* 71:1-21.

890 Kay RF. 1975. The functional adaptations of primate molar teeth. *Am J Phys Anthropol* 43:195-
891 216.

- 1
2
3
4 892 Kay RF. 1977. The evolution of molar occlusion in Cercopithecidae and early catarrhines. Am J
5 893 Phys Anthropol 46:327-352.
6
7 894 Kay RF. 1981. The nut-crackers – a new theory of the adaptations of the Ramapithecinae. Am J
8 895 Phys Anthropol 55(2):141-151.
9
10 896 Kay RF. 1984. On the use of anatomical features to infer foraging behavior in extinct primates.
11 897 In: Rodman PS, Cant JGH, editors. Adaptations for Foraging in Nonhuman Primates:
12 898 Contributions to an Organismal Biology of Prosimians, Monkeys, and Apes. New York:
13 899 Columbia University Press. p 21-53.
14
15 900 Kay RF, Covert HH. 1984. Anatomy and behavior of extinct primates. In: Chivers DJ, Wood BA,
16 901 Bilsborough A, editors. Food Acquisition and Processing in Primates. New York: Springer
17 902 US. p 467-508.
18
19 903 Kay RF, Hiiemae KM. 1974a. Jaw movement and tooth use in recent and fossil primates. Am J
20 904 Phys Anthropol 40:227-256.
21
22 905 Kay RF, Hiiemae KM. 1974b. Jaw movement and tooth use in recent and fossil primates.
23 906 American Journal of Physical Anthropology 40:227-256.
24
25 907 Kay RF, Hiiemae KM. 1974c. Mastication in Galago crassicaudatus, a cinefluorographic and
26 908 occlusal study. In: Martin RD, Doyle GA, Walker AC, editors. Prosimian Biology. London:
27 909 Duckworth. p 501-530.
28
29 910 Kay RF, Sheine WS. 1979. On the relationship between chitin particle size and digestibility in the
30 911 primate *Galago senegalensis*. Am J Phys Anthropol 43:195-216.
31
32 912 Kay RF, Simons EL. 1980. The ecology of Oligocene African Anthropoidea. Int J Primatol 1:21-37.
33 913 Kirk EC, Simons EL. 2000. Diet of fossil primates from the Fayum depression of Egypt: A
34 914 quantitative analysis of molar shearing. J Hum Evol 40:203-229.
35
36 915 Lanyon JM, Sanson GD. 1986. Koala (*Phascolarctos cinereus*) dentition and nutrition. II.
37 916 Implications of tooth wear in nutrition. J Zool 209:169-181.
38
39 917 Ledogar JA, Winchester JM, St. Clair EM, Boyer DM. 2013. Diet and dental topography in
40 918 pitheciine seed predators. Am J Phys Anthropol 150(1):107-121.
41
42 919 López-Torres S, Selig KR, Prufrock KA, Lin D, Silcox MT. 2018. Dental topographic analysis of
43 920 paromomyid (Plesiadapiformes, Primates) cheek teeth: more than 15 million years of
44 921 changing surfaces and shifting ecologies. Hist Biol 30(1-2):76-88.
45
46 922 Lucas PW. 2006. Dental Functional Morphology: How Teeth Work. Cambridge: Cambridge
47 923 University Press. 355 p.
48
49 924 Lucas PW, Constantino PJ, Wood B, Lawn BR. 2008. Dental enamel as a dietary indicator in
50 925 mammals. BioEssays 30:374-385.
51
52 926 McCarthy CT, Ní Annaidh A, Gilchrist MD. 2010. On the sharpness of straight edge blades in
53 927 cutting soft solids: Part II—Analysis of blade geometry. Eng Fract Mech 77(3):437-451.
54
55 928 McHenry K, Bajcsy P. 2008. An overview of 3D data content, file formats and viewers. Urbana,
56 929 IL: National Center for Supercomputing Applications. 1-21 p.
57
58 930 McLeod MN, Minson DJ. 1969. Sources of variation in the *in vitro* digestibility of tropical
59 931 grasses. Grass and Forage Science 24(3):244-249.
60
61 932 Mills JRE. 1955. Ideal dental occlusion in the primates. Dental Practnr and Dent Rec 6:47-61.
62
63 933 Mills JRE. 1963. Occlusion and Malocclusion of the Teeth of Primates. In: Brothwell DR, editor.
64 934 Dental Anthropology. Oxford: Pergamon Press. p 29-52.
65

1
2
3
4 935 Mills JRE. 1967. A comparison of lateral jaw movements in some mammals from wear facets on
5 936 the teeth. *Archs Oral Biol* 12:645-661.
6
7 937 Mills JRE. 1973. Evolution of Mastication in Primates. In: Montagna W, Zingesser MR, editors.
8 938 Symposia of the Fourth International Congress of Primatology. Basel: S. Karger. p 65-81.
9
10 939 Molnar S, Gantt DG. 1977. Functional implications of primate enamel thickness. *Am J Phys*
11 940 *Anthropol* 46:447-454.
12 941 Nishihara T. 1995. Feeding ecology of Western Lowland gorillas in the Nouabalè-Ndoki National
13 942 Park, Congo. *Primates* 36(2):151-168.
14
15 943 Pampush JD, Duque AC, Burrows BR, Daegling DJ, Kenney WF, McGraw WS. 2013. Homoplasmy
16 944 and thick enamel in primates. *J Hum Evol* 64(3):216-224.
17 945 Pampush JD, Spradley JP, Morse PE, Griffith D, Gladman JT, Gonzales LA, Kay RF. 2018. Adaptive
18 946 wear-based changes in dental topography associated with atelid (Mammalia: Primates)
19 947 diets. *Biol J Linn Soc* 124(4):584-606.
20
21 948 Pampush JD, Spradley JP, Morse PE, Harrington AR, Allen KL, Boyer DM, Kay RF. 2016a. Wear
22 949 and its effects on dental topography measures in howling monkeys (*Alouatta palliata*).
23 950 *Am J Phys Anthropol* 161(4):705-721.
24
25 951 Pampush JD, Winchester JM, Morse PE, Vining AQ, Boyer DM, Kay RF. 2016b. Introducing
26 952 molaR: a new R package for quantitative topographic analyses of teeth (and other
27 953 topographic surfaces). *J Mamm Evol* 23(4):397-412.
28
29 954 Parker GA, Maynard Smith J. 1990. Optimality theory in evolutionary biology. *Nature* 348:27-33.
30 955 Pineda-Munoz S, Lazagabaster IA, Alroy J, Evans AR. 2017. Inferring diet from dental
31 956 morphology in terrestrial mammals. *Method Ecol Evol* 8:481-491.
32
33 957 Plummer M, Best N, Cowles K, Vines K. 2006. CODA: Convergence Diagnosis and Output
34 958 Analysis for MCMC. *R News* 6:7-11.
35
36 959 Popowicz TE, Fortelius M. 1997. On the cutting edge: tooth blade sharpness in herbivorous and
37 960 faunivorous mammals. *Ann Zool Fenn* 34:73-88.
38 961 Pruetz JD. 2006. Feeding ecology of savanna chimpanzees at Fongoli, Senegal. In: Hohmann G,
39 962 Robbins MM, Boesch C, editors. *Feeding Ecology in Apes and Other Primates*.
40 963 Cambridge: Cambridge University Press. p 161-182.
41
42 964 R Core Team. 2017. R: A language and environment for statistical computing. Vienna, Austria: R
43 965 Foundation for Statistical Computing.
44 966 Reilly GA, McCormack BAO, Taylor D. 2004. Cutting sharpness measurement: a critical review.
45 967 *Journal of Materials Processing Technology* 153-154:261-267.
46
47 968 Renaud S, Ledevin R. 2017. Impact of wear and diet on molar row geometry and topography in
48 969 the house mouse. *Arch Oral Biol* 81:31-40.
49
50 970 Revell LJ. 2012. phytools: An R package for phylogenetic comparative biology (and other things).
51 971 *Method Ecol Evol* 3:217-223.
52 972 Ross CF, Iriarte-Diaz J. 2014. What does feeding system morphology tell us about feeding? *Evol*
53 973 *Anthropol* 23(3):105-120.
54
55 974 Ross CF, Iriarte-Diaz J. 2014. What does feeding system morphology tell us about feeding?
56 975 *Evolutionary Anthropology: Issues, News, and Reviews* 23(3):105-120.
57 976 Schaller GB. 1963. *The Mountain Gorilla*. Chicago: University of Chicago Press.
58
59 977 Schwartz GT. 2000. Taxonomic and functional aspects of the patterning of enamel thickness
60 978 distribution in extant large-bodied hominoids. *Am J Phys Anthropol* 111:221-224.

1
2
3
4 979 Seilacher A. 1973. Fabricational noise in adaptive morphology. *Syst Zool* 22(4):451-465.
5 980 Selig KR, Khalid W, Silcox MT. 2021. Mammalian molar complexity follows simple, predictable
6 981 patterns. *P Natl Acad Sci USA* 118(1):e2008850118.
7 982 Selig KR, López-Torres S, Sargis EJ, Silcox MT. 2019. First 3D dental topographic analysis of the
8 983 enamel-dentine junction in non-primate Euarchontans: contribution of the enamel-
9 984 dentine junction to molar morphology. *J Mamm Evol* 26:587-598.
10 985 Sheine WS, Kay RF. 1977. An analysis of chewed food particle size and its relationship to molar
11 986 structure in the primates *Cheirogaleus medius* and *Galago senegalensis* and insectivoran
12 987 *Tupaia glis*. *Am J Phys Anthropol* 47:15-20.
13 988 Sheine WS, Kay RF. 1982. A model for comparison of masticatory effectiveness in primates. *J*
14 989 *Morph* 172:139-149.
15 990 Shellis RP, Beynon AD, Reid DJ, Hiiemae KM. 1998. Variations in molar enamel thickness among
16 991 primates. *J Hum Evol* 35:507-522.
17 992 Skinner MM, Evans AR, Smith T, Jernvall J, Tafforeau P, Kupczik K, Olejniczak AJ, Rosas A,
18 993 Radovčić J, Thackeray JF, Toussaint M, Hublin JJ. 2010. Brief communication:
19 994 Contributions of the enamel-dentin junction shape and enamel deposition to primate
20 995 molar crown complexity. *Am J Phys Anthropol* 142(1):157-163.
21 996 Spradley JP, Pampush JD, Morse PE, Kay RF. 2017. Smooth operator: Observations on the
22 997 effects of different mesh retriangulation protocols on the computation of Dirichlet
23 998 normal energy. *Am J Phys Anthropol* 163(3):94-109.
24 999 Strait S. 1993. Molar morphology and food texture among small-bodied insectivorous
25 1000 mammals. *J Mammal* 74:391-402.
26 1001 Strait SG. 1997. Tooth use and the physical properties of food. *Evol Anthropol* 5(6):199-211.
27 1002 Taylor AB. 2006. Feeding behavior, diet, and the functional consequences of jaw form in
28 1003 orangutans, with implications for the evolution of *Pongo*. *J Hum Evol* 50:377-393.
29 1004 Thierry G, Guy F, Lazzari V. 2017. Investigating the dental toolkit of primates based on food
30 1005 mechanical properties: Feeding action does matter. *Am J Primatol* 79:e22640.
31 1006 Ungar PS. 2004. Dental topography and diets of *Australopithecus afarensis* and early *Homo*. *J*
32 1007 *Hum Evol* 46(5):605-622.
33 1008 Ungar PS, Kay RF. 1995. The dietary adaptations of European Miocene catarrhines. *P Natl Acad*
34 1009 *Sci USA* 92:5479-5481.
35 1010 Ungar PS, M'Kirera F. 2003. A solution to the worn tooth conundrum in primate functional
36 1011 anatomy. *P Natl Acad Sci USA* 100(7):3874-3877.
37 1012 Ungar PS, Williamson M. 2000. Exploring the effects of tooth wear on functional morphology: A
38 1013 preliminary study using dental topographic analysis. *Palaeontol Electron* 3(1):1-18.
39 1014 Venkataraman VV, Glowacka H, Fritz J, Clauss M, Seyoum C, Nguyen N, Fashing PJ. 2014. Effects
40 1015 of dietary fracture toughness and dental wear on chewing efficiency in geladas
41 1016 (*Theropithecus gelada*). *Am J Phys Anthropol* 155:17-32.
42 1017 Vogel ER, van Woerden JT, Lucas PW, Utami Atmoko SS, van Schaik CP, Dominy NJ. 2008.
43 1018 Functional ecology and evolution of hominoid molar enamel thickness: *Pan troglodytes*
44 1019 *schweinfurthii* and *Pongo pygmaeus wurmbii*. *J Hum Evol* 55:60-74.
45 1020 Wall CE, Vinyard CJ, Johnson KR, Williams SH, Hylander WL. 2006. Phase II jaw movements and
46 1021 masseter muscle activity during chewing in *Papio anubis*. *Am J Phys Anthropol* 129:215-
47 1022 224.
48
49
50
51
52
53
54
55
56
57
58
59
60
61
62
63
64
65

1
2
3
4
5
6
7
8
9
10
11
12
13
14
15
16
17
18
19
20
21
22
23
24
25
26
27
28
29
30
31
32
33
34
35
36
37
38
39
40
41
42
43
44
45
46
47
48
49
50
51
52
53
54
55
56
57
58
59
60
61
62
63
64
65

1023 Watts DP. 1984. Composition and variability of mountain gorilla diets in the central Virungas.
1024 Am J Primatol 7:323-356.

1025 Williams SH, Kay RF. 2001. A comparative test of adaptive explanations for hypsodonty in
1026 ungulates and rodents. J Mamm Evol 8(3):207-229.

1027 Winchester JM, Boyer DM, St. Clair EM, Gosselin-Ildari AD, Cooke SB, Ledogar JA. 2014. Dental
1028 topography of platyrrhines and prosimians: Convergence and contrasts. Am J Phys
1029 Anthropol 153:29-44.

1030 Zuccotti LF, Williamson MD, Limp WF, Ungar PS. 1998. Technical Note: Modeling primate
1031 occlusal topography using geographic information systems technology. Am J Phys
1032 Anthropol 107:137-142.

[Click here to view linked References](#)

1
2
3
4
5
6
7
8
9
10
11
12
13
14
15
16
17
18
19
20
21
22
23
24
25
26
27
28
29
30
31
32
33
34
35
36
37
38
39
40
41
42
43
44
45
46
47
48
49
50
51
52
53
54
55
56
57
58
59
60
61
62
63
64
65

Sign-Oriented Dirichlet Normal Energy: Aligning Dental Topography and Dental Function in the R package mo1aR.

James D. Pampush^{1,2}, Paul E. Morse^{3,4}, Edward J. Fuselier⁵, ~~Simon Chapple~~⁶, Matthew [MJ](#). Skinner^{6,7}, and Richard F. Kay^{3,8}

¹Department of Exercise Science, High Point University, High Point, NC 27260

²Department of Physician Assistant Studies, High Point University, High Point, NC 27260

³Department of Evolutionary Anthropology, Duke University, Durham, NC 27708

⁴Florida Museum of Natural History, University of Florida, Gainesville, FL 32611

⁵Department of Mathematical ~~Sciences~~, High Point University, High Point, NC 27260

⁶School of Anthropology and Conservation, University of Kent, Canterbury, UK CT2 7NR

⁷Department of Human Evolution, Max Planck Institute for Evolutionary Anthropology, Leipzig, Germany 04103

⁸Division of Earth and Climate Sciences, Nicholas School, Duke University, Durham NC 27708

Key Words:

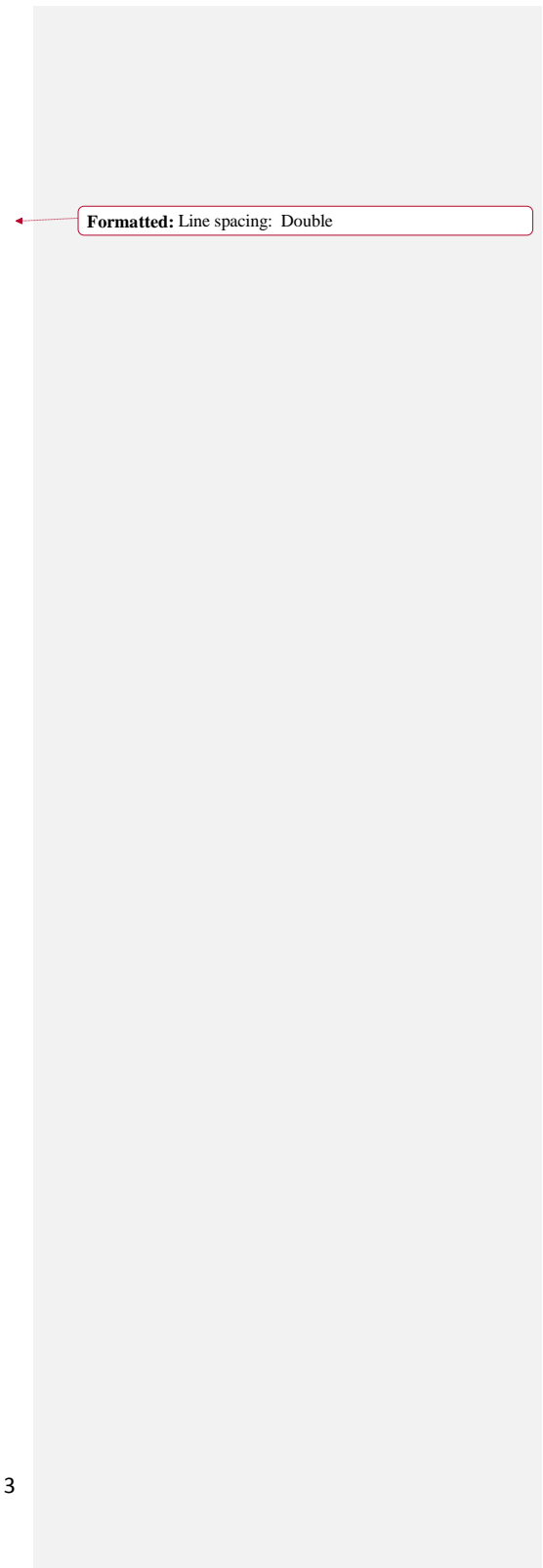
DNE; crenulated enamel; occlusal sulci; enamel furrows; dental sharpness; curvature sign orientation

1
2
3
4
5
6
7
8
9
10
11
12
13
14
15
16
17
18
19
20
21
22
23
24
25
26
27
28
29
30
31
32
33
34
35
36
37
38
39
40
41
42
43
44
45
46
47
48
49
50
51
52
53
54
55
56
57
58
59
60
61
62
63
64
65
66

Abstract

Dirichlet normal energy (DNE) is a dental topography measurement aimed at capturing occlusal sharpness and has shown promise for its ability to sort primate molars according to perceived shearing ability. ~~However, initial applications~~ As initially implemented, ~~of~~ this measurement does not differentiate concave versus convex contributions to surface sharpness. This is problematic because the DNE-signal derived from concave aspects of an occlusal surface measures a sharp ‘edge’ oriented inward towards the enamel dentine junction rather than outward towards food contact. The inclusion of concave DNE in dietary analyses of molars possessing deep occlusal sulci—such as those found among hominoids—inflates the perceived functional sharpness of these teeth. Concave-inflated DNE values can be misleading, being interpreted as indicating that a particular taxon is more adapted for processing fibrous food than is warranted. The modification of the DNE measurement introduced here ‘Sign-oriented DNE’ alleviates this problem by elimination of concave sharpness from analyses, allowing investigations to focus on features of occlusal surfaces plausibly linked to shearing, cutting, or shredding of food materials during Phases I and II of the masticatory power stroke. Convex DNE is just as effective at sorting non-hominoid primate molars into traditional dietary categories as the initial applications of the orientation-blind version of the measurement, and produces more theoretically coherent results from hominoid molars. Focusing on- and improving the connection between measurement and occlusal function will enhance the ability of dental topography to make meaningful contributions to our collective understanding of species’ dietary ecologies.

1
2
3
4
5
6
7
8
9
10
11 67
12
13 68
14
15
16
17
18
19
20
21
22
23
24
25
26
27
28
29
30
31
32
33
34
35
36
37
38
39
40
41
42
43
44
45
46
47
48
49
50
51
52
53
54
55
56
57
58
59
60
61
62
63
64
65



Formatted: Line spacing: Double

1
2
3
4
5
6
7
8
9
10
11 69 **Introduction:**
12
13 70 Originally introduced by Ungar and colleagues (e.g., Zuccotti et al. 1998; Ungar and
14
15 71 Williamson 2000; Ungar and M'Kirera 2003), dental topographic (DT) analysis is a rapidly
16
17 72 growing and diversifying approach ~~to-aimed at~~ studying the morphological, functional, and
18
19 73 adaptive properties of mammalian teeth. Using scanned and digitized dental surfaces, ~~dental~~
20
21 74 ~~topography~~DT measurements quantitatively characterize the surface topography of tooth
22
23 75 crowns. Some prominent DT measurements include orientation patch count (Evans et al. 2007),
24
25 76 relief index (Boyer 2008), average surface slope (Dennis et al. 2004), and the focus of this work:
26
27 77 an estimate of surface sharpness known as Dirichlet normal energy (DNE, Bunn et al. 2011),
28
29 78 ~~that is the focus of this work.~~ DNE and ~~these~~ other DT measurements offer many advantages
30
31 79 over homology-based dental measures, such as shearing quotient (SQ; see: Kay and Simons
32
33 80 1980; Kay 1984; Anthony and Kay 1993; Strait 1993; Ungar and Kay 1995; Kirk and Simons
34
35 81 2000), or crown height (Williams and Kay 2001; Damuth and Janis 2011). Paramount among the
36
37 82 topography measurements' advantages is that they can be applied to teeth without requiring
38
39 83 dental landmarks, as they are quantitative characterizations of whole or partial tooth surfaces.
40
41 84 By side-stepping homology, these measurements can be applied to ~~variably~~ worn teeth (e.g.,
42
43 85 Ungar and Williamson 2000; Ungar and M'Kirera 2003; Pampush et al. 2018)—whose
44
45 86 identifiable landmarks (discrete cusp tips and crests) are often obscured by wear—and ~~permits~~
46
47 87 they permit comparisons among clades that may not share homologous features (e.g., Evans et
48
49 88 al. 2007; Harper et al. 2019; Selig et al. 2021). Generally speaking, DT measurements
50
51 89 overwhelmingly derived their perceived usefulness from their ability to assign objective and
52
53 90 distinct values to teeth supposedly possessing differing dietary adaptations (see below). The
54
55
56
57
58
59
60
61
62
63
64
65

1
2
3
4
5
6
7
8
9
10
11
12
13
14
15
16
17
18
19
20
21
22
23
24
25
26
27
28
29
30
31
32
33
34
35
36
37
38
39
40
41
42
43
44
45
46
47
48
49
50
51
52
53
54
55
56
57
58
59
60
61
62
63
64
65

underlying assumption here is that within the context of mammalian mastication, DT measurements are reflective of the functional abilities of occlusal surfaces. However, uncritical acceptance of this assumption paves the way for misapplication or misinterpretation of DT measurements, particularly when applying them to teeth which are structurally distinct from reference samples. Before more thoroughly evaluating DNE, it is best to review what is understood about dental function and what might be learned about dental morphology from the use of DT measurements.

Associating dental topography and dental function

To date, there has been inconsistent and incomplete efforts made to connect dental topography measurement with models or assessments of tooth function. Stepping away from dental landmarks has hindered the interpretive footing of some ~~of these topography~~DT measurements since modeling of how teeth move and interact during mastication has traditionally been framed around the interaction of various named features presumed to have functional relevance (e.g., cusp apices). ~~That is~~Put differently, dental landmarks provide the essential vocabulary in characterizing exactly which and how ~~and what~~ parts of teeth are brought together to reduce food. Initially, studies of mammalian masticatory movements were based on manipulation of dried skulls and jaws where researchers focused on how the cusps of upper and lower teeth might complement one another (Butler 1952; Mills 1955; 1963; 1967; Butler 1973; Mills 1973). Models of mastication experienced a leap forward with the advent of cinefluorography and its application to mammals and primates exhibiting 'primitive' dental morphologies (Crompton and Hiiemae 1967; Crompton and Hiiemae 1969; Kay and Hiiemae 1974c; Kay and Hiiemae 1974b; Hiiemae 1978). Cinefluorographic recordings showed that

1
2
3
4
5
6
7
8
9
10
11
12
13
14
15
16
17
18
19
20
21
22
23
24
25
26
27
28
29
30
31
32
33
34
35
36
37
38
39
40
41
42
43
44
45
46
47
48
49
50
51
52
53
54
55
56
57
58
59
60
61
62
63
64
65

mastication follows a rhythmic pattern arranged in two basic modes. Cycles in both modes consist of a closing movement in which the lower jaws are approximated, giving way to a power stroke when forces are applied between teeth and food. The two modes of mastication are distinguishable by the degree of occlusion in their power strokes. In the initial mode, once a bite of food is separated and brought into the mouth, the upper and lower cheek teeth are closed around it, coarsely reducing the food, and mixing it with saliva ~~while in preparationing it~~ for finer trituration. This so-called ‘puncture-crushing’ mode does not involve the direct occlusion of molars during its power stroke, and is not tightly constrained by ~~nor particularly~~ informative of ~~the~~ the form-function relationship of molar structure. In a second subsequent ‘chewing’ mode of the power stroke, ~~informally called ‘chewing,’~~ smaller food boluses are tightly pressed between teeth during the power stroke. During this second mode of mastication, precise contacts between the teeth guide and constrain masticatory movements. It is during this second operation of the power stroke—or intercuspal phase (Ross and Iriarte-Diaz 2014)—where molar form becomes relevant to masticatory function. It has been convincingly established that the complementary features of occluding molars work to reduce food while the mandibular molars are brought upward and medially, processing food between the interdigitating cusps (Crompton and Hiiemae 1970; Hiiemae and Kay 1972; Kay and Hiiemae 1974a; Hiiemae 1978; 1984). In primates and other mammals with conservative dental morphology, most or all of the features we identify as ‘shearing’ crests come into occlusion during the initial upward and mediolingually directed ~~first~~ Phase I of the chewing power stroke (Crompton 1971; Kay 1975; 1977). When the teeth are fully interdigitated (in centric occlusion), the upper molar protocones (and hypocones, if present) are seated in the talonid and trigonid

1
2
3
4
5
6
7
8
9
10
11
12
13
14
15
16
17
18
19
20
21
22
23
24
25
26
27
28
29
30
31
32
33
34
35
36
37
38
39
40
41
42
43
44
45
46
47
48
49
50
51
52
53
54
55
56
57
58
59
60
61
62
63
64
65

basins of the lower molars, respectively. Movement into this position is followed by a Phase II movement out of centric occlusion when the surfaces of the talonid and trigonid are dragged across the protocone and hypocone. The degree of force applied between the teeth during the two phases has been debated (Wall et al. 2006; Ross and Iriarte-Diaz 2014), but certainly forces sufficient to produce a distinctive pattern of scratches on planar attrition wear surfaces are achieved during Phase II.

The adaptive significance of mammalian cheek-tooth morphology and mastication is realized with the observation that—not only are the varied forms seemingly optimized to efficiently triturate particular types of food materials—but that the morphological differences fit within the functional expectations for how chewing works (Butler 1939; Kay 1975; Lucas 2006). Early studies of primate molars established that species that feed on different proportions of fruit, leaves, and insects have different molar structure and that common adaptive patterns were acquired independently-convergently in many clades. Primate frugivores have small teeth for their adult body size with relatively short molar crest lengths and crushing-grinding basins (Kay 1975). In contrast, leaf-eating species tend to have larger teeth for their adult body size with longer, sharper molar crests and larger crushing-grinding basins. These observations made with standard dental measurements such as SQ have proven insightful, partly because these measures were intentionally designed to capture functionally relevant information based on models of how teeth interact during mastication, but also because they were explicitly linked to a performance metric: chewed food particle size (Sheine and Kay 1977; Kay and Sheine 1979; Sheine and Kay 1982). Since it is well established that the digestibility (extractable energy), especially of high-fiber plant foods-materials is

1
2
3
4
5
6
7
8
9
10
11
12
13
14
15
16
17
18
19
20
21
22
23
24
25
26
27
28
29
30
31
32
33
34
35
36
37
38
39
40
41
42
43
44
45
46
47
48
49
50
51
52
53
54
55
56
57
58
59
60
61
62
63
64
65

~~materially significantly~~ improved when they are more finely triturated (McLeod and Minson 1969; Sheine and Kay 1977; Kay and Covert 1984), the connection between dental measures and performance allowed researchers to convincingly link their observations to adaptive scenarios (e.g., Kay 1984; Kay and Covert 1984; Anthony and Kay 1993; Kirk and Simons 2000; Allen et al. 2015).

In contrast to standard dental measures, the landmark-free approach which advantages the ~~dental topography~~DT measurements also has the effect of disassociating them from models of tooth function and performance. Topography measurements are abstract expressions of surface-wide dental ~~morphology-form~~ that ~~may segregate different morphologies, but~~ do not necessarily follow a clear functional rationale. To be functionally insightful, measurements used to assess dental morphology must be correlated with performance outcomes—which is best assessed by chewed-food particle size and/or chew strokes or chewing time—but can also be inferred through other means. Otherwise, ~~when detached from homology~~ these measurements are ~~unmoored just~~ abstractions of the morphology, ~~wherein two dramatically different dental Bauplan~~ē with little-to-no clear resemblance might generate identical DT values. Outside of ~~testing explicitly functional hypotheses, it is unclear what value DT measurements would hold in a phylogenetic context since the measures can disguise homoplasy as homology, and while they may still be useful for tracking broad changes or trends in tooth form, they cannot inform adaptive hypotheses or dietary reconstructions without clearer links to the known modes of masticatory function.~~

In practice, there may be three ways of showing or inferring that a ~~topography~~DT measurement is capturing functionally relevant information about dental morphology to prove

- Formatted: Font: Italic
- Formatted: Font: Italic, No underline
- Formatted: No underline

1
2
3
4
5
6
7
8
9
10
11 179 useful in testing adaptive hypotheses. First, a measurement could be experimentally grounded
12
13 180 to a functional effect if it is shown to be correlated with chewed-food particle sizes or chewing
14
15 181 time/chew-stroke count. This must be done using a set of dental morphologies whose disparity
16
17 182 of forms at least encompasses the precision of the measurement, while also controlling for as
18
19 183 many aspects of food material properties and chewing mechanics as possible. As mentioned
20
21 184 above, we believe this to be the ideal approach for ecologically ground-truthing these
22
23 185 measurements, and might be best achieved with a thoughtfully designed experiment on captive
24
25 186 or opportunistically collected dead animals (e.g., Lanyon and Sanson 1986; Renaud and Ledevin
26
27 187 2017). Some progress has been made ~~to address this central issue~~ toward making these
28
29 188 correlations. In gelada baboons (*Theropithecus*), Venkataraman et al. (2014) studied food
30
31 189 toughness, and fecal particle size (FPS, as a surrogate for swallowed particle~~food~~ size) in the
32
33 190 field, matched with age-graded topographic metrics on teeth from museum collections. They
34
35 191 found that FPS is similar between prime and old adults in the wet season, when food fracture
36
37 192 toughness was at a minimum, but older adults were less efficient (higher FPS) than prime
38
39 193 individuals in the dry season when food toughness was highest. They linked these findings to
40
41 194 topography-DT measurements (declining relief index and orientation patch count; DNE was not
42
43 195 measured) in older individuals. But this study did not directly compare occlusal topographies
44
45 196 with FPS, limiting confidence in their results. A number of other studies on primates have
46
47 197 reported on the relationships among FPS, age, and molar topography (Ungar 2004; Glowacka et
48
49 198 al. 2016; Thiery et al. 2017) but none considers all three together, and clear documentation of
50
51 199 the relationship between chewed-particle size and topography measurements has remained
52
53 200 elusive.

1
2
3
4
5
6
7
8
9
10
11 201 A second approach employs the comparative method, where by topography
12
13 202 measurements are inferred to be functionally relevant if they successfully differentiate dental
14
15 203 morphologies. Currently this second technique is how most dental topography measurements
16
17 204 derive their presumed efficacy—via demonstrations of their successful re-sorting of mammalian
18
19 205 teeth into traditional heuristic dietary categories (e.g., insectivore, folivore, frugivore, etc., see:
20
21 206 Evans et al. 2007; Winchester et al. 2014). With the specimens' dietary categories assigned *a*
22
23 207 *priori* on the basis of field observations, these kinds of such studies often show that these
24
25 208 measurements are likely capturing functionally relevant properties of dental surfaces; possibly
26
27 209 even quantifying the same features researchers have previously used to qualitatively sort teeth
28
29 210 into dietary groups. However, in the case of some DT measurements, these inferences are
30
31 211 based on the interpretation of patterns arising from uncertain processes; without clarity on
32
33 212 precisely which ~~at~~ tooth features are being measured and how these measures directly relate to
34
35 213 masticatory function, dental topography is relegated to a black box operation that produces
36
37 214 results constrained to analogy and lacking in functional insight. That is, even if the new
38
39 215 measurement seems to identify patterns in teeth, those patterns need to correlate with
40
41 216 function to be insightful. In contrast, classic and simpler measurements like SQ have already
42
43 217 provided the core ecological insights and analogical frameworks these new topography-DT
44
45 218 measurements aim to make more 'objective,' and do so with clear underlying functional
46
47 219 rationale. Without a clear correlation with some element of masticatory performance, the new
48
49 220 dental topography measurements will remain hamstrung in their ability to speak to the
50
51 221 functional capabilities of unusual occlusal morphologies (such as those encountered in wear
52
53
54
55
56
57
58
59
60
61
62
63
64
65

1
2
3
4
5
6
7
8
9
10
11
12
13
14
15
16
17
18
19
20
21
22
23
24
25
26
27
28
29
30
31
32
33
34
35
36
37
38
39
40
41
42
43
44
45
46
47
48
49
50
51
52
53
54
55
56
57
58
59
60
61
62
63
64
65

series, or in extinct organisms for whom no straightforward modern analog exists),
undermining their core purpose.

A third method relies on appealing to first principles while associating the
measurements derived from teeth (e.g., sharpness as assessed with DNE) with the functional
outcomes of their interactions with food materials (i.e., the ability of interdigitating tooth
surfaces to reduce the particle size of chewed food). Through a deductive reasoning process
starting with examination of the dental properties supposedly being captured by the various
measurements, researchers might then conclude that the results of particular measurements
must anticipate certain masticatory outcomes. Deductive logic of this kind, though largely
theoretical, is still necessary for the attainment of measurement consistency, and for
articulating the relationship between the captured-measured features and functional
outcomes.

Ultimately, to be useful in a dietary ecology context, these highly abstract
measurements of dental morphology should be grounded to masticatory function using all
three of the above stated approaches. They should: [1] correlate with a performance metric, [2]
effectively capture observable patterns among study specimens, and [3] offer clear underlying
functional rationale(s). Until there is clarity and certainty regarding what these various
the
value of these measurements values mean in functional terms (if at all), researchers employing
these kinds of DT measurements should remain skeptical of the biological relevance
interpretations arising from any surprising or incongruous dental topography findings. Put
differently in other words, if the topography-DT measurement values from a particular taxon
do not conform to *a priori* expectations (e.g., molars with apparently blunt cusps yielding

1
2
3
4
5
6
7
8
9
10
11
12
13
14
15
16
17
18
19
20
21
22
23
24
25
26
27
28
29
30
31
32
33
34
35
36
37
38
39
40
41
42
43
44
45
46
47
48
49
50
51
52
53
54
55
56
57
58
59
60
61
62
63
64
65

surprisingly high values of sharpness), researchers would be better served to question the measurements themselves (or the protocol for producing them), rather than attempting to rewrite the known feeding ecology of the taxon under consideration.

In this paper, we introduce an important modification to how the dental topography measurement DNE is expressed, by labeling and sorting the surface according to the orientation (concave vs convex) of its curvature. This is operationalized in a revision to the R package `molar` (Pampush et al. 2016b), and is expected to produce a more functionally coherent link between the DNE measurement and and chewing efficiencyfunctional sharpness of occlusal surfaces. In presenting sign-oriented DNE, we explore four interrelated goals. [1] First, decompose the calculation of DNE and assess the components' associations with dental performance. As will be shown below, while there is solid rationale to consider DNE the best estimate of *functional* occlusal sharpness among the current suite of dental topography-DT measuresmeasurements, not all aspects of its final summation can be deductively linked to masticatory performance. In particular, the concave-orientedconcave-oriented component of total surface sharpness is likely confounding the link between DNE measurement values and realized dental performance and should be eliminated from the measurement in future applications. [2] Second, reanalysis of previously published primate dental surfaces will show that the isolated convex DNE component retains its correlations with diets high in fiber/exoskeleton consumption. The proposed modification to DNE not only better aligns the measure with current models of chewing mechanics but should also improve its precision since concave, non-masticatory edges are eliminated from the final summation of specimen DNE values. [3] We demonstrate below that this proposed modification to the DNE measurement is

1
2
3
4
5
6
7
8
9
10
11 266 non-trivial by examining great ape (Hominoidea) molars in comparison to other primate teeth.
12
13 267 It will be observed that not all primates (let alone mammals generally) possess similar ratios of
14
15 268 convex to concave dental surface curvature, such that the concave surface contribution to the
16
17 269 final DNE surface values cannot be dismissed as commonly held ‘noise’ when making adaptive
18
19 270 comparisons or interpretations. Furthermore, we will argue that without convincingly
20
21 271 connecting concave DNE to the same measurement objectives as convex DNE, the comingling
22
23 272 of these two components into one value produces functional and interpretive incoherence. [4]
24
25 273 Fourth, and finally, we examine the effects and interaction that scaling, scanning, and
26
27 274 processing of teeth into digital surfaces has on the ratio between concave and convex
28
29 275 components of DNE values. We will examine whether the differences among the digital
30
31 276 surfaces analyzed here are non-allometric products of the underlying morphology or artifacts of
32
33 277 the digitization process for completing the measurements. It is our expectation that these
34
35 278 analyses and alterations to the DNE calculation will make it more consistent and reliable across
36
37 279 the varied dental morphologies of mammalian taxa, and guide researchers in applying DNE for
38
39 280 meaningful ecological and evolutionary insights.

40
41 281 **Methods:**

42
43 282 *Measurement background and decomposition of Dirichlet normal energy (goal 1)*

44
45 283 When viewed from first principles (*à la* deductively), not all purported measurements of
46
47 284 topographic surface sharpness—a valuable property of teeth to measure given its expected link
48
49 285 with the ability to slice through tough or crack-arresting materials (Lucas 2006)—are similarly
50
51 286 effective and/or consistent in a dietary ecology framework. Orientation patch count (OPC), for
52
53
54
55
56
57
58
59
60
61
62
63
64
65

1
2
3
4
5
6
7
8
9
10
11
12
13
14
15
16
17
18
19
20
21
22
23
24
25
26
27
28
29
30
31
32
33
34
35
36
37
38
39
40
41
42
43
44
45
46
47
48
49
50
51
52
53
54
55
56
57
58
59
60
61
62
63
64
65

instance, is designed to count the number of 'breakage sites'¹ on a molar and is coarsely correlated with the proportion of fiber in a species' diet across broad mammalian groups (Evans et al. 2007). Ecologists have taken this to mean that the count of breakage sites tracks the cutting ability of teeth (e.g., Evans and Janis 2014), since dietary fibers are generally work-limited for break down (Strait 1997; Lucas 2006). That is, fibrous materials need to be cut with continuous application of force, whereas stress-limited materials which will catastrophically fail when enough force is applied. While the comparative analyses seem to demonstrate the efficacy of OPC, considering the calculation of the measurement—which begins by sorting contiguous aspects of the tooth surface according to whichever direction the feature faces within an eight compass directions framework (see Evans et al. 2007; Evans and Janis 2014) — suggests that it is set up to analyze lophodont teeth. In fact, OPC has proven most effective when deployed in clades possessing lophodont taxa, and it does not seem to correlate with dietary fiber content among clades possessing more basal tribosphenic designs This measurement assumes that the boundaries between differently oriented patches represent cutting 'tools,' and therefore the OPC value is presumed to correlate with the number of cutting components thus estimating the tooth's ability to process fiber. OPC may be effective when employed comparing the highly disparate teeth of certain mammalian orders, but issues of precision and coherence emerge when considering an object like a hemisphere, which possess no cutting ridges yet will produce an OPC measure of eight (Pampush et al. 2016a). These problems, as well as the general performance of the measurement, have led some researchers

¹ 'Breakage sites' are defined by van der Glas et al. (1992; pg. 105) as "part of the occlusal surface of the post-canine teeth which is suitable for the breaking of particles of a particular size." Most dental morphologists take this to mean the outward facing crests and cusps of molars.

1
2
3
4
5
6
7
8
9
10
11
12
13
14
15
16
17
18
19
20
21
22
23
24
25
26
27
28
29
30
31
32
33
34
35
36
37
38
39
40
41
42
43
44
45
46
47
48
49
50
51
52
53
54
55
56
57
58
59
60
61
62
63
64
65

~~to conclude that OPC cannot be used for finer comparisons of dietary ecology or that it loses efficacy when applied to groups with conservative dental morphologies~~ (Pineda-Munoz et al. 2017). One might interpret this to mean that the measurement seems to work when the boundaries between patches are sharp edges associated with crests, but begins to come apart when teeth lack crests, for instance, even a simple hemisphere has an OPC value of eight (because some part of the hemisphere will face each of the 8-compass directions) but at best has only one ‘breakage site’ at the apex of the hemisphere. This limited functional correspondence likely explains the success of the measurement in certain applications (e.g., Evans et al. 2007; Evans and Janis 2014) while OPC’s use among bunodont dentitions has yielded fewer insights (e.g., Winchester et al. 2014).

On the other hand, Dirichlet normal energy (DNE) —even as conventionally implemented— is one of the more promising measurements because of the way it characterizes dental surfaces. DNE is a unitless and directionless, assessment of surface sharpness. It follows that if DNE is indeed measuring sharpness in a functionally meaningful way, then we would expect animals routinely consuming tough foods like fibrous leaves and other plant parts (or insect exoskeletons) to have overall-sharper occlusal surfaces—and correspondingly higher DNE values—as has been previously demonstrated with some comparative studies (e.g., Winchester et al. 2014). Furthermore, when DNE is mapped onto a model tooth surface, the areas exhibiting the greatest Dirichlet energy density tend to correspond to the portions of the tooth making functional contact during Phase I occlusion (see chewing mechanics above). Together, these observations suggest that DNE is capturing functionally a functionally-relevant measurement properties of a dental surface.

1
2
3
4
5
6
7
8
9
10
11
12
13
14
15
16
17
18
19
20
21
22
23
24
25
26
27
28
29
30
31
32
33
34
35
36
37
38
39
40
41
42
43
44
45
46
47
48
49
50
51
52
53
54
55
56
57
58
59
60
61
62
63
64
65

The DNE of a surface is estimated with the formula:

$$DNE = \sum e(p) \times area(p) \quad \text{Eqn (1)}$$

where $e(p)$ is the Dirichlet energy density about point p given by the formula:

$$e(p) = \left(\frac{1}{r_a}\right)^2 + \left(\frac{1}{r_b}\right)^2 \quad \text{Eqn (2)}$$

As can be seen from the underlying Dirichlet energy density calculation, sharpness is estimated for each point on the analyzed surface by summing the two squared reciprocal radii of osculating circles (r_a and r_b) found in the planes of principle curvature about each point. Point-based sharpness values are summed over the entire surface to give a ‘total surface’ DNE measure (for visuals and worked example, see SOM of Pampush et al. 2016a).

Particularly relevant to the underlying calculations in the DNE measurement is the use of osculating circle radii to assess sharpness. The use of osculating circles appears to be one of the more successful approaches researchers have found to quantify sharpness (e.g., Popowicz and Fortelius 1997; Evans et al. 2005; Hainsworth et al. 2008), a property which has otherwise proven surprisingly difficult to measure (for review see Reilly et al. 2004). In one standout study of knife blades, Hainsworth and colleagues (2008) demonstrated a relationship between osculating circle radii and performance (see also: McCarthy et al. 2010). While controlling for the force involved and the material being stabbed, Hainsworth et al. (2008) measured the osculating circle radii of blade edges before using the knives in a series of stabbing experiments. From their results Hainsworth et al. (2008) note two key findings: First, they show that osculating circle radii (i.e., morphology measurement) are correlated with knife penetration (i.e., performance measurement), meaning that the measurement can be used to predict functionality. The second point their data makes is the way the two measurements are

1
2
3
4
5
6
7
8
9
10
11
12
13
14
15
16
17
18
19
20
21
22
23
24
25
26
27
28
29
30
31
32
33
34
35
36
37
38
39
40
41
42
43
44
45
46
47
48
49
50
51
52
53
54
55
56
57
58
59
60
61
62
63
64
65

correlated. They show that the smaller the osculating circle radius (i.e., the finer the knife edge) the deeper the stabbing depth—interestingly—in a negative correlation which resembles the formula $y = -\sqrt{x}$ (see Fig. 10 Hainsworth et al. 2008). These results can be algebraically manipulated to present a positive linear correlation between osculating circle radii and stabbing penetration by taking the reciprocal of the radii and squaring them. This mirrors the manipulation occurring within the Dirichlet energy density measurement (Eqn 2) with the minor difference that Dirichlet energy density is measuring sharpness in two dimensions (two orthogonal radii) instead of one. If sharpness is quantified in this manner and summed across all points on the surface, it produces Equation 1 from above. Therefore, one can interpret DNE as a natural surface-wide extension of the osculating circle approach to measuring sharpness.

Examining the underlying DNE calculation provides some insights into the expected performance of the measurement, with two items particularly worth noting. [1] The measurement does not account for the orientation of the sharp edge, since ~~the an~~ osculating circle can be placed above or below the surface and simply has to trace the curve of the point. As the reciprocal radii are always squared to produce the Dirichlet energy density measure, the positive or negative signs of the radial values are eliminated (Dirichlet energy density is always expressed as ~~an absolute positive~~ value). [2] While squaring of the reciprocal radii linearize their relationship to performance, it also has the mathematical effect of relegating most of the surface to irrelevance in the final summation. Put differently, in a surface composed of irregular curvatures (like a tooth with sharp cusps and crests, but relatively gently-curving walls and basins) a small amount of the surface area accounts for the vast majority of the total DNE value. In concert, the orientation blindness and the emphasis on relatively small portions of the

1
2
3
4
5
6
7
8
9
10
11
12
13
14
15
16
17
18
19
20
21
22
23
24
25
26
27
28
29
30
31
32
33
34
35
36
37
38
39
40
41
42
43
44
45
46
47
48
49
50
51
52
53
54
55
56
57
58
59
60
61
62
63
64
65

surface to define the total DNE value require researchers to be particularly cognizant of what exactly it is they are measuring, especially if they plan to use ~~these~~those results to draw ecological or adaptive inferences.

From the perspective of tooth shearing ability, a major flaw in the ~~current~~conventional application of DNE as a measure of surface sharpness is its inability to distinguish concave from convex components of sharpness. If DNE's utility as a dietary signal is derived from its capturing of occlusal sharpness in a *functional* context (as opposed to a strictly morphological assessment), then occlusal sulci, the often deep and sharp grooves on tooth surfaces, may be creating an interpretive problem. As currently implemented, in-folded creases such as occlusal sulci are summed as sharp elements just as are ridges and crests even though the 'sharp' component of these grooves is oriented towards the inner dentine of the tooth. With the current understanding of mastication, it is hard to imagine how deep and sharp sulci could assist in slicing up food. Due to this lack of accounting for sharpness orientation, conventional DNE measurements of tooth surfaces that combine sharp crests with crenulations and/or deep sulci ~~run the risk of~~may misinforming functional/adaptive interpretations. During normal mastication, dietary materials are unlikely to make contact with or be deformed by the nadirs of the deep occlusal sulci, and in the event that they do, during these interactions they are being 'cupped' not 'split' as they are at cusp tips or along crests and shearing ridges. Thus, when sharp, deep sulci are present to a high degree, scholars may interpret high values of DNE as pointing to elevated cusp and ridge sharpness, when instead the occlusal 'sharpness' measured by DNE is ~~a function of~~disproportionately derived from inwardly-directed, sharply concave occlusal sulci. This may lead to the understandable misinterpretation that a species is

1
2
3
4
5
6
7
8
9
10
11
12
13
14
15
16
17
18
19
20
21
22
23
24
25
26
27
28
29
30
31
32
33
34
35
36
37
38
39
40
41
42
43
44
45
46
47
48
49
50
51
52
53
54
55
56
57
58
59
60
61
62
63
64
65

adapted to masticate higher levels of dietary fiber than its teeth are actually equipped to efficiently process—provided DNE is being used as a proxy for functional masticatory surface sharpness.

A simple solution is at hand to better align DNE as a functionally relevant measurement of masticatory morphology: Investigated surfaces can be partitioned into concave and convex components (described below), ~~and allowing~~ researchers ~~can to~~ disregard the concave aspect of DNE and focus their ~~functional examinations and~~ interpretations on the outwardly sharp convex DNE value. The convex component of the DNE summation represents the aspect of the tooth expected to make direct ~~contact~~ contact with food materials, and therefore actually be used in food breakdown.

Software and data collection

The R package `molAR` is a suite of tools for performing dental topographic analyses (Pampush et al. 2016b). The package allows researchers to measure the following from PLY-format files (McHenry and Bajcsy 2008) that represent dental surfaces: Dirichlet normal energy (DNE), orientation patch count (OPC), orientation patch count rotated (OPCR), surface slope (m), and relief index (RFI). The package also contains tools for performing analyses of measurement accuracy and quality, as well as visualization of these measures on digital surface models. The updated version `molAR 5.0` contains a modification to the `DNE()` function incorporating a new user-adjustable argument *kappa*, which enables users to set the inflection point for defining the concave versus convex portions of the occlusal surface (for specific details of the calculation, and for an extreme example of sign-oriented DNE applied to a convex-dominated tooth, see Online Resources 1 and 2). The default value of *kappa* is set at 0, meaning

1
2
3
4
5
6
7
8
9
10
11 1415 that the function will partition the surface into concave and convex portions according to a
12
13 1416 neutral or zero measurement of curvature. Users can adjust *kappa* anywhere between -2 to 2,
14
15 1417 with negative values biasing the boundary towards concave curvature values, meaning that
16
17 1418 *kappa*=-1 will result in a reduced area being defined as concave, while *kappa*=1 will have an
18
19 1419 enlarged area of the surface designated as concave. The new DNE() function separately
20
21 1420 aggregates the concave and convex contributions to the total DNE value, as well as the surface
22
23 1421 area measurements, for the analyzed surface. As is standard when applying DNE to dental
24
25 1422 surfaces (e.g., Bunn et al. 2011; Winchester et al. 2014; Pampush et al. 2016b), PLY-~~surface~~
26
27 1423 faces with a vertex on the boundary, and those faces with Dirichlet energy densities ~~in~~-above
28
29 1424 the 99.9th-percentile are excluded from the final DNE summation (though users can adjust
30
31 1425 these parameters in the molAR DNE() function). Therefore, the function otherwise makes no
32
33 1426 changes to the way DNE is ~~quantified~~calculated—the total DNE of a surface is constant
34
35 1427 regardless of the value of *kappa*—but this novel parameter permits deeper insight into the
36
37 1428 relative contributions (concave or convex) to total DNE.- Additionally, users can adjust *kappa* to
38
39 1429 isolate the most concave or convex portions of a surface for more detailed analysis.

40
41 1430 Surfaces derived from dental scans of 234 minimally worn lower second molars (M₂)
42
43 1431 were analyzed for this study. The sample includes 100 strepsirrhine specimens, 8 tarsiers
44
45 1432 specimens (i.e., ‘prosimians;’ 26 total species) and 107 platyrrhine specimens (21 species) from
46
47 1433 the data set of Winchester et al. (2014) ~~data set~~, downloaded from *MorphoSource.org* (Figure
48
49 1434 1, Online Resource Table S1; Boyer et al. 2016). These surfaces were combined with unworn
50
51 1435 lower second molar surfaces of the hominoids; *Gorilla gorilla* (N=6), *Pongo pygmaeus* (N=6),
52
53 1436 and *Pan troglodytes* (N=7) either downloaded from *MorphoSource.org* or from *human-fossil-*

1
2
3
4
5
6
7
8
9
10
11 137 *record.org* (Online Resource Table S1). -In preparation for measuring DNE, all the surfaces were
12
13 138 processed uniformly following protocols detailed elsewhere (e.g., Pampush et al. 2016a;
14
15 139 Spradley et al. 2017), whereby the M₂ tooth crown was digitally segmented away from adjacent
16
17 140 teeth as well as ~~the specimen's~~ roots using Avizo 9.5 (FEI Houston, Hillsboro, OR). ~~Q~~Any
18
19 141 occlusal surface damage ~~such as pits, cracks, and spalled enamel was~~ere digitally repaired
20
21 142 during segmentation. If the damage was so extensive as to obscure the original surface
22
23 143 contours the specimen was discarded. Digital surfaces were generated without smoothing from
24
25 144 the segmentation results. After cropping to the enamel cervix, surfaces were simplified and
26
27 145 remeshed to ~10,000 faces, smoothed 20 iterations in *Avizo*, and exported as PLY files for
28
29 146 analysis in R following previously published recommendations (Spradley et al. 2017).

30
31 147 Several different types of data were collected from each of the digitized dental surfaces
32
33 148 and specimens. ~~S~~First, sign-orientedign oriented DNE was measured on each dental surface in
34
35 149 *molAR* 5.0 with the contributions from the concave and convex areas of the tooth partitioned
36
37 150 using the default *kappa* value of 0 (see Online Resource 1 for technical details of curve
38
39 151 orientation assignment). The partitioned tooth surface area was also measured. DNE ratio
40
41 152 (DNE-R) and surface area ratio (SA-R) were both calculated as concave portion divided by
42
43 153 convex portion. Additional DNE parameters for outlier and boundary exclusion were left at their
44
45 154 default values (Pampush et al. 2016b). Each of the non-hominoid taxa was assigned into a
46
47 155 traditional heuristic dietary category (i.e., insectivore, folivore, frugivore, etc.) following the
48
49 156 same designations used by Winchester et al. (2014) when they originally published these
50
51 157 surfaces. Additionally, three different scaling measures were collected; species mean body
52
53 158 mass for all available taxa was recovered from the literature, tooth length was taken directly
54
55
56
57
58
59
60
61
62
63
64
65

1
2
3
4
5
6
7
8
9
10
11
12
13
14
15
16
17
18
19
20
21
22
23
24
25
26
27
28
29
30
31
32
33
34
35
36
37
38
39
40
41
42
43
44
45
46
47
48
49
50
51
52
53
54
55
56
57
58
59
60
61
62
63
64
65

from the surfaces themselves, and scanning resolution (~~in millimeters~~) was recorded for each specimen.

To investigate the dietary signal ~~quality~~ from the isolated convex component of DNE, the Winchester et al. (2014) data set was reanalyzed comparing convex DNE with traditional dietary categories using a phylogenetically controlled Markov-chain Monte Carlo sampled generalized linear model (MCMCgImm) through the R package `MCMCgImm` (Hadfield 2010). The advantage of using the MCMCgImm rather than a simple phylogenetically controlled least-squares regression (i.e., PGLS, see Grafen 1989), is that in the former, data entries do not need to be reduced to species averages and instead individual specimen measures can be used [as we have done here](#).

A series of ~~other additional~~ MCMCgImms were performed to investigate scaling allometry of concave DNE and the ~~DNE-R ratio~~. Logit-transformed ~~DNE-R ratios~~ were compared with log-transformed tooth length, log-transformed body mass, and scanning resolution in models incorporating all taxa, and within each of the taxonomic groupings. In keeping with prior dental topography studies that have grouped strepsirrhines and tarsiers from this data set together into the ecomorphological (and now systematically defunct) category ‘prosimians’ (Boyer 2008; Bunn et al. 2011; Winchester et al. 2014), we employ this ~~moniker-nomen~~ and compare these taxa with platyrrhines and hominoids. The phylogenetic tree used for these analyses was downloaded from 10k trees (Arnold et al. 2010) and reflects the modern cladistic systematic consensus that there are two basal clades of primates, Strepsirrhini and Haplorhini, the latter consisting of anthropoids and tarsiers. All MCMCgImm analyses employed a sampling rate of 50, a burn-in of 3,000, and were iterated 250,000 times.

1
2
3
4
5
6
7
8
9
10
11
12
13
14
15
16
17
18
19
20
21
22
23
24
25
26
27
28
29
30
31
32
33
34
35
36
37
38
39
40
41
42
43
44
45
46
47
48
49
50
51
52
53
54
55
56
57
58
59
60
61
62
63
64
65

All MCMCglmm posterior distributions were tested for convergence using the R package `coda` (Plummer et al. 2006).

In addition to the MCMCglmms, non-phylogenetically controlled ANOVAs were performed examining logit-transformed DNE-R and surface area ratios SA-R sorted by taxonomic groupings to gain insights into potential grade effects using base R functions (R Core Team 2017). Finally, logit-transformed DNE-R and surface area ratios SA-R were compared with diet in phylogenetically controlled ANOVAs within prosimians and platyrrhines using the R package `phytools` (Revell 2012).

Results

Summary statistics describing the mean values of DNE, convex DNE, concave DNE, convex surface area, and concave surface area (with $\kappa=0$) are organized by taxonomic group and diet in Table 12. The DNE ratio (DNE-R) and surface area ratios (SA-R)—both (defined as concave/convex—) are presented in heat-map style in Table 23, illustrating that while the hominoids have much higher DNE-ratio-values, they possess relatively low concave to convex surface area ratios SA-R values. Pie charts organized by taxonomic group and diet visually present these ratios in Figure 2A and B. All raw data, including the surface files used to perform these calculations are available in Online Resource 3.

Examination of convex DNE's diet-based sorting ability shows (as expected) that insectivores and folivores tend to have higher convex DNE values than those of frugivores and omnivores, reflecting their overall sharper cusps and crests (Table 34). These trends are visualized in the colored histogram in Figure 33, and the differences between conventional (i.e. total) DNE and convex DNE are shown in the box plots of Figure 2C4.

1
2
3
4
5
6
7
8
9
10
11
12
13
14
15
16
17
18
19
20
21
22
23
24
25
26
27
28
29
30
31
32
33
34
35
36
37
38
39
40
41
42
43
44
45
46
47
48
49
50
51
52
53
54
55
56
57
58
59
60
61
62
63
64
65

Multiple MCMCglmm results are presented in Table [45](#), describing the statistical relationships between DNE-[R-ratio](#) and two measures of size, tooth length and average species body mass. MCMCglmm models in these analyses employed the entire data set as well as specific examinations of the taxonomic groupings. The overall distributions of tooth length and average species body mass are visualized against logit-transformed DNE-[R-ratio](#) in Figure [4A](#) and [B5](#). Three of these models returned significant correlations: DNE-[R-ratio](#) is significantly correlated with tooth length across all specimens, and DNE-[R-ratio](#) is also significantly correlated with tooth length within great apes, but not within the other groups. Finally, DNE-[R-ratio](#) is significantly correlated with average species body mass within great apes, but not within or across the other groups.

Significant correlations exist between DNE-[R-ratio](#) and scan resolution across all specimens and within great apes, as well as between concave DNE and scan resolution across all specimens and within apes. Table [56](#) presents the results of MCMCglmm analyses comparing scanning resolution with two measures: DNE-[R-ratio](#) and concave DNE. Like the other set of MCMCglmm analyses, these use several different specimen partitions—across all specimens, and then within each of the groupings (i.e., prosimians, platyrrhines, and great apes). The relationship between scan resolution and logit-transformed DNE-[R-ratio](#) is plotted in Figure [4C6A](#), and between scan resolution and concave DNE in Figure [4D6B](#). In both cases, these significant relationships appear to be driven by gorillas, which required much lower resolutions during scanning due to their significantly larger size than even the other apes.

In a *post hoc* analysis aimed at investigating the relationship between scanning resolution ~~and against~~ concave DNE ~~and /~~ DNE-[ratio-R](#), we scanned a single maxillary molar (M^2)

1
2
3
4
5
6
7
8
9
10
11
12
13
14
15
16
17
18
19
20
21
22
23
24
25
26
27
28
29
30
31
32
33
34
35
36
37
38
39
40
41
42
43
44
45
46
47
48
49
50
51
52
53
54
55
56
57
58
59
60
61
62
63
64
65

of *Pan troglodytes* at three different resolutions (9, 18, and 36 μm), and then subjected the different scans to the previously described processing regime of simplifying, remeshing, and smoothing to end up with three different $\sim 10,000$ face PLY files. The DNE-ratio-R (concave/convex) for these surfaces is highest for the 9 μm resolution scan at 0.875, followed by a precipitous drop off to a DNE-ratio-R of 0.514 at the 18 μm scale. The 36 μm scan has a DNE-ratio-R of 0.431 as the relationship appears to level-off (see Online Resource 3 for plots and Online Resource Table S2 for raw values). From this analysis it is safe to conclude that as scanning resolution decreases, the amount of concave DNE contained in digitized models of teeth decreases much more quickly than does the amount of convex DNE. Thus, if any of the specimens scanned for these analyses would be biased with methodological inflation of concave DNE it would be the specimens scanned at the finest resolution. Therefore, the inflated concave DNE values observed in these great ape molars in our sample are unlikely to be an artifact of lower scanning resolution.

Conventional ANOVAs comparing logit-transformed DNE-R and surface area ratios across the taxonomic groups indicates significant differences among these groupings (Table 67). This is suggestive of a grade shift between great apes and the other taxa within this sample. Furthermore, phylogenetically-controlled ANOVAs examining logit-transformed DNE-R and surface area ratios SA-R within the prosimian and platyrrhine groupings show only one significant relationship to diet, among prosimians and DNE-R-ratio. These additional ANOVAs further suggest that the increase in DNE-R and surface area ratios SA-R is not a product of diet, but rather suggests historical contingency in the *Bbaupläne* of these primate molars.

Discussion:

1
2
3
4
5
6
7
8
9
10
11 547 *Utility of convex DNE for studies of dietary ecology (goal 2)*
12
13 548 Conventional Dirichlet normal energy is regarded as a proxy for surface sharpness (Bunn
14
15 549 et al. 2011; Winchester et al. 2014; Pampush et al. 2016b), a property expected to correlate
16
17 550 with fibrous and tough diets in primates (Kay 1975; Lucas 2006). However, when decomposed
18
19 551 and critically assessed for their functional implications, not all components of the conventional
20
21 552 DNE measurement can be deductively associated with a *functionally* sharp occlusal surface (i.e.,
22
23 553 a surface consisting of blades that might be expected to interact with and cut food). Notably,
24
25 554 concave ~~aspects-components~~ of the occlusal surface ~~sometimes-culminate-in~~ can consist of very
26
27 555 sharp and deep crevices; ~~however, such the sharp edge of these~~ concave features ~~is-are~~
28
29 556 oriented towards the enamel dentine junction and would not be expected to directly interact
30
31 557 with a food bolus. Obviously, this presents an explanatory challenge to researchers using
32
33 558 conventional DNE to ascribe dietary characteristics from occlusal surfaces. Rather than arguing
34
35 559 that concave sulci have a functional shearing role during mastication, a more plausible stance is
36
37 560 to argue that concave DNE contributes ‘noise’ when the -measurement is used as to assess a
38
39 561 tooth’s shearing ability. Concave ‘noise’ of this kind is likely to play a role to some degree
40
41 562 among nearly all mammalian molars, since complex mammalian cheek teeth are almost always
42
43 563 characterized by ~~concave-both crevices~~ and ~~convex-components~~ crests. For the continued
44
45 564 application of DNE among primates, it is reassuring to note that the isolated convex component
46
47 565 of DNE—measured from the portion of the occlusal surface oriented toward food contact—is
48
49 566 correlated with fibrous diets needing masticatory cutting, supporting Winchester et al.’s (2014)
50
51 567 general conclusions (Table 34, Figures 2C and 34). The reanalyzed Winchester et al. (2014) data
52
53 568 set of prosimian and platyrrhine primates shows that insectivorous and folivorous taxa from

1
2
3
4
5
6
7
8
9
10
11
12
13
14
15
16
17
18
19
20
21
22
23
24
25
26
27
28
29
30
31
32
33
34
35
36
37
38
39
40
41
42
43
44
45
46
47
48
49
50
51
52
53
54
55
56
57
58
59
60
61
62
63
64
65

both groups exhibit higher convex DNE values than their more frugivorous or omnivorous/durophagous relatives (Figures 2C3 and 34). Close inspection of the regions of the molars that produce the highest levels of convex DNE show that they are associated with 'shearing crests' used in Phase I of the chewing power stroke (Figure 57), further underscoring that convex DNE is capturing functionally relevant information. It should be noted however, that the prosimians and platyrrhines contained in the Winchester et al. (2014) data set all exhibit fairly similar ratios of convex to concave DNE ratios (DNE-R Table 23). Thus the switch to analyzing only the convex DNE component had little to no effect on the relative arrangement of measured specimen values—and therefore pertinent dietary inferences—of these taxa. Given these results, conventional DNE analyses which have previously looked at prosimians, platyrrhines, and other close relatives are unlikely to gain new ecological insights with this revision to the DNE measurement, even if the measure is now more theoretically consistent with current models of tooth function (e.g., Ledogar et al. 2013; Winchester et al. 2014; López-Torres et al. 2018; Selig et al. 2019; Selig et al. 2021). However, this new approach does appear to have implications for analyses of great ape molars (see below), and potentially other taxa characterized by different ratios of concave to convex DNE.

Taxonomic differences and the functionality of concave DNE (goal 3)

In contrast to the measures taken from prosimians and platyrrhines, great ape molars tend to exhibit large amounts of highly concentrated concave DNE (i.e., DNE arising from the concave areas of the occlusal surface; Table 13, Figure 2A). This concave DNE contribution is particularly striking among apes because of the relatively small amount of surface area it is derived from (for examples of surfaces see Figures 2A, 2B and 57). ~~That is, as compared to the~~

1
2
3
4
5
6
7
8
9
10
11 591 ~~prosimians and platyrrhines analyzed in this work, these great apes tend to have much lower~~
12
13 592 ~~percentages of their total occlusal surface area in concave orientation (Table 3).~~ In the case of
14
15 593 great apes, this concave DNE contribution is likely confounding the interpretive power of the
16
17 594 conventional (i.e., total-surface) DNE measurement (~~Figure 6, Figure 8) since because~~ the sharp
18
19 595 edges of these concave features are oriented inward towards the enamel-dentine junction, and
20
21 596 are certainly not being used to shred, slice, or cut food ~~materials~~. When the outsized concave
22
23 597 contribution to total DNE is included during dietary interpretation of great apes, they cluster
24
25 598 with ~~folivorous-primate folivores (or insectivorous) primates~~ (Figure 2C4). Such a finding could
26
27 599 be interpreted as indicating that great ape occlusal surfaces are relatively sharp compared with
28
29 600 other primates, and suggestive of adaptation for shearing-based mastication of highly fibrous or
30
31 601 mechanically tough diets. However, this interpretation does not square with the ecologically
32
33 602 well-characterized great ape diets typically full of fruit, nuts, ~~meat, and~~ herbaceous vegetation,
34
35 603 ~~and occasionally meat~~ (e.g., Watts 1984; Nishihara 1995; Pruett 2006; Taylor 2006; Kanamori et
36
37 604 al. 2010). Mountain gorillas, on the other hand, are known to be highly folivorous (Schaller
38
39 605 1963; Fossey and Harcourt 1977; Watts 1984), but were not analyzed here; our sample is
40
41 606 composed of western lowland gorillas characterized by more frugivorous diets (Doran et al.
42
43 607 2002; Doran-Sheehy et al. 2009). When the ape molars are assessed for only convex DNE, their
44
45 608 measures fall out with the convex DNE measurements of the platyrrhines and prosimian
46
47 609 ~~specimens-species~~ Winchester et al. (2014) labeled as omnivores (Figure 2C5). This omnivore
48
49 610 designation reflects not only the reported diversity of great ape diets, but likely the current
50
51 611 precision of the DNE measurement when trying to characterize dietary adaptation on
52
53 612 generalized occlusal morphologies.
54
55
56
57
58
59
60
61
62
63
64
65

1
2
3
4
5
6
7
8
9
10
11 613 The preponderance of sharp sulci on ape teeth begs the question as to whether there
12
13 614 might be some relationship with tooth function or if their presence is related to how tooth
14
15 615 enamel develops. Regarding the morphogenesis of the ape occlusal sulci (and therefore the
16
17 616 measured concave DNE), Butler (1956) noted that sulci normally correspond in position to
18
19 617 valleys in the surface of the dentine. He suggested that they may be greatly exaggerated in
20
21 618 depth owing to a localized failure of enamel formation, an epiphenomenon of the restriction of
22
23 619 the vascular supply to the ameloblasts lying in the depths of the sulcus. If Butler is correct, deep
24
25 620 sulci would be an example of fabricational noise (Seilacher 1973). In keeping with Butler's
26
27 621 (1956) model, for the comparatively thick-enameled primates like hominins-Homo,
28
29 622 Australopithecus, Paranthropus or Pongo (Grine and Martin 1988; Shellis et al. 1998) the deep
30
31 623 occlusal sulci are possibly the spandrellic consequence of the evolution of thicker enamel driven
32
33 624 by the need to overcome stresses directed normal to the occlusal plane and/or exposure to
34
35 625 dietary abrasives and wear (Kay 1981; Vogel et al. 2008; Pampush et al. 2013). In such a
36
37 626 scenario, the enamel thickness of the cusps is the principal target of selection and the
38
39 627 thickening of the cuspal enamel should prove sufficient by itself to achieve functional
40
41 628 competence with~~out~~ or without the accompanying sulci. However this potential process cannot
42
43 629 explain the presence of all great ape deep occlusal sulci because not all have evolved thickened
44
45 630 molar enamel (Molnar and Gantt 1977). Indeed, many Miocene apes have thick enamel without
46
47 631 deep occlusal sulci (Alba et al. 2010). Another complication is the degree to which dentine
48
49 632 surface complexity is echoed in the outer enamel surface, a relationship with considerable
50
51 633 variation among primates, and particularly so among the great apes (Skinner et al. 2010).
52
53 634 Further research is needed to determine the potential functional value of the highly crenulated
54
55
56
57
58
59
60
61
62
63
64
65

1
2
3
4
5
6
7
8
9
10
11 635 occlusal basins often found, for example, in *Pongo* and [the platyrrhine](#) *Chiropotes* (Vogel et al.
12
13 636 2008; Ledogar et al. 2013). Whatever the ultimate cause, our results indicate that the concave
14
15 637 DNE contributed from the sulci and inward crenulations of hominoid molars should not be
16
17 638 ~~conflated-viewed as with~~ tooth sharpness, as it relates to the ability of teeth to cut through
18
19 639 tough foods.

20
21 640 The occlusal sulci on hominoid (including human) molars are not necessarily functionless
22
23 641 morphogenic byproducts, although as noted above, that remains a distinct possibility. Yet,
24
25 642 before applying an abstract and complex measurement like DNE in the study of occlusal sulcus
26
27 643 morphology, it is worth asking some basic questions to better frame ecological hypotheses to
28
29 644 consciously avoid the sharpshooter fallacy² (see Evers 2017). What function do the sulci serve
30
31 645 other than to separate the tooth into discrete cusps and crests? How exactly should researchers
32
33 646 use a measurement like DNE to functionally assess concavely oriented sulci within their
34
35 647 ecological hypothesis? Perhaps the sulci serve as ‘stress sinks’ during crushing actions, acting in
36
37 648 concert with buttressing features like the ‘protostylid’ and ‘trigonid crest’ to protect the non-
38
39 649 renewable enamel from cracks and catastrophic failure as some have speculated (Benazzi et al.
40
41 650 2013). If this is the case, then before applying DNE (or any other abstract topographical
42
43 651 measurement) it is worth examining what kind of sulcus morphology would best accommodate
44
45 652 this role and how concave DNE might correlate with that morphology. One way to approach
46
47 653 this is to use the optimality criterion (Parker and Maynard Smith 1990), which argues that a

50
51 ² As explained by Evers (2017), the sharpshooter fallacy arises when particular outcomes are assessed without
52 proper context and perceived patterns are erroneously assumed to be linked to some underlying cause. This fallacy
53 is illustrated with a parable about a poor marksman who shoots without aiming at a barn and later paints targets
54 around the bullet holes. Researchers can fall victim to this fallacy if they indiscriminately apply complex
55 measurements like DNE to morphologies without specific expectations for what they are trying to measure.

1
2
3
4
5
6
7
8
9
10
11 654 morphology is well suited to counter particular loading regimes if it evenly distributes stress
12
13 655 throughout the structure, thereby avoiding the production of failure points. It is well known
14
15 656 that enamel cracks form from concentrated stress (Lucas 2006; Lucas et al. 2008), and sharp
16
17 657 deep sulci engender stress concentrations during loading (Benazzi et al. 2013). Cracks, even in
18
19 658 deep sulci, expose the underlying dentine to bacterial colonization and the development of
20
21 659 dental caries. In fact, deep occlusal sulci are associated with dental caries with or without
22
23 660 cracks in the enamel (Brown 1970). All other things being equal, a better morphology for
24
25 661 countering masticatory crushing loads would involve parabolic shaped cusps and sulcal basins
26
27 662 which would more evenly distribute stresses (Lucas 2006; Constantino et al. 2011). As this work
28
29 663 has shown, sharp deep sulci correlate with high concave DNE values, and thus transitively, high
30
31 664 concave DNE should correlate with the production of large stress concentrations in sulci during
32
33 665 heavy masticatory loading. Given the framework of this functional hypothesis, concave DNE
34
35 666 should be *negatively* correlated with countering-enabling stress dissipation during hard object
36
37 667 feeding. Furthermore, if sharp, deep occlusal sulci are stress-sinks for crushing hard foods, then
38
39 668 these features should be associated with other adaptations for hard-object feeding like thick
40
41 669 enamel. The taxon possessing the largest average concave DNE in our sample is the relatively
42
43 670 thin-enameled *Gorilla gorilla*, not the thick-enameled hard-object feeder *Pongo pygmaeus*
44
45 671 (Schwartz 2000), producing an incoherent functional complex the reverse of expectations under
46
47 672 the is-hypothesis stress-sink hypothesis.

48
49 673 Considering the above, when applying conventional DNE to a dental surface we find
50
51 674 ourselves at something of an interpretive impasse. Convex DNE measures outward facing
52
53 675 sharpness, plausibly linked to cutting ability and correlated with dietary toughness and fiber
54
55
56
57
58
59
60
61
62
63
64
65

1
2
3
4
5
6
7
8
9
10
11
12
13
14
15
16
17
18
19
20
21
22
23
24
25
26
27
28
29
30
31
32
33
34
35
36
37
38
39
40
41
42
43
44
45
46
47
48
49
50
51
52
53
54
55
56
57
58
59
60
61
62
63
64
65

content, while concave DNE measures inward facing sharpness which is likely engendering stress concentrations that are seemingly maladaptive for crushing loads and have no plausible functionality for shearing. Given this framing, we see no value in combining these two sources of DNE into a single measurement, since they are likely tracking very different functional (or even fabricational) consequences of the dental morphology, one directed outward toward the food bolus and the other inward to the internal structure of the tooth. Additionally, it has been shown that concave and convex DNE are not necessarily correlated across taxa, and if comingled into a single measurement, researchers ~~have no idea~~cannot discern whether they are measuring outward or inward oriented sharpness (~~Figure 8~~). Perhaps deep occlusal sulci have some functional role only realized with sufficient dental wear, but such a hypothesis is yet to be articulated or tested. Until there is some demonstrable functional benefit for sharp concave sulci included in the functional complex associated with shearing, researchers using DNE as a sharpness proxy to study feeding ecology and adaptation are best advised to disregard concave DNE and focus on the convex DNE component.

Effects of scaling and digitization on DNE ratios (goal 4)

While measures of convex DNE align the great apes with other primate omnivores, a central question remains, why do these great ape molars show such radically higher values of concave DNE and therefore significantly different ~~DNE-R-ratios~~ than their prosimian and platyrrhine relatives (Table 23, Figures 2 and 68)? Despite the mathematical proofs indicating that the DNE measurement is unitless (see Bunn et al. 2011; Pampush et al. 2016a), the size disparity among the taxa of this study naturally point towards two inter-related forms of allometric scaling concerns: methodological and biological. Methodologically, to produce

1
2
3
4
5
6
7
8
9
10
11
12
13
14
15
16
17
18
19
20
21
22
23
24
25
26
27
28
29
30
31
32
33
34
35
36
37
38
39
40
41
42
43
44
45
46
47
48
49
50
51
52
53
54
55
56
57
58
59
60
61
62
63
64
65

faithful digital models of their molars, the specimens in this study were necessarily scanned at different resolutions. It is therefore possible that the increased relative amount of concave DNE among great apes is the byproduct of different scan resolutions. The non-ape teeth used in this study were scanned at a resolution of 10 and 18 μm , but the apes were scanned at lower 23–65 μm resolutions. There are detectable trends between DNE ratio-R and concave DNE with scan resolution across the entire sample (Table 56, Figures 46), however closer inspection of these results suggests that this relationship is driven by the gorilla sample. Gorillas exhibit not only the largest size of any of the specimens in the sample, but also exhibit the largest DNE ratio-R values (concave to convex, Table 23). Within only the prosimians and platyrrhines, both of which have specimens scanned at the 10 and 18 μm resolutions, there are no differences in the DNE ratio-R or quantities of concave DNE (Table 56, Figure 46). The findings within prosimians and platyrrhines the non-ape sample in, of which some specimens have been scanned at roughly half the resolution of others in the sample, suggest that the inflated concave DNE measures characteristic of great apes are not the result of scanning differences. This interpretation is further supported by the theoretical premise Moreover, a that lower scan resolution should cause features such as narrow crests and sulci to be represented as blunter rather than sharper edges on digitized surface models—the reverse of our findings. Indeed, in our *post-hoc* analysis of an upper chimp of a chimpanzee scanned at three different resolutions, both convex and concave DNE was observed to decrease with coarser resolutions, but the concave DNE does so much more dramatically than does the convex DNE component (Online Resource 4).

1
2
3
4
5
6
7
8
9
10
11 1719 Having discounted a methodological origin for our observations, we conclude that there
12
13 1720 is something biologically different about great ape molars apart from their size, which is
14
15 1721 producing these concave DNE results. The other size-based analyses presented in Table 45, and
16
17 1722 Figure 45 support this suggestion. In a pattern very similar to the resolution analyses, when
18
19 1723 compared with tooth length, DNE-R-ratio is significantly correlated across the whole data set as
20
21 1724 well as within the apes but not within any other subsets of the specimens (Table 45, Figure
22
23 1725 45B). The analyses of species body mass averages against DNE-R-ratio (Figure 45A) showed
24
25 1726 significant correlation within apes, but not within prosimians, within platyrrhines, or across the
26
27 1727 specimens generally. Additionally, the non-phylogenetically controlled ANOVAs comparing
28
29 1728 DNE-R and surface-area-ratios SA-R among the three groups confirm that apes stand apart from
30
31 1729 the other primates analyzed here (Table 67). In concert, these findings suggest that the DNE-R
32
33 1730 ratio results are not the product of scaling problems associated with producing the
34
35 1731 measurement nor the result of some sort of primate-wide scaling mechanism phenomenon;
36
37 1732 rather they are a phenomenon exclusive seem to be related to the biology of great ape dental
38
39 1733 structure alone. Researchers might speculatively associate the higher levels of concave DNE
40
41 1734 found on great ape molars with processes of evolving relatively thicker enamel (Molnar and
42
43 1735 Gantt 1977), developmental interactions with the underlying dentine surface—which is
44
45 1736 typically more complex in apes (Skinner et al. 2010)—or to a functional stress-dissipating role
46
47 1737 (Benazzi et al. 2013), but as discussed above, further research is required to explore these
48
49 1738 hypotheses and their consequences.

50 1739 **Conclusions**

51
52
53
54
55
56
57
58
59
60
61
62
63
64
65

1
2
3
4
5
6
7
8
9
10
11 740 Dirichlet normal energy (DNE) is one of several new and potentially useful dental
12
13 741 topographic measurements with relevance for understanding tooth function and inferring
14
15 742 dietary behavior in extinct primates. This study analyzes DNE's ability to provide functionally
16
17 743 relevant insights when employed in dietary ecology studies of primate (and mammalian) cheek
18
19 744 teeth. Following the deductive decomposition of the measurement into its concave and convex
20
21 745 components, we propose a modification to the DNE measurement whereby the concave and
22
23 746 convex portions of the occlusal surface are partitioned into their separate contributions to the
24
25 747 total surface-wide DNE measure. The interpretive consequences of this refinement are
26
27 748 explored, and several major conclusions ~~can be drawn~~reached: [1] DNE's value is found in its
28
29 749 ability to capture functional properties of occlusal surfaces (specifically the ability to reduce the
30
31 750 size of food particles by shearing and/or cutting), and should be employed in the context of
32
33 751 *functional* dietary ecology hypotheses. [2] The value of DNE as a functional signal is undermined
34
35 752 by considering the combined concave and convex contributions to total surface-wide DNE ~~as~~
36
37 753 ~~has been practiced in prior studies~~. These separate components of occlusal morphology have
38
39 754 distinct (and uncorrelated) functional consequences, the former being associated with the
40
41 755 ability of teeth to comminute food and the latter of uncertain significance but possibly related
42
43 756 to attenuating internal stresses or an artifact of enamel growth. Therefore, combining the two
44
45 757 produces incoherence in the functional interpretation of DNE values. [3] In the specific case of
46
47 758 great apes and (speculatively) other mammals exhibiting similar occlusal features on their
48
49 759 molars (e.g., some bears, ~~pigs~~bunodont artiodactyls, sea otters etc.), sharply grooved and
50
51 760 inwardly oriented sulci or furrows contribute 'sharpness' components ~~that are not~~whose
52
53 761 functionally has not been established and may not be relevant to the ability of the tooth to cut
54
55
56
57
58
59
60
61
62
63
64
65

1
2
3
4
5
6
7
8
9
10
11 762 tough foods, and therefore add ‘noise’ to the functional utility of the total DNE signal,
12
13 763 potentially misleading ~~ascriptions inferences about the~~ diet of investigated taxa. [4]
14
15 764 Consideration of convex DNE in isolation retains and refines the validity of previous findings
16
17 765 regarding relationships between occlusal sharpness and consumption of dietary fiber, whether
18
19 766 that be chitinous insect / exoskeletons or cellulose plant fiber, while also aligning those taxa
20
21 767 with sharply concave surfaces (i.e., great apes) with the functional expectations the
22
23 768 measurement was originally intended to reflect. [5] Methodologically, ~~large~~ quantities of
24
25 769 concave DNE do not appear to be artifacts of the scanning and digitization process, but rather
26
27 770 seem to be derived from something distinct about the morphogenesis of particular mammalian
28
29 771 teeth. Given these findings, this refinement to DNE should help researchers using it to bring
30
31 772 new insights to dietary-reconstruction debates involving molars with deep occlusal sulci, such
32
33 773 as those found among hominins.

34
35 774 Dental topography measures offer great promise for bringing new insights to our
36
37 775 collective understanding of the function and adaptation of molar teeth, particularly in the
38
39 776 integrated context of dental lifespans. However, researchers need to articulate their questions
40
41 777 carefully while incorporating the assumptions and capabilities of these abstract quantifications
42
43 778 of morphology in their studies, and resist being seduced by the ‘objectivity’ the derived
44
45 779 numerical values seem to present. The presented refinement and discussion of DNE here
46
47 780 should help researchers effectively and intelligently deploy this measurement, and the other
48
49 781 dental topography measurements should be similarly explored for improvements and
50
51 782 coherence.

52 783

53
54
55
56
57
58
59
60
61
62
63
64
65

1
2
3
4
5
6
7
8
9
10
11
12
13
14
15
16
17
18
19
20
21
22
23
24
25
26
27
28
29
30
31
32
33
34
35
36
37
38
39
40
41
42
43
44
45
46
47
48
49
50
51
52
53
54
55
56
57
58
59
60
61
62
63
64
65

Acknowledgements

This research was supported by the National Science Foundation Grant Nos. 2018769 and 2018779; a Leakey Foundation grant for the project titled “Hominin dental topography in 4D: A novel assessment of diet;” the European research Council (ERC) under the European Union’s Horizon 2020 research and innovation programme (grant agreement no. 819960), and the Max Planck Society. For access to CT scans of extant apes, we thank the Museum für Naturkunde – Leibniz Institute for Evolution and Biodiversity Science (Frieder Myer and Christiane Funk), and the Max Planck Institute for Evolutionary Anthropology (C. Boesch, J-J. Hublin), and special thanks to Simon Chapple and Mykolas Imbrasas who were involved in directly transferring scans. Finally, we also thank the editors (D. Croft) and two anonymous reviewers for their whose helpful comments on early versions of this manuscript improved this work immensely. We declare no known conflicts of interest.

Figure Captions:

Figure 1: Radial plot of phylogenetic tree used in analyses, downloaded from 10k Trees (Arnold et al. 2010). Colored points at end of each tip indicate species’ dietary category. Colored text of binomina indicates grouping used for analyses.

Figure 2: A and B sSummary pie charts showing average convex and concave contributions to subsets of the sample. Platyrrhines and prosimians are sorted by dietary categories following Winchester et al. (2014). Apes (plotted with red) are grouped according to genus. Upper plots A illustrate convex and concave proportions of surface DNE. Lower plots B illustrate convex and concave proportions of M₂ surface area. Note the significantly larger percentage of concave DNE derived from ape molars, despite smaller percentage of concave surface area as compared to the other primates analyzed here. C Overlaid boxplots of conventional (i.e., ‘Total’) DNE that incorporates DNE from the concave portions of the tooth crown (in faded colors) and convex DNE (in bolder colors). Prosimians and platyrrhines are sorted by dietary categories following Winchester et al. (2014), while apes are grouped by genus.

Figure 3: Histogram of entire dental sample’s convex DNE distribution. Colored circles represent individual specimens and their dietary category. Apes are included among omnivores.

1
2
3
4
5
6
7
8
9
10
11
12
13
14
15
16
17
18
19
20
21
22
23
24
25
26
27
28
29
30
31
32
33
34
35
36
37
38
39
40
41
42
43
44
45
46
47
48
49
50
51
52
53
54
55
56
57
58
59
60
61
62
63
64
65

Figure 4: Overlaid boxplots of conventional (i.e., 'Total') DNE that incorporates DNE from the concave portions of the tooth crown (in faded colors) and convex DNE (in bolder colors). Prosimians and platyrrhines are sorted by dietary categories following Winchester et al. (2014), while apes are grouped by genus.

Figure 45: Scatter plots comparing logit-transformed DNE-R-ratio (ratio of concave to convex DNE) with measures of taxon size and scanning resolution. (A) Log-transformed average species body mass, collected from the literature. (B) Log-transformed tooth length measured from the digital surfaces. (C) Logit-transformed DNE ratio (concave/convex) with scanning resolution; (D) concave DNE alone. The platyrrhines and prosimians were all scanned at either 10 or 18 μm resolutions, whereas apes required lower scanning resolutions due to their larger size.

Figure 6: Scatter plots comparing decompositions of the DNE measurement with scan resolution. (A) Logit-transformed DNE ratio (concave/convex) with scanning resolution; (B) concave DNE alone. The platyrrhines and prosimians were all scanned at either 10 or 18 μm resolutions, whereas apes required lower scanning resolutions due to their larger size.

Figure 57: M₂s models of representative M₂ specimens from each taxonomic grouping, all to the same scale in occlusal and oblique perspectives. Left images in each pair illustrate sign-oriented DNE (scaled consistently among all specimens) in log-scale to improve visualization of surface curvature. Right images in each pair illustrate convex and concave regions of the M₂ surfaces. Note that in contrast to prosimian and platyrrhine folivores and insectivores, these *Pongo* and *Gorilla* M₂s show both relatively lower, more rounded cusps, and smaller, more discretized concave regions corresponding to grooves and sulci. The narrow nature of these concave regions accounts for the relatively lower concave area observed in ape molars (Figure 2B), but also generates high DNE values (Figure 68).

Figure 68: Bar plots showing the relative contribution to total DNE from each face on the surface of the representative specimens illustrated in Figure 57. Face DNE values are ordered from most concave to most convex and colored consistently with the DNE plots in Figure 57. Open circle along x-axis represents the inflection point where surface orientation transitions from concave to convex (i.e., neutral or 'flat' orientation). Pie charts embedded in the plots show the relative contributions to DNE from the concave and convex portions of each surface. Note the relatively steep slopes of the prosimian and platyrrhine concave faces, while the apes show much shallower slopes, indicating the larger number of concave faces making significant contributions to total DNE.

1
2
3
4
5
6
7
8
9
10
11
12
13
14
15
16
17
18
19
20
21
22
23
24
25
26
27
28
29
30
31
32
33
34
35
36
37
38
39
40
41
42
43
44
45
46
47
48
49
50
51
52
53
54
55
56
57
58
59
60
61
62
63
64
65

Alba DM, Fortuny J, Moyà-Solà S. 2010. Enamel thickness in the Middle Miocene great apes *Anoiapithecus*, *Pierolapithecus*, and *Dryopithecus*. *Proc Biol Sci* 277:2237-2245.

Allen KL, Cooke SB, Gonzales LA, Kay RF. 2015. Dietary inference from upper and lower molar morphology in platyrrhine primates. *PLoS ONE* 10(3):e0118732. doi:0118710.0111371/journal.pone.0118732.

Anthony M, Kay RF. 1993. Tooth form and diet in ateline and alouattine primates: reflections on the comparative method. *Am J Sci* 293A:356-382.

Arnold C, Matthews LJ, Nunn CL. 2010. The 10kTrees Website: A new online resource for primate phylogeny. *Evol Anthropol* 19:114-118.

Benazzi S, Nguyen HH, Kullmer O, Hublin JJ. 2013. Unravelling the functional biomechanics of dental features and tooth wear. *PLoS ONE* doi:DOI 10.1371/journal.pone.0069990.

Boyer DM. 2008. Relief index of second mandibular molars is a correlate of diet among prosimian primates and other euarchontan mammals. *J Hum Evol* 55:1118-1137.

Boyer DM, Gunnell GF, Kaufman S, McGeary T. 2016. MorphoSource - Archiving and sharing 3D digital specimen data. *Paleont Soc P* 22:157-181.

Brown JP. 1970. Rat molar morphology and dental caries. *Caries Res* 4:49-55.

Bunn JM, Boyer DM, Lipman Y, St. Clair EM, Jernvall J, Daubechies I. 2011. Comparing Dirichlet normal surface energy of tooth crowns, a new technique of molar shape quantification for dietary inference, with previous methods in isolation and in combination. *Am J Phys Anthropol* 145:247-261.

Butler PM. 1939. Studies of the mammalian dentition—Differentiation of the post-canine dentition. *Proc Zool Soc Lond* 109(1):1-36.

Butler PM. 1952. The milk-molars of Perissodactyla, with remarks on molar occlusion. *Proc Zool Soc Lond* 121(4):777-817.

Butler PM. 1956. The ontogeny of molar pattern. *Biol Rev* 31:30-70.

Butler PM. 1973. Molar wear facets of early Tertiary North American primates. In: Zingesser MR, editor. *Craniofacial Biology of Primates: Symp Fourth Int Cong Primatology Vol 3: Karger, Basel.* p 1-27.

Constantino PJ, Lee JJ-W, Morris D, Lucas PW, Hartstone-Rose A, Lee W-K, Dominy NJ, Cunningham A, Wagner M, Lawn BR. 2011. Adaptation to hard-object feeding in sea otters and hominins. *J Hum Evol* 61:89-96.

Crompton AW. 1971. The origin of the tribosphenic molar. In: Kermack DM, Kermack KA, editors. *Early Mammals.* p 65-87.

Crompton AW, Hiiemae K. 1969. Functional occlusion in tribosphenic molars. *Nature* 222:678-679.

Crompton AW, Hiiemae KM. 1967. Molar occlusion and mandibular movements during occlusion in the American opossum, *Didelphis marsupialis* L. *Zool J Linn Soc* 49:21-47.

Crompton RH, Hiiemae KM. 1970. Molar occlusion and mandibular movements during occlusion in the American opossum, *Didelphis marsupialis* L. *Zool J Lin Soc* 49(1):21-47.

Damuth J, Janis CM. 2011. On the relationship between hypsodonty and feeding ecology in ungulate mammals, and its utility in palaeoecology. *Biol Rev* 86:733-758.

Dennis JC, Ungar PS, Teaford MF, Glander KE. 2004. Dental topography and molar wear in *Alouatta palliata* from Costa Rica. *Am J Phys Anthropol* 125(2):152-161.

1
2
3
4
5
6
7
8
9
10
11
12
13
14
15
16
17
18
19
20
21
22
23
24
25
26
27
28
29
30
31
32
33
34
35
36
37
38
39
40
41
42
43
44
45
46
47
48
49
50
51
52
53
54
55
56
57
58
59
60
61
62
63
64
65

Doran DM, McNeilage A, Greer D, Bocian C, Mehlman P, Shah N. 2002. Western lowland gorilla diet and resource availability: New evidence, cross-site comparisons, and reflections on indirect sampling methods. *Am J Primatol* 58(3):91-116.

Doran-Sheehy DM, Mongo P, Lodwick J, Conklin-Brittain NL. 2009. Male and female western gorilla diet: preferred foods, use of fallback resources, and implications for ape versus old world monkey foraging strategies. *Am J Phys Anthropol* 140(4):727—738.

Evans AR, Hunter J, Fortelius M, Sanson GD. 2005. The scaling of tooth sharpness in mammals. *Ann Zool Fenn* 42:603-613.

Evans AR, Janis CM. 2014. The evolution of high dental complexity in the horse lineage. *Ann Zool Fenn* 51:73-79.

Evans AR, Wilson GP, Fortelius M, Jernvall J. 2007. High-level of similarity of dentitions in carnivorans and rodents. *Nature* 445:78-81.

Evers JLH. 2017. The Texas sharpshooter fallacy. *Human Reproduction* 32(7):1363.

Fossey D, Harcourt AH. 1977. Feeding ecology of free-ranging mountain gorillas (*Gorilla gorilla beringei*). In: Clutton-Brock TH, editor. *Primate Ecology*. New York: Academic Press. p 415-447.

Glowacka H, McFarlin SC, Catlett KK, Mudakikwa A, Bromage TG, Cranfield MR, Stoinski TS, Schwartz GT. 2016. Age-related changes in molar topography and shearing crest length in a wild population of montain gorillas from Volcanoes National Park, Rwanda. *Am J Phys Anthropol* 160(1):3-15.

Grafen A. 1989. The phylogenetic regression. *Phil Trans R Soc Lond B* 326(1233):119-157.

Grine FE, Martin LB. 1988. Enamel thickness and development in *Australopithecus* and *Paranthropus*. In: Grine FE, editor. *Evolutionary History of the "Robust" Australopithecines*. New York: Aldine de Gruyter.

Hadfield JD. 2010. MCMC methods for multi-response generalized linear mixed models: The MCMCglmm R package. *J Statistical Software* 33(2):1-22.

Hainsworth SV, Delaney RJ, Rutty GN. 2008. How sharp is sharp? Towards quantification of the sharpness and penetration ability of kitchen knives used in stabbings. *Int J Legal Med* 122(4):289-291.

Harper T, Parras A, Rougier GW. 2019. *Reigitherium* (Meridiolestida, Mesungulatoidea) an enigmatic Late Cretaceous mammal from Patagonia, Argentina: morphology, affinities, and dental evolution. *J Mamm Evol* 26:447-478.

Hiiemae KM. 1978. Mammalian mastication: a review of the activity of the jaw muscles and movements they produce in chewing. In: Butler PM, Joysey KA, editors. *Development, Function and Evolution of Teeth*. London: Academic Press. p 359-398.

Hiiemae KM. 1984. Functional aspects of primate jaw morphology. In: Chivers DJ, Hladik CH, editors. *Food Acquisition and Processing in Nonhuman Primates*. London: Acadmeic Press. p 257-281.

Hiiemae KM, Kay RF. 1972. Tends in the evolution of primate mastication. *Nature* 240:486-487.

Kanamori T, Kuze N, Bernard H, Malim TP, Kohshima S. 2010. Feeding ecology of Bornean orangutans (*Pongo pygmaeus morio*) in Danum Valley, Sabah, Malasia: A 3-year record including two mast fruitings. *Am J Primatol* 71:1-21.

Kay RF. 1975. The functional adaptations of primate molar teeth. *Am J Phys Anthropol* 43:195-216.

1
2
3
4
5
6
7
8
9
10
11
12
13
14
15
16
17
18
19
20
21
22
23
24
25
26
27
28
29
30
31
32
33
34
35
36
37
38
39
40
41
42
43
44
45
46
47
48
49
50
51
52
53
54
55
56
57
58
59
60
61
62
63
64
65

Kay RF. 1977. The evolution of molar occlusion in Cercopithecidae and early catarrhines. *Am J Phys Anthropol* 46:327-352.

Kay RF. 1981. The nut-crackers – a new theory of the adaptations of the Ramapithecinae. *Am J Phys Anthropol* 55(2):141-151.

Kay RF. 1984. On the use of anatomical features to infer foraging behavior in extinct primates. In: Rodman PS, Cant JGH, editors. *Adaptations for Foraging in Nonhuman Primates: Contributions to an Organismal Biology of Prosimians, Monkeys, and Apes*. New York: Columbia University Press. p 21-53.

Kay RF, Covert HH. 1984. Anatomy and behavior of extinct primates. In: Chivers DJ, Wood BA, Bilsborough A, editors. *Food Acquisition and Processing in Primates*. New York: Springer US. p 467-508.

Kay RF, Hiiemae KM. 1974a. Jaw movement and tooth use in recent and fossil primates. *Am J Phys Anthropol* 40:227-256.

Kay RF, Hiiemae KM. 1974b. Jaw movement and tooth use in recent and fossil primates. *American Journal of Physical Anthropology* 40:227-256.

Kay RF, Hiiemae KM. 1974c. Mastication in *Galago crassicaudatus*, a cinefluorographic and occlusal study. In: Martin RD, Doyle GA, Walker AC, editors. *Prosimian Biology*. London: Duckworth. p 501-530.

Kay RF, Sheine WS. 1979. On the relationship between chitin particle size and digestibility in the primate *Galago senegalensis*. *Am J Phys Anthropol* 43:195-216.

Kay RF, Simons EL. 1980. The ecology of Oligocene African Anthropeidea. *Int J Primatol* 1:21-37.

Kirk EC, Simons EL. 2000. Diet of fossil primates from the Fayum depression of Egypt: A quantitative analysis of molar shearing. *J Hum Evol* 40:203-229.

Lanyon JM, Sanson GD. 1986. Koala (*Phascolarctos cinereus*) dentition and nutrition. II. Implications of tooth wear in nutrition. *J Zool* 209:169-181.

Ledogar JA, Winchester JM, St. Clair EM, Boyer DM. 2013. Diet and dental topography in pitheciine seed predators. *Am J Phys Anthropol* 150(1):107-121.

López-Torres S, Selig KR, Prufrock KA, Lin D, Silcox MT. 2018. Dental topographic analysis of paromyid (Plesiadapiformes, Primates) cheek teeth: more than 15 million years of changing surfaces and shifting ecologies. *Hist Biol* 30(1-2):76-88.

Lucas PW. 2006. *Dental Functional Morphology: How Teeth Work*. Cambridge: Cambridge University Press. 355 p.

Lucas PW, Constantino PJ, Wood B, Lawn BR. 2008. Dental enamel as a dietary indicator in mammals. *BioEssays* 30:374-385.

McCarthy CT, Ní Annaidh A, Gilchrist MD. 2010. On the sharpness of straight edge blades in cutting soft solids: Part II—Analysis of blade geometry. *Eng Fract Mech* 77(3):437-451.

McHenry K, Bajcsy P. 2008. An overview of 3D data content, file formats and viewers. Urbana, IL: National Center for Supercomputing Applications. 1-21 p.

McLeod MN, Minson DJ. 1969. Sources of variation in the *in vitro* digestibility of tropical grasses. *Grass and Forage Science* 24(3):244-249.

Mills JRE. 1955. Ideal dental occlusion in the primates. *Dental Practnr and Dent Rec* 6:47-61.

Mills JRE. 1963. Occlusion and Malocclusion of the Teeth of Primates. In: Brothwell DR, editor. *Dental Anthropology*. Oxford: Pergamon Press. p 29-52.

1
2
3
4
5
6
7
8
9
10
11
12
13
14
15
16
17
18
19
20
21
22
23
24
25
26
27
28
29
30
31
32
33
34
35
36
37
38
39
40
41
42
43
44
45
46
47
48
49
50
51
52
53
54
55
56
57
58
59
60
61
62
63
64
65

Mills JRE. 1967. A comparison of lateral jaw movements in some mammals from wear facets on the teeth. *Archs Oral Biol* 12:645-661.

Mills JRE. 1973. Evolution of Mastication in Primates. In: Montagna W, Zingeser MR, editors. *Symposia of the Fourth International Congress of Primatology*. Basel: S. Karger. p 65-81.

Molnar S, Gantt DG. 1977. Functional implications of primate enamel thickness. *Am J Phys Anthropol* 46:447-454.

Nishihara T. 1995. Feeding ecology of Western Lowland gorillas in the Nouabalè-Ndoki National Park, Congo. *Primates* 36(2):151-168.

Pampush JD, Duque AC, Burrows BR, Daegling DJ, Kenney WF, McGraw WS. 2013. Homoplasy and thick enamel in primates. *J Hum Evol* 64(3):216-224.

Pampush JD, Spradley JP, Morse PE, Griffith D, Gladman JT, Gonzales LA, Kay RF. 2018. Adaptive wear-based changes in dental topography associated with atelid (Mammalia: Primates) diets. *Biol J Linn Soc* 124(4):584-606.

Pampush JD, Spradley JP, Morse PE, Harrington AR, Allen KL, Boyer DM, Kay RF. 2016a. Wear and its effects on dental topography measures in howling monkeys (*Alouatta palliata*). *Am J Phys Anthropol* 161(4):705-721.

Pampush JD, Winchester JM, Morse PE, Vining AQ, Boyer DM, Kay RF. 2016b. Introducing molar: a new R package for quantitative topographic analyses of teeth (and other topographic surfaces). *J Mamm Evol* 23(4):397-412.

Parker GA, Maynard Smith J. 1990. Optimality theory in evolutionary biology. *Nature* 348:27-33.

Pineda-Munoz S, Lazagabaster IA, Alroy J, Evans AR. 2017. Inferring diet from dental morphology in terrestrial mammals. *Method Ecol Evol* 8:481-491.

Plummer M, Best N, Cowles K, Vines K. 2006. CODA: Convergence Diagnosis and Output Analysis for MCMC. *R News* 6:7-11.

Popowicz TE, Fortelius M. 1997. On the cutting edge: tooth blade sharpness in herbivorous and faunivorous mammals. *Ann Zool Fenn* 34:73-88.

Pruetz JD. 2006. Feeding ecology of savanna chimpanzees at Fongoli, Senegal. In: Hohmann G, Robbins MM, Boesch C, editors. *Feeding Ecology in Apes and Other Primates*. Cambridge: Cambridge University Press. p 161-182.

R Core Team. 2017. R: A language and environment for statistical computing. Vienna, Austria: R Foundation for Statistical Computing.

Reilly GA, McCormack BAO, Taylor D. 2004. Cutting sharpness measurement: a critical review. *Journal of Materials Processing Technology* 153-154:261-267.

Renaud S, Ledevin R. 2017. Impact of wear and diet on molar row geometry and topography in the house mouse. *Arch Oral Biol* 81:31-40.

Revell LJ. 2012. phytools: An R package for phylogenetic comparative biology (and other things). *Method Ecol Evol* 3:217-223.

Ross CF, Iriarte-Diaz J. 2014. What does feeding system morphology tell us about feeding? *Evol Anthropol* 23(3):105-120.

Ross CF, Iriarte-Diaz J. 2014. What does feeding system morphology tell us about feeding? *Evolutionary Anthropology: Issues, News, and Reviews* 23(3):105-120.

Schaller GB. 1963. *The Mountain Gorilla*. Chicago: University of Chicago Press.

Schwartz GT. 2000. Taxonomic and functional aspects of the patterning of enamel thickness distribution in extant large-bodied hominoids. *Am J Phys Anthropol* 111:221-224.

1
2
3
4
5
6
7
8
9
10
11
12
13
14
15
16
17
18
19
20
21
22
23
24
25
26
27
28
29
30
31
32
33
34
35
36
37
38
39
40
41
42
43
44
45
46
47
48
49
50
51
52
53
54
55
56
57
58
59
60
61
62
63
64
65

Seilacher A. 1973. Fabricational noise in adaptive morphology. *Syst Zool* 22(4):451-465.

Selig KR, Khalid W, Silcox MT. 2021. Mammalian molar complexity follows simple, predictable patterns. *PNAS* 118(1):e2008850118.

Selig KR, López-Torres S, Sargis EJ, Silcox MT. 2019. First 3D dental topographic analysis of the enamel-dentine junction in non-primate Euarchontans: contribution of the enamel-dentine junction to molar morphology. *J Mamm Evol* 26:587-598.

Sheine WS, Kay RF. 1977. An analysis of chewed food particle size and its relationship to molar structure in the primates *Cheirogaleus medius* and *Galago senegalensis* and insectivoran *Tupaia glis*. *Am J Phys Anthropol* 47:15-20.

Sheine WS, Kay RF. 1982. A model for comparison of masticatory effectiveness in primates. *J Morph* 172:139-149.

Shellis RP, Beynon AD, Reid DJ, Hiiemae KM. 1998. Variations in molar enamel thickness among primates. *J Hum Evol* 35:507-522.

Skinner MM, Evans AR, Smith T, Jernvall J, Tafforeau P, Kupczik K, Olejniczak AJ, Rosas A, Radović J, Thackeray JF, Toussaint M, Hublin JJ. 2010. Brief communication: Contributions of the enamel-dentin junction shape and enamel deposition to primate molar crown complexity. *Am J Phys Anthropol* 142(1):157-163.

Spradley JP, Pampush JD, Morse PE, Kay RF. 2017. Smooth operator: Observations on the effects of different mesh retriangulation protocols on the computation of Dirichlet normal energy. *Am J Phys Anthropol* 163(3):94-109.

Strait S. 1993. Molar morphology and food texture among small-bodied insectivorous mammals. *J Mammal* 74:391-402.

Strait SG. 1997. Tooth use and the physical properties of food. *Evol Anthropol* 5(6):199-211.

Taylor AB. 2006. Feeding behavior, diet, and the functional consequences of jaw form in orangutans, with implications for the evolution of *Pongo*. *J Hum Evol* 50:377-393.

Thieri G, Guy F, Lazzari V. 2017. Investigating the dental toolkit of primates based on food mechanical properties: Feeding action does matter. *Am J Primatol* 79:e22640.

Ungar PS. 2004. Dental topography and diets of *Australopithecus afarensis* and early *Homo*. *J Hum Evol* 46(5):605-622.

Ungar PS, Kay RF. 1995. The dietary adaptations of European Miocene catarhines. *PNAS* 92:5479-5481.

Ungar PS, M'Kirera F. 2003. A solution to the worn tooth conundrum in primate functional anatomy. *PNAS* 100(7):3874-3877.

Ungar PS, Williamson M. 2000. Exploring the effects of tooth wear on functional morphology: A preliminary study using dental topographic analysis. *Palaeontol Electron* 3(1):1-18.

Venkataraman VV, Glowacka H, Fritz J, Clauss M, Seyoum C, Nguyen N, Fashing PJ. 2014. Effects of dietary fracture toughness and dental wear on chewing efficiency in geladas (*Theropithecus gelada*). *Am J Phys Anthropol* 155:17-32.

Vogel ER, van Woerden JT, Lucas PW, Utami Atmoko SS, van Schaik CP, Dominy NJ. 2008. Functional ecology and evolution of hominoid molar enamel thickness: *Pan troglodytes schweinfurthii* and *Pongo pygmaeus wurmbii*. *J Hum Evol* 55:60-74.

Wall CE, Vinyard CJ, Johnson KR, Williams SH, Hylander WL. 2006. Phase II jaw movements and masseter muscle activity during chewing in *Papio anubis*. *Am J Phys Anthropol* 129:215-224.

1
2
3
4
5
6
7
8
9
10
11
12
13
14
15
16
17
18
19
20
21
22
23
24
25
26
27
28
29
30
31
32
33
34
35
36
37
38
39
40
41
42
43
44
45
46
47
48
49
50
51
52
53
54
55
56
57
58
59
60
61
62
63
64
65

Watts DP. 1984. Composition and variability of mountain gorilla diets in the central Virungas. *Am J Primatol* 7:323-356.

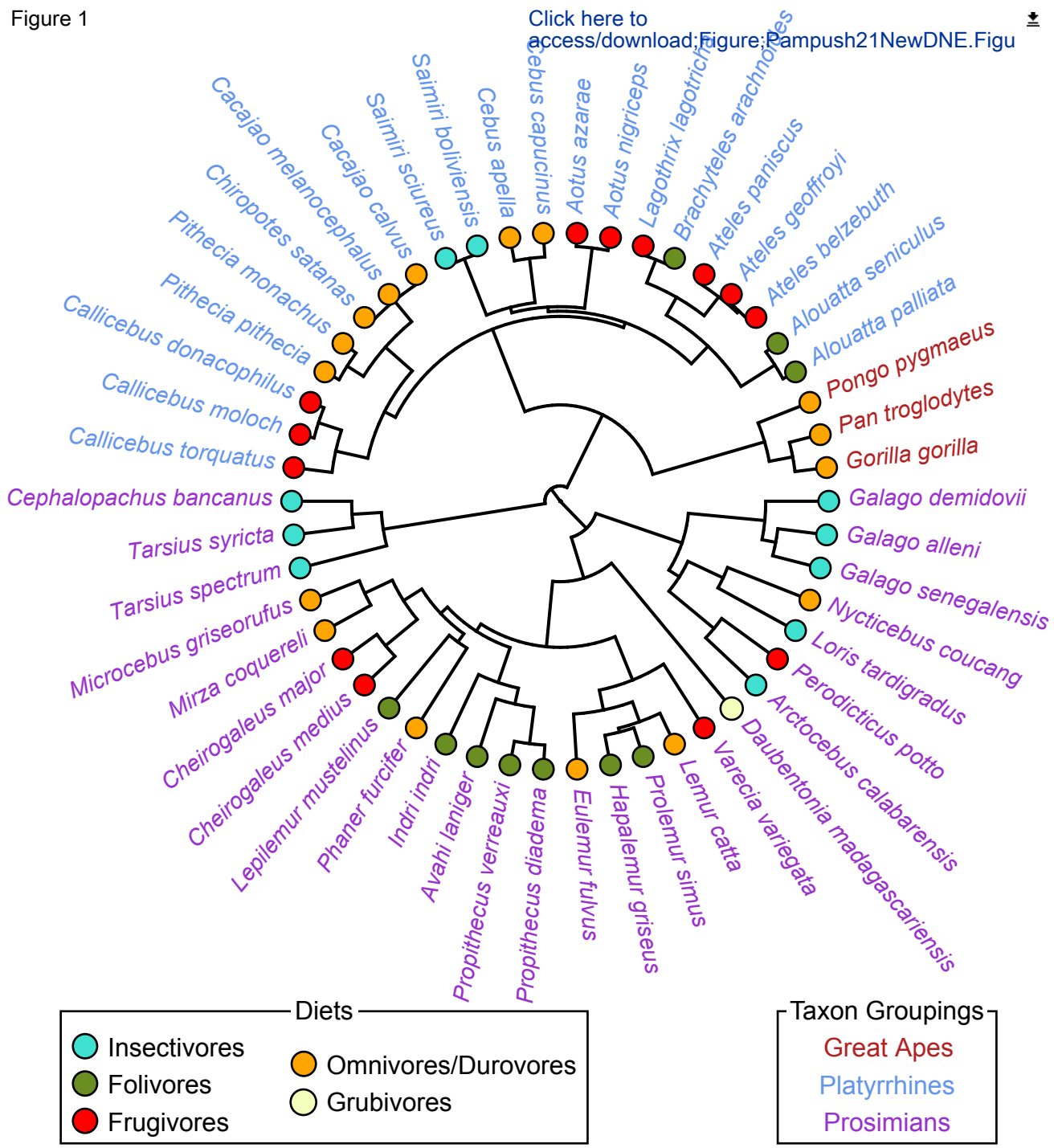
Williams SH, Kay RF. 2001. A comparative test of adaptive explanations for hypsodonty in ungulates and rodents. *J Mamm Evol* 8(3):207-229.

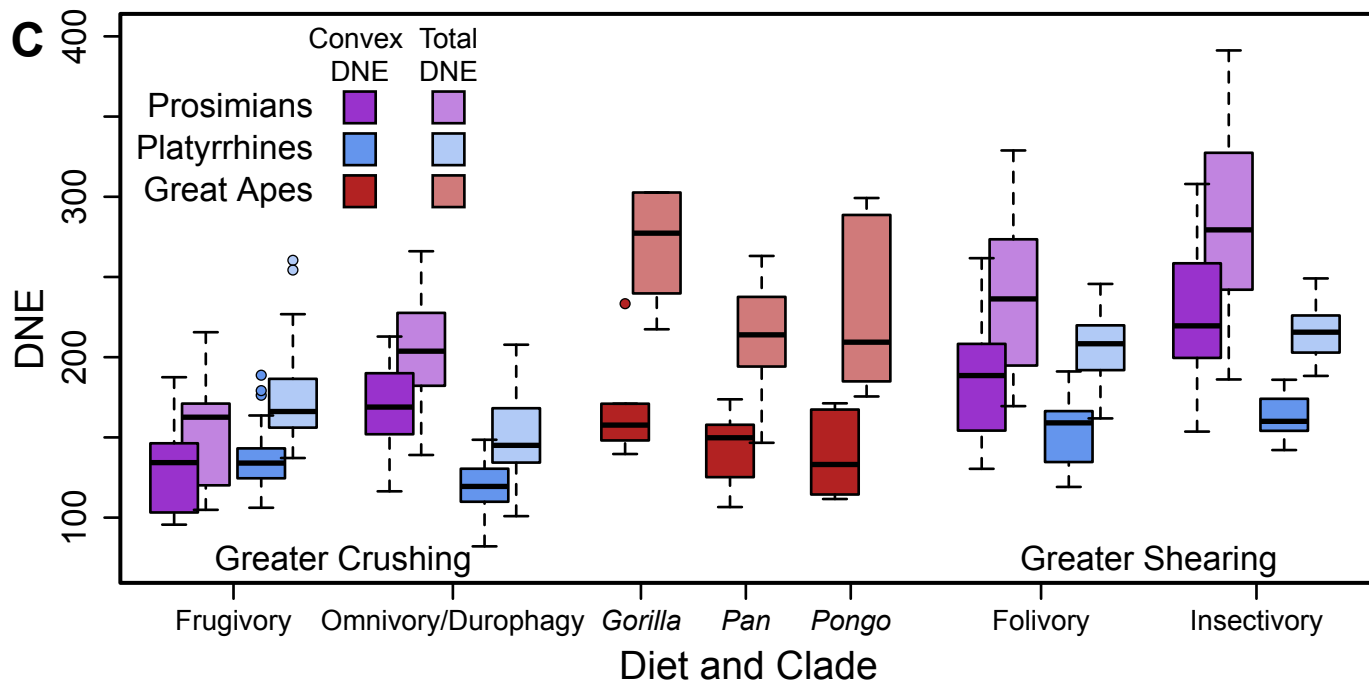
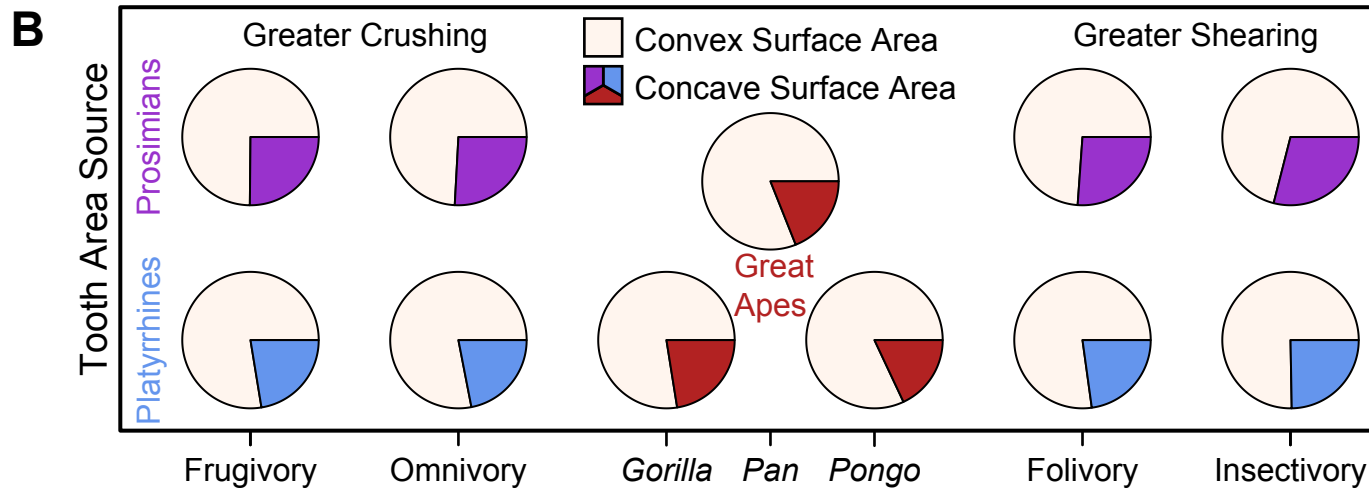
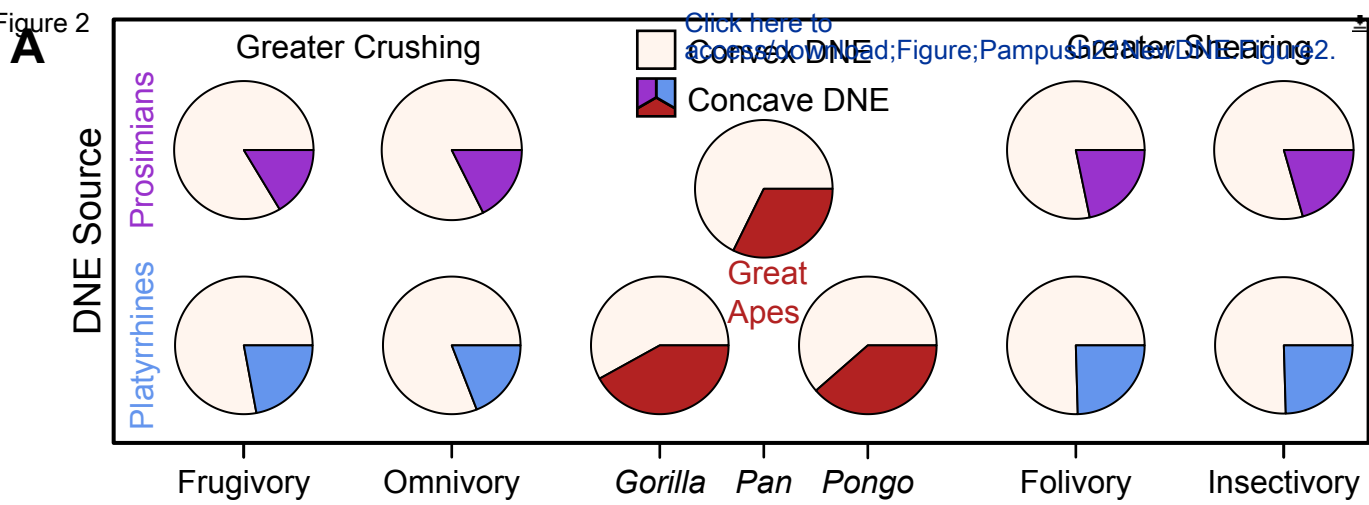
Winchester JM, Boyer DM, St. Clair EM, Gosselin-Ildari AD, Cooke SB, Ledogar JA. 2014. Dental topography of platyrrhines and prosimians: Convergence and contrasts. *Am J Phys Anthropol* 153:29-44.

Zuccotti LF, Williamson MD, Limp WF, Ungar PS. 1998. Technical Note: Modeling primate occlusal topography using geographic information systems technology. *Am J Phys Anthropol* 107:137-142.

Figure 1

Click here to access/download;Figure;Pampush21NewDNE.Figu





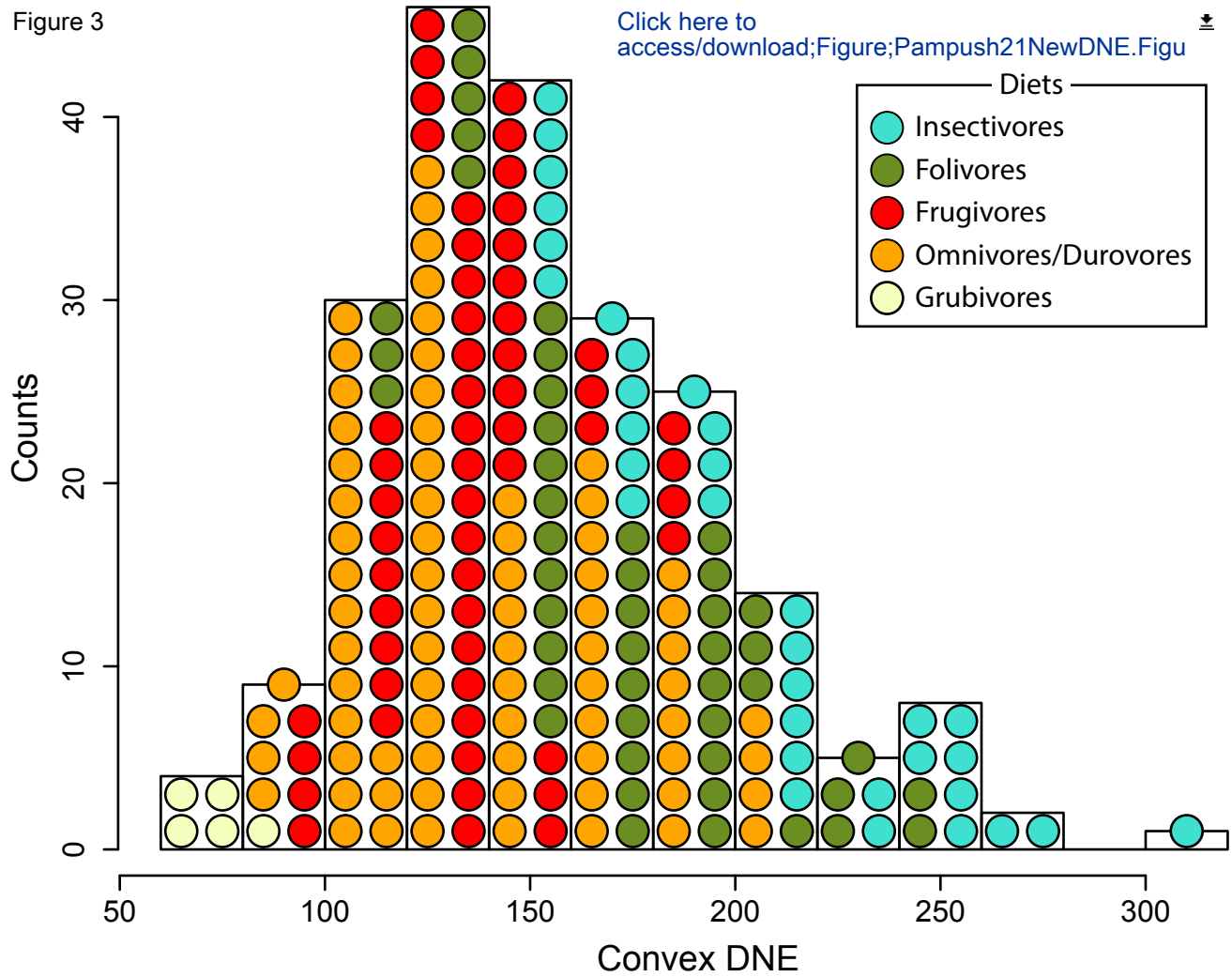
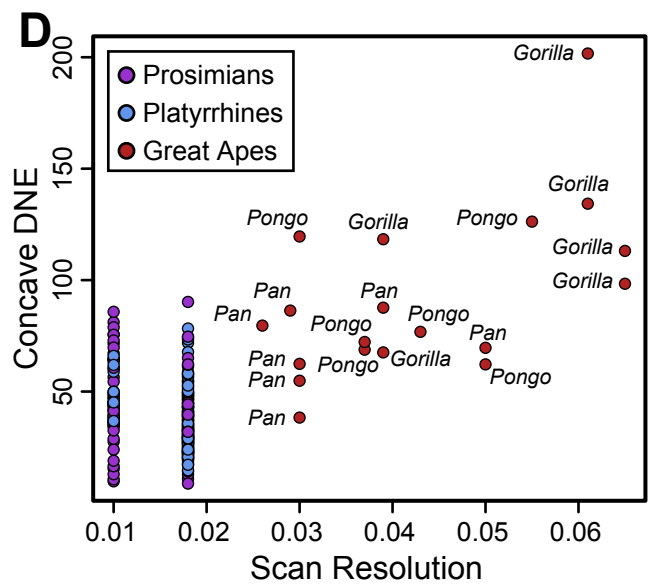
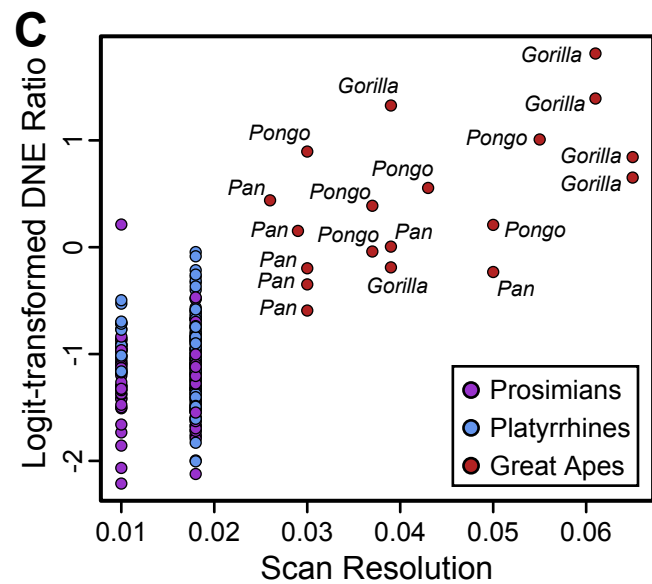
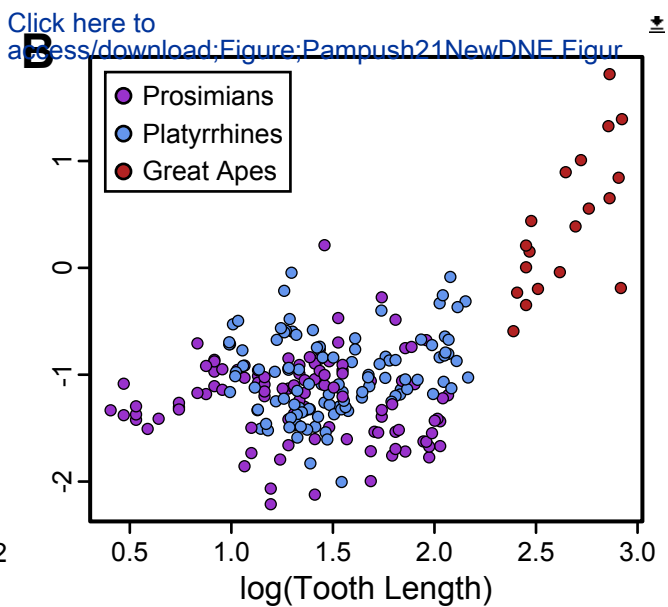
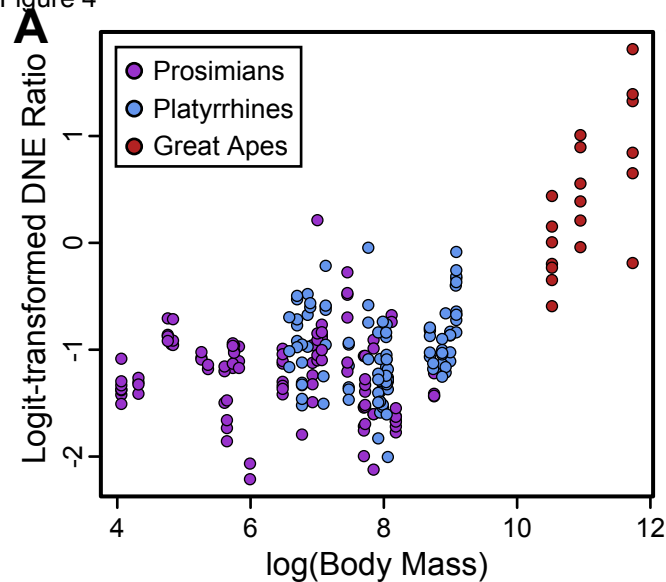


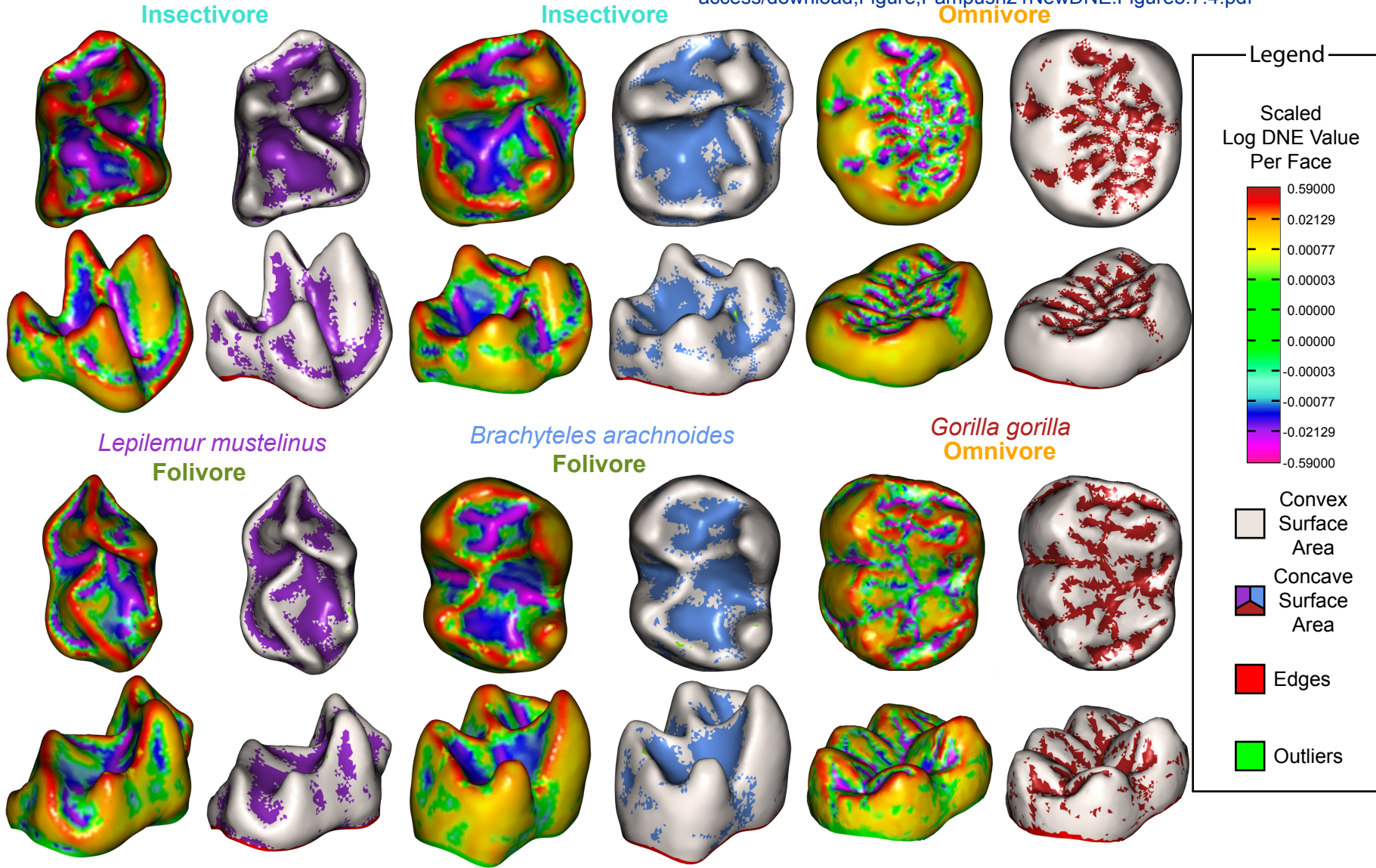
Figure 4



Prosimians

Platyrrhines

Click here to [access/download;Figure;Pampush21NewDNE_Figur](#)



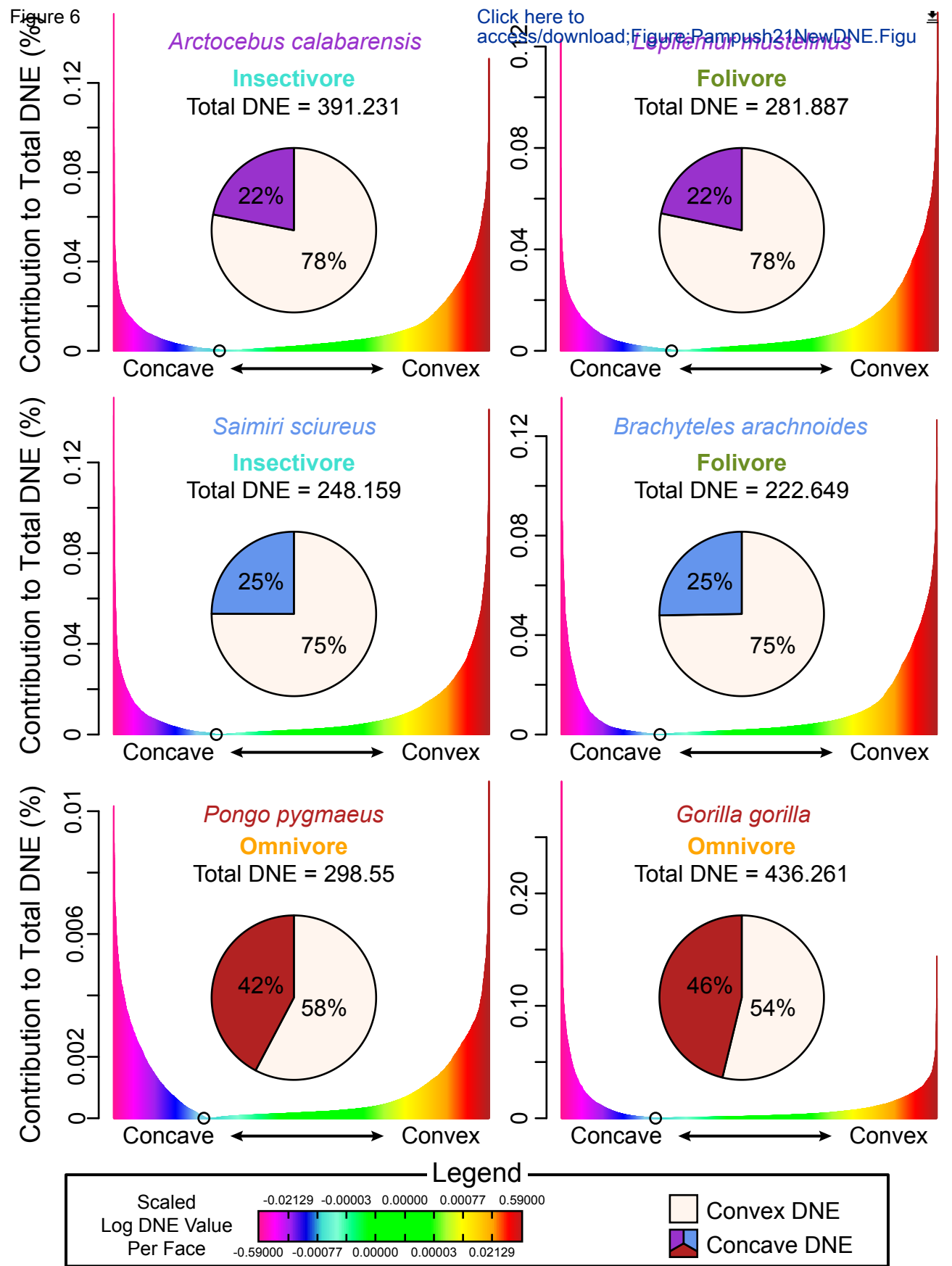


Table 1: Mean DNE values

Group	Diet/Genus	Mean Total DNE +/- SD	Mean Convex DNE +/- SD	Mean Concave DNE +/- SD	Mean Convex Area +/- SD	Mean Concave Area +/- SD
Prosimians	Folivory	237.55±48.47	185.88±35.42	51.66±16.58	34.99±23.781	12.38±7.15
	Frugivory	155.44±35.15	129.93±30.27	25.50±11.04	28.21±15.67	9.47±6.79
	Insectivory	278.75±53.50	221.33±39.25	57.42±15.71	11.12±4.84	4.53±1.92
	Omnivory	205.37±30.73	169.22±25.49	36.15±8.26	19.28±13.46	6.72±4.72
Platyrrhines	Folivory	202.94±24.63	153.11±22.15	49.82±8.62	92.07±12.46	27.21±4.12
	Frugivory	174.80±28.71	136.22±17.85	38.56±12.74	36.05±18.34	10.42±5.10
	Durophagy /Omnivory	147.39±21.96	119.26±14.95	28.13±9.86	29.95±5.98	8.41±1.65
	Insectivory	214.49±20.81	163.67±13.68	50.82±9.56	13.25±1.23	4.35±0.62
Apes	<i>Gorilla</i>	291.21±77.44	168.99±34.28	122.22±44.97	422.03±37.69	122.41±13.66
	<i>Pan</i>	211.77±40.01	143.38±23.93	68.39±17.99	213.39±20.57	49.92±1.99
	<i>Pongo</i>	227.16±53.48	139.52±26.91	87.63±27.81	291.03±61.98	63.92±15.12

Table 2: Ratio Values.

Group	Diet/Genus	Concave/Convex DNE Ratio (DNE-R)	Concave/Convex Surface Area Ratio (SA- R)
Prosimii	Folivory	0.227	0.353
	Frugivory	0.196	0.336
	Insectivory	0.259	0.408
	Omnivory	0.213	0.348
Platyrrhines	Folivory	0.325	0.295
	Frugivory	0.283	0.289
	Durophagy/Omnivory	0.235	0.281
	Insectivory	0.311	0.328
Apes	<i>Gorilla</i>	0.723	0.290
	<i>Pan</i>	0.476	0.233
	<i>Pongo</i>	0.628	0.219

Notes: Heat-map table shows higher values with darker cell backgrounds and lower values with paler cell backgrounds.

Table 3: Phylogenetically controlled MCMCglmm results comparing convex DNE with diet using Winchester et al. (2014) sample

	Posterior Mean	l-95% CI	u-95% CI	eff. Sample	<i>p</i>
(Intercept)	129.083	82.515	181.224	5294	<0.001
Folivory	40.014	2.953	76.822	5160	0.0352
Frugivory	19.053	-16.629	50.935	5479	0.2757
Grubivory	-57.463	-146.868	27.158	5813	0.1951
Insectivory	87.303	46.187	128.102	4940	<0.001
Omnivory	34.236	-8.181	76.016	4940	0.1081

Notes: Posterior Mean = average posterior effect size; l-95% CI lower confidence interval on effect size; u-95% CI = upper confidence interval on effect size; eff.Sample = effective sample size; *p* = probability.

Table 4: MCMCglmm results of size analyses

Model	post.coeff (95CI range)	eff.sample	pMCMC
All Specimens	0.5144	5440	0.002
DNE-R~Tooth Length	(0.166-0.846)		
Prosimians	0.2611	4940	0.285
DNE-R~Tooth Length	(-0.223-0.739)		
Platyrrhines	0.3078	5990	0.291
DNE-R~Tooth Length	(-0.264-0.888)		
Apes	2.369	4335	0.002
DNE-R~Tooth Length	(1.066-3.632)		
All Specimens	0.1353	4940	0.055
DNE-R~Body Mass	(-0.007-0.267)		
Prosimians	-0.022	4940	0.790
DNE-R~Body Mass	(-0.187-0.141)		
Platyrrhines	0.080	4940	0.630
DNE-R~Body Mass	(-0.275-0.399)		
Apes	0.8736	5711	0.006
DNE-R~Body Mass	(0.385-1.416)		

Notes: post.coeff = posterior correlation coefficient. eff.sample= effective sample size.
pMCMC= MCMC specific probability

Table 5: MCMCglmm results of resolution analyses

Model	post.coeff (95CI range)	eff.sample	pMCMC
All Specimens	14.868	4940	0.012
DNE-R~Scan Resolution	(3.130-25.837)		
Prosimians	-4.630	4940	0.702
DNE-R~Scan Resolution	(-27.994-20.506)		
Platyrrhines	-28.417	4940	0.567
DNE-R~Scan Resolution	(-126.821-76.203)		
Apes	26.555	787.4	0.039
DNE-R~Scan Resolution	(4.173-50.032)		
All Specimens	894.97	4940	<0.001
concave DNE~Scan Resolution	(437.88-1405.28)		
Prosimians	-421.47	4940	0.342
concave DNE~Scan Resolution	(-1258.91-445.14)		
Platyrrhines	-2007.579	4940	0.227
concave DNE~Scan Resolution	(-5519.13-1327.141)		
Apes	1621.22	3480	0.020
concave DNE~Scan Resolution	(319.49-2827.97)		

Notes: post.coeff = posterior correlation coefficient. eff.sample= effective sample size.
pMCMC= MCMC specific probability

Table 6: ANOVA of Ratios Comparing Phylogenetic Groups

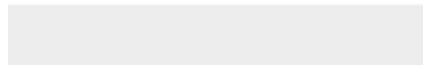
Model	DF	F-value	P-value
DNE-R~Phylogenetic Group	2	130.8	<0.001
SA-R~Phylogenetic Group	2	54.55	<0.001

Table 7: Phylogenetic ANOVA of Ratios Comparing Diets within Phylogenetic Groups

Model	F-value	P-value
Prosimians DNE-R~Diet	7.738	0.044
Prosimians SA-R~Diet	7.393	0.051
Platyrrhines DNE-R~Diet	1.345	0.710
Platyrrhines SA-R~Diet	2.186	0.506



Click here to access/download
Supplemental Material
Online Resources Cover Page.pdf





Click here to access/download
Supplemental Material
Online Resource 1.pdf



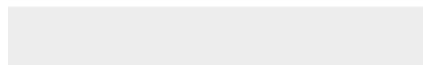
Click here to access/download
Supplemental Material
Online Resource 2.pdf



Click here to access/download

Supplemental Material

50d5b7c9-84b0-4bd0-9803-e3a8dbd1726b





Click here to access/download
Supplemental Material
Online Resource 4.pdf

Change of Authorship for:

Sign-Oriented Dirichlet Normal Energy: Aligning Dental Topography and Dental Function in the R package mo1aR.

Both Mykolas Imbrasas and Simon Chapple, graduate students at the University College London have requested to have their names moved to the acknowledgements. Upon reflect they did not feel their contributions rose to the level of authorship.

Thank you.